Creep of gel-spun polyethylene fibres : improvements by impregnation and crosslinking

Creep of Gel-Spun Polyethylene Fibres
-
Improvements by Impregnation and Crosslinking

CIP-DATA Library Technische Universiteit Eindhoven

Jacobs, Martinus J.N.

Creep of gel-spun polyethylene fibres : Improvements by impregnation and crosslinking / by Martinus J. N. Jacobs, Eindhoven : Technische Universiteit
Eindhoven, 1999. - Proefschrift. - ISBN 90-386-2741-6
NUGI 813
Trefwoorden: polymeren ; mechanische eigenschappen / polyetheen ; kruip / vezeltechnologie ; gelspinnen / crosslinken
Subject headings: polymers ; mechanical properties / polyethylene ; creep / fibretechnology ; gelspinning / crosslinking

Druk: Universiteitsdrukkerij TU Eindhoven

Creep of Gel-Spun Polyethylene Fibres
-
Improvements by Impregnation and Crosslinking

Proefschrift

ter verkrijging van de graad van doctor aan de Technische Universiteit Eindhoven, op gezag van de Rector Magnificus, prof.dr. M. Rem, voor een commissie aangewezen door het College voor Promoties in het openbaar te verdedigen op dinsdag 7 december 1999 om 16.00 uur

door
Martinus Johanna Nicolaas Jacobs
geboren te Dongen

Dit proefschrift is goegekeurd door de promotoren:

prof.dr. P.J. Lemstra
prof.dr. I.M. Ward, FRS

Copromotor:

dr. C.W.M. Bastiaansen

Opgedragen aan mijn vader
N.B. Jacobs, ✞ 1988

The solution/gel-spinning process, invented in the late 70-s at DSM, enables the production of fibres, based on ultra-high molecular weight polyethylene, with outstanding mechanical properties. Fibres with breaking loads up to 4 GPa and Young's moduli up to 150 GPa are produced commercially nowadays. However, the long term mechanical properties do not match the excellent short term properties. Especially creep is limiting for long term loading of the fibre, this is relevant for many applications of the fibres, for example in ropes, cables and composites. Moreover, many other possible applications are not even considered because of the creep behaviour of the fibre.

Routes for improving the creep properties of gel-spun fibres are subjected to a number of limitations. The fibres are produced by ultra-drawing as-spun filaments and any chemical modification before drawing interferes with the drawing process, and with the ultimate properties of the drawn fibres. Significant improvements have been reported by using branched or modified polyethylenes. However the merits have been overestimated as the creep properties are mostly reported at comparable, and relatively low, draw ratio. For improving the creep properties by modification of the drawn fibre, it is imperative that chain rupture is minimised. For example, crosslinking by means of high energy irradiation failed, because of a too high chain scission rate and resulted only in degradation of the chains, and hence, in a increase of the creep.

The creep rate of highly oriented fibres is determined by the rate of chain diffusion through crystalline segments. For describing the permanent creep, the concept of thermally activated processes is applied and exended to a molecular level. At least two parallel processes, are required for describing the relation between stress and the flow creep rate. Each process is characterised by a limiting strain rate, determined by the average thermally activated diffusion rate of the chains contributing to that process, by an activation energy and an activation volume. The activation volume of each process, the stress sensitivity, is proportional to the inverse of the number of the contributing chains.

The creep, the reversible as well as the irreversible creep, scales with the draw ratio such that fibres of different draw ratio loaded with the same force show the same creep. This observation is explained by assuming that the number of stress bearing chains in a fibre is invariant under drawing, and furthermore that the resistance of the stress bearing chains is constant.

The two-process model description is used to identify the options for improving the irreversible creep properties. Two methods are available for improving the creep resistance, a) enlargement of the number of chains that contribute to the load, and b) increase of the slip resistance of (at least a fraction of) the polymer segments. The options for improving the creep resistance at relatively high stress levels, for instance by increasing the molecular weight or the draw ratio, are limited. For improving the creep resistance at lower stress levels, reinforcement of the network process is the only option. This option offers the best opportunities for post drawing modification of fibres.

Photochemical and thermally induced crosslinking are suitable for crosslinking gel-spun polyethylene fibres, because chain scission is only a secondary effect. Adding the required initiator to the fibre before drawing has disadvantages; it interferes with the fibre production process, and furthermore a high concentration of initiator is required. Post-drawing impregnation of the fibres is not trivial because of the high density and high crystallinity of the fibre. In the present research, two methods have applied and evaluated: vapour phase impregnation and supercritical fluid assisted impregnation.

Fibres of different draw ratio have been crosslinked by UV irradiation, after vapour phase impregnation with chlorine containing UV-initiators at room temperature. The crosslink efficiency decreases with increasing draw ratio. The strength of the network formed is highest in fibres of intermediate draw ratio, and lower in both less and more highly drawn fibres. The flow creep is suppressed (up to a stress of 0.6 GPa) in fibres of different draw ratio, while the reversible creep is not influenced. The treatment should be performed in an inert atmosphere in order to reduce loss of short term mechanical properties.

Supercritical fluid assisted impregnation is a powerful technique for impregnation of (polymeric) materials. Dyeing in supercritical carbondioxide is being developed as an environmentally friendly method for colour dyeing polymeric fibres. Gel-spun polyethylene fibres of different draw ratio have been crosslinked by UV-irradiation, after impregnation with benzophenone in supercritical CO2. The creep resistance is improved significantly, especially at intermediate loads, up to 1 GPa. The creep improvement can be attributed fully to an increase of the network strength. Crosslinking furthermore results in a lower stress relaxation rate, and in an increase of the thermal resistance.

The studies into the creep of fibres of different draw ratio and the crosslinking of these fibres have resulted in information that is relevant to structural models. A model is proposed, wherein in a fibre at an intermediate stage of drawing consist mainly of fibrillar units, that consist of chains with a high degree of chain extension, sandwiched between the fibrils there is a small fraction containing chains with a low degree of extension. At subsequent drawing, or deformation due to creep, the fibrillar domains elongate, and interfibrillar chains are reeled in and become part of the extended chain phase. Reactants can penetrate in the layers between the extended chain domains. Impregnation and UV-irradiation results in grafting and crosslinking this phase, and both interfere with reeling in of the chains.

Chapter 1 Introduction

1.1 Strong polymeric fibres

In the last three decades of the 20th century, significant progress has been made in exploiting the intrinsic properties of the macromolecular chain concerning ultimate mechanical properties, especially in the field of 1-dimensional objects such as fibres.

Two major routes can be discerned which are completely different in respect to the starting (base) materials, namely *rigid* as opposed to *flexible* macromolecules [1].

The prime examples of rigid chain polymers are the aromatic polyamides (aramids), notably poly(p-phenylene terephthalamide), PPTA, currently produced under the trade names Kevlar® (Du Pont) and Twaron® (Akzo Nobel). More recent developments include the PBO (poly-(phenylene benzobisoxazole)) fibre, produced by Toyobo under the trade name Zylon®, and the experimental fibre M-5 developed by Akzo Nobel based on PIPD (polypyridobisimidazole) [2]. The latter fibre shows a much better compressive strength compared with the other polymeric fibres [3].

The *primus inter pares* of a high-performance fibre based on flexible macromolecules is undoubtedly polyethylene. X-ray studies show that the crystal modulus, viz. the Young's modulus in the chain direction, is the highest amongst all flexible macromolecules [4,5], see Table 1.1, related to the small chain cross section and the packing in an orthorhombic unit cell. The only technical problem is to extend and align the intrinsically flexible polyethylene chains into a parallel register in order to exploit the high chain stiffness.

In the case of rigid chains, the polymer chemist has built-in the intrinsic rigidity in the chain, for example PBO and the M-5 fibre. In the case of PPTA, poly(p-phenylene terephthalamide), the building block of the aramid fibre, the molecule is not strictly a rigid (rod) chain, as the ratio of the contour length over the persistence length is about 4 in dilute solutions [6], but the chain is sufficiently stiff to obtain chain extension and alignment during spinning from nematic solutions.

In the case of conventional flexible and (stereo)regular polymer molecules, the chains tend to fold upon solidification/crystallisation and in order to exploit the intrinsic possibilities in 1-D structures, routes have been developed to transform folded-chain crystals into chain-extended structures as will be discussed extensively in the next chapter. These routes have been realised and currently high strength and high modulus fibres based on ultra-high molecular weight polyethylene, approaching the theoretical Young's modulus, are produced by DSM (Dyneema®) and its licensee Allied Signal (Spectra®), and Toyobo (Dyneema®) , the DSM partner in Japan.

Table 1.1 Estimated ultimate Young's moduli of flexible chain polymers derived from X-Ray studies on oriented fibres [4,5]

Material	X-Ray Modulus (GPa)
Polyethylene (PE)	235
Poly(vinyl alcohol) (PVAL)	230
Poly(ethylene terephthalate) (PETP)	110
Polyamide-6 (PA-6)	175
Polypropylene (i-PP)	40

1.2 Development of strong PE fibres

The development of the high modulus and high strength polyethylene fibres has followed a tortuous path. High-strength/high-modulus fibres based on ultra-high molecular weight polyethylene (UHMW-PE) are being produced commercially by the so-called solution(gel)- spinning process, developed at DSM, since 1983. Figure 1.1 shows the development of the stiffness of oriented polyethylene fibres/tapes in this century. The result of the pioneering work of Ward and co-workers in the 70-s, and the quantum leap in properties since 1980 can be inferred from figure 1.1.

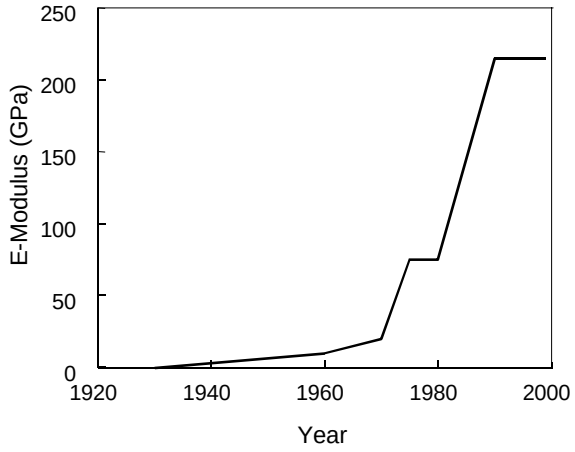

Figure 1.1 The development of the Young's modulus of polyethylene in this century

A full description of the history and the scientific background of the development of strong polyethylene fibres and an analysis of the limiting properties is given in chapter 2. The key concepts and developments leading to the present state are presented briefly below.

In 1932, Carothers and Hill predicted that polymers enable the realisation of strong and stiff materials. They formulated the essential conditions for the realisation of very strong polymeric materials [7], viz. long chain linear molecules in an extended chain conformation, and in a parallel (crystalline) register with the chain axis.

Estimates of the high chain modulus of polymeric chains were made as early as 1936 by Meyer and Lotmar [8] for cellulose. Based on vibrational spectroscopy and force constants, they calculated the chain modulus to be 77–120 GPa. In 1960 Treloar [9] made similar calculations on the properties of (extended) polymeric chains, and he calculated for polyethylene a Young's modulus of 182 GPa! These calculations and related estimates concerning the stiffness of an extended polymer chain triggered researchers to pursue chain extension via various methods and techniques.

Ward and co-workers [10-12] at the University of Leeds have made major contributions in the 70-s concerning the realisation of strong/stiff polyethylene fibres

by melt-spinning and subsequent (semi) solid-state drawing of linear polyethylene. By optimising polymer composition and process conditions, highly oriented polyethylene fibres could be made. The fibres possessed a relatively high Young's modulus (up to 70 GPa), and a strength level up to 1.5 GPa. Melt-spinning and drawing, however, encounter some limits. With increasing molar mass, the melt-viscosity becomes prohibitive high for spinning and, moreover, the drawability in the solid-state decreases with increasing molecular weight, as will be discussed extensively in chapter 2.

An alternative for melt-processing is processing via a solution, to circumvent high viscosity. Academic studies concerning chain-extension in dilute solutions were made by Mitsuhashi (13) and later by Pennings et al. [14] in extensional flow fields generated in a Couette type apparatus. Pennings made, using this technique, so-called shish-kebab type fibrils. The maximum modulus was about 25 GPa, because the fraction of extended chains could not be made large enough [15], see further chapter 2.

In subsequent studies, Zwijnenburg and Pennings [16] demonstrated that oriented polyethylene structures based on UHMW-PE could be generated by their so-called surface-growth technique. By optimising the process conditions, the fraction of extended chains, and consequently the mechanical properties of the structures were maximised [17]. They could produce oriented PE structures possessing a strength over 3 GPa and a corresponding Young's modulus of appr. 100 GPa. The process, however, is extremely slow and, moreover, due to the decreasing concentration (polymer depletion) in the equipment, the resulting polyethylene fibrous structures possessed a varying thickness (the thickness decreases with time).

At the end of the seventies, a technological break-through was realised by Smith and Lemstra at DSM. They demonstrated in 1979 the possibility of producing UHMW-PE fibres with high mechanical properties, by solution-spinning from a non-oriented semi-dilute solution, followed by ultra-drawing [18,19,20]. Strength and moduli over 3 GPa and 100 GPa respectively were reported. This gel-spinning (or solution(gel)-spinning) process [21], patented world-wide is still the basis for all commercially produced high-strength and high-modulus UHMW-PE fibres.

The ultra-drawability of UHMW-PE processed via a semi-dilute solution is readily demonstrated by a simple laboratory test [22]. A film made by dissolving a small amount of 1-2 % UHMW-PE in a hot solvent (many solvents can be used, such as: xylene, decaline, paraffin oil or paraffin wax, a convenient solvent being xylene), homogenising the solution, pouring it out in a cooled tray so that crystallisation occurs, and removing the solvent (when using xylene by evaporation), can be drawn easily on a hot shoe (at 120°C) up to 40-100 times, compared with melt processed film, which can be drawn 5-6 times at maximum. Obviously, via solution(gel)-spinning or solvent-casting a favourable structure/morphology is generated for ultra-drawing, viz. chain-extension, even in the dry state!

In industrial processes, a suspension of solvent and UHMW-PE powder is fed to an extruder, the powder is dissolved at elevated temperature and the solution is homogenised in the extruder barrel. Via a metering pump, the solvent is fed to a spinneret containing typical several hundreds of orifices. Quenching the as-spun filaments can be done in air [22] or in water [23] or in an extracting medium [24].

It is difficult to classify solution(gel)-spinning according to industrial standards, viz. solution- vs. dry-spinning vs. melt-spinning. Lammers (4) classifies the gel-spinning process, described by Smith and Lemstra [19], as a special dry-spinning process, because the quenching medium (water) is inert, therefore only a single active liquid (solvent) is used. Some researchers still consider solution(gel)-spinning as a mysterious process involving ‘gels’ [25].

The fact is that the spinning solutions of UHMW-PE, the spin dope, are homogeneous solutions in a thermodynamic sense, viz. UHMW-PE is dissolved on a molecular scale. The as-spun filaments, containing a lot of solvent, obtain a gelly appearance upon quenching since the polymer molecules crystallise and the connected crystallites are surrounded by the solvent and the solvent is the majority component. The topology of the chains, see chapter 2, is determined and fixed by this gelation/crystallisation procedure and results in a superdrawable precursor. The removal of solvent, either by evaporation and/or extraction, prior or during drawing, will and should not change the induced chain topology, under the condition that the temperature does not surpass the dissolution or melting temperature.

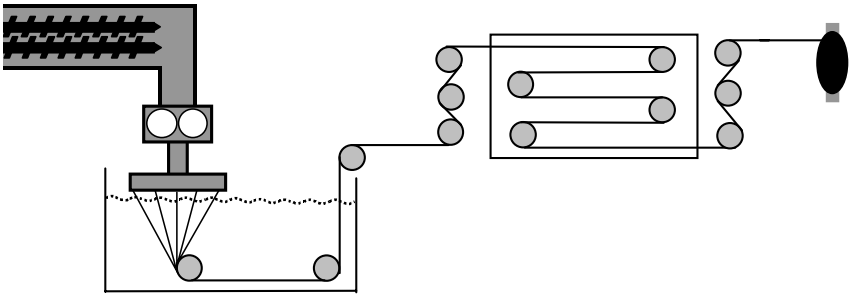

Figure 1.2: Schematic of the gel-spinning process

Industrial processes have been developed by DSM and Toyobo [26], Allied Signal [27] and Mitsui Petrochemical Company [28]. The industries involved reported only few details on the research into process development and optimisation of commercial gel-spinning process in the scientific literature. The large number of patents, related to the gel-spinning process, however demonstrates the vigorous industrial research and development that followed the publication of the possibilities of the gel-spinning process in 1981 [29]. A recent patent search revealed, see figure 1.3, that more than 350 patents have been filed for producing ultra-strong polyethylene fibres by gel-spinning before the end of 1998. The figure also shows the number of patents related to improvement of the creep properties of such fibres.

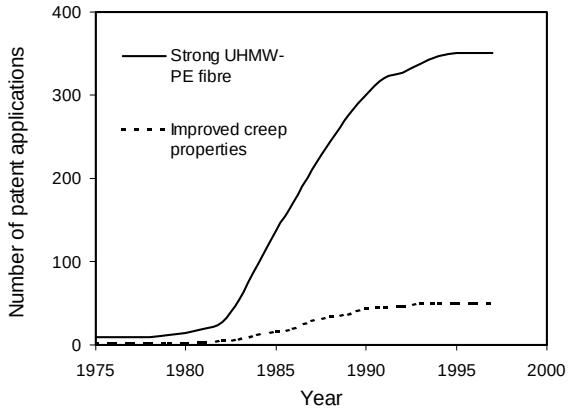

Figure 1.3 The cumulative number of patent applications related to the gel-spinning process from 1975 until 1997

The technique for producing high strength and high modulus polyethylene fibres is either described as solution-spinning or as gel-spinning. In this thesis the process will be referred to as gel-spinning.

1.3 Applications of gel-spun UHMW-PE fibres

In the years after the introduction of commercially produced fibres, gel-spun polyethylene fibres have been used, or suggested for use, in widely different applications. Figure 1.4 gives the most important commercial applications of gel-spun UHMW-PE fibres.

Figure 1.4 shows that most applications are either in ropes/nets or in products for ballistic protection. Long-term properties related to deformation and creep are relevant to, or limiting for, all rope and cable applications and for nearly all applications listed under the heading miscellaneous. Table 1.2 gives a more detailed listing of the application of gel-spun UHMW-PE fibres.

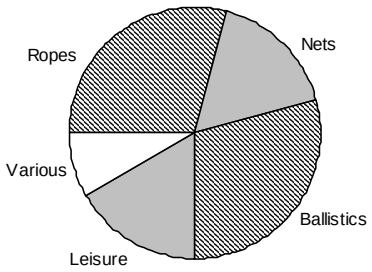

Figure 1.4 Application segments of gel-spun fibres [30).

Table 1.2 Major applications of gel- spun polyethylene fibres [30]

Ropes and Cables	**Ballistic protection**	**Miscellaneous**
Towing lines	Bullet proof vests	Sails
Mooring/anchor lines	Inserts for vests	Motor helmets
Yacht ropes	Helmets	Cut resistant gloves
Long lines	Car amour panels	Radomes
Trawl nets	Spall liners	Dental floss
Fish farms	Ballistic blankets	Speaker cones
Parapent lines	Containment shields	Cryogenic composites

The properties which motivate the use of highly oriented gel-spun UHMW-PE fibres include: high (specific) strength and stiffness (all applications), a low density, a high energy absorption capability (ballistic protection, composites), a high sound speed (ballistic protection, speaker cones), flexibility, (ropes, nets), good di-electric properties (radomes), and good chemical resistance.

Properties which are limiting the use of the fibres in specific applications are: creep (ropes and composites that require loading during prolonged periods, especially when the use temperature is above ambient), low compression strength (composites), low melting temperature (composites), low adhesion (composites), and low transverse strength (ropes, due to a weak lateral strength the fibres are prone to fibrillate, composites). Improvement of one ore more of those limiting properties, can be expected to increase the range of possible applications.

1.4 Properties of commercially produced gel-spun fibres

Fibres with outstanding short-term mechanical properties can be produced by the solution(gel)-spinning process. In the laboratory, fibres with a Young's modulus up to 220 GPa and strength more than 7 GPa (even up to 9.9 GPa) have been made [31, 32]. Table 1.3 gives the mechanical properties of commercially produced UHMW-PE fibres.

Table 1.3 Short term mechanical properties of commercially available gel-spun fibres [33,34]

Tensile strength	2.7-4	GPa
Tensile modulus	90-170	GPa
Tensile strain to failure	2.5-4	%
Compressive yield stress	0.07-0.09	GPa
Energy absorption capacity	50-70 10^6	J/m^3

The mechanical properties, especially the modulus, the strength and the strain at rupture are functions of the temperature and loading time. These aspects are considered in chapter 2.

Some physical properties relevant for the applications mentioned are given in table 1.4. Several of the physical properties reflect the high orientation and chain extension: the sound speed is related to the tensile modulus and density by $c = \sqrt{(E/\rho)}$, The negative coefficient of linear thermal expansion and high axial heat conductivity are due to the high degree of chain extension.

Table 1. 4 Physical properties of gel-spun fibres [33,34]

Density	970-980	kg/m^3
Crystallinity	80-90	%
Sound speed	10-12 10^3	m/s
Relative dielectric constant	2.2-2.4	-
Dielectric loss factor	10^{-4}	-
Melting point	142-152	°C
Coefficient of linear thermal expansion	-12 10^{-6}	K^{-1}
Thermal conductivity	20-40	W/mK

Gel-spun UHMW-PE fibres possess a good chemical resistance, the feedstock properties are enhanced by the high density and high crystallinity. An inconvenience is the low interaction with matrices, and the difficulty to impregnate or dye a fibre.

1.5 Long term properties of gel-spun UHMW-PE fibres

Several characteristics that are limiting the use of gel-spun polyethylene fibres are related to the limited interactions between the polyethylene chains, viz. only weak Van der Waals forces. Creep and creep rupture are seriously limiting the stress that can be carried for a prolonged time [35-38]. The low compression yield stress and the low shear-stress, are limiting its use in structural composites. The low lateral strength of the fibres, lower than that of the non-oriented polymer, causes the fibre to be sensitive to abrasion, and is limiting to the shear strength of composites reinforced with gel-spun UHMW-PE fibres.

The fact that only weak Van der Waals interactions are operative between polyethylene chains, is on the one hand a disadvantage, as mentioned above, but on the other hand is also essential for the success of processing UHMW-PE into high-performance fibres. Once the constraints (entanglements, as will be discussed in chapter 2) are removed prior to the drawing operation, UHMW-PE can be transformed easily into oriented structures, possessing highly extended chains, in contrast to polymers with a higher interaction between the molecules (chapter 2).

The drawing operation, however, is not fundamentally different from creep experiments, albeit the processes involve a different time-temperature scale. During drawing, polyethylene chains are transformed from a folded into an extended-chain conformation involving slippage of chains. During creep tests, the same mechanisms are involved concerning slippage of chains defects. Solution(gel)-spinning results in an ultra-drawable precursor fibre, that is subsequently drawn. The process that makes UHMW-PE more drawable, reduces the number intermolecular interactions (viz. entanglements), and thus results in a greater sensitivity to creep.

Much research has been done for improving the resistance against long term loading, by increasing the strength of the intermolecular interactions or by increasing the resistance of chains against slip [39-51].
Increasing the resistance of chains against slip has been performed by adding bulky side groups to the chain, methyl side groups [48,49], ethyl or butyl groups [50], chlorine atoms [51]. Again the potential of such schemes for improving the properties

of gel-spun fibres is limited, because the side groups interfere with the drawing process.

Crosslinking is another way to improve intermolecular interactions, and has been tried for gel-spun UHMW-PE fibres [40,42-47]. Crosslinking has improved the long-term mechanical properties of gel-spun polyethylene fibres only very slightly or not at all. High energy radiation crosslinking of drawn gel-spun UHMW-PE fibres only resulted in a degradation of their short term as well as long term mechanical properties [40,42,44], whereas this method is relatively successful for melt-spun polyethylene fibres (40).

The discrepancy between the excellent short term strength of UHMW-PE fibres, and the long term mechanical properties still exists. It motivates the search into a better understanding of the creep behaviour and into the possibilities to improve the long term properties.

Many structural models describe the distribution of the crystalline and non crystalline domains and these models are used for explaining the observed properties of highly drawn gel-spun fibres [52-61]. Some of the models assume that the supermolecular structure is not relevant for the mechanical behaviour and relate the fibre properties to the chain properties and their interactions [52-54], without taking a supermolecular structure into account. Other models have a hierarchical super-molecular structure; v.s. the properties and interactions of the smaller structural units [55-57,61] determine the properties of larger units. In these hierarchical models stronger units are connected by weaker links.
A fibre contains nearly perfect crystalline domains and non-crystalline defect sites. The non-crystalline defects determine the strength of the fibres [44], and are sites where the fibre is accessible for modification. As a main objective of this research is to influence the creep behaviour of gel-spun UHMW-PE fibres by post treatment.

1.6 Objectives of this study

Creep of gel-spun fibres is limiting for some of its present uses, and it prevents expansion in other, deformation critical, applications. The first part of this thesis is

aimed at extending the knowledge of the creep behaviour of gel-spun fibres and the influence of some major process parameters. The second deals with improving the creep properties of the fibres.

1.7 Scope of the thesis

In chapter 2, a review is presented on the processing of polyethylene, on the various options for attaining high chain orientation and chain extension, and on the limitations that are intrinsic to the polyethylene chain and its interactions.

In chapter 3, the models that describe the deformation and creep of (gel-spun) polyethylene fibres are analysed, and developed further to a molecular level.

In chapter 4, the general creep properties of highly oriented polyethylene fibres, and the influence of some important process parameters, are described.

In chapter 5 a survey is given on available literature and patents concerning research aimed at improving the creep resistance of highly oriented polyethylene fibres.

Chapter 6 deals with the modification of gel-spun UHMW-PE fibres by means of vapour phase impregnation with chlorine containing compounds, followed by UV-irradiation.

Chapter 7 deals with supercritical CO_2 assisted impregnation and UV crosslinking of UHMW-PE fibres.

In chapter 8 the structure of the gel-spun fibres is discussed. On the one hand, because the structure determines the relation between the molecular processes and the macroscopically observed deformation and creep behaviour. On the other hand, because the possibilities of impregnation and modification of the fibres are determined by structural details.

1.8 References

1 P.J. Lemstra, R. Kirschbaum, T. Ohta, H. Yasuda, Developments in Oriented Polymers-2, I.M. Ward, (Ed.), (1987), Elseviers Applied Science, London,39

2 M. Lammers, E.A. Klop, M.G. Nordholt, D.J. Sikkema, Polymer, **39**, (1998), 5999

3 M. Lammers, Ph-D Thesis, ETH Zürich, (1998), ch. 6

4 T. Nishino, H. Okhubo, K.J. Nakamae, Macomol. Sci., Phys., **B31**, (1992), 191

5 E.K. Nakamae, T. Nishino, Advances in X-ray analysis, **35**, (1992), 545

6 W. Fang Hwang, Proc. Int. symp. Fibre Sci. Technol. (ISF), Hakone, (1985), 39

7 W. Carothers and J.W. Hill, J. Amer. Chem. Soc., **54**, (1992),1579

8 K.H. Meyer, W. Lotmar, Helv. Chim. Acta, **19**, (1936), 68

9 L.R.G. Treloar, Polymer, **1**, 1960, 95

10 G. Cappacio, T.A. Crompton and I.M. Ward, J. Polym. Sci., B, Polym. Phys.,**14**,(1976), 1641

11 G. Cappacio, I.M. ward, Polym. Eng. and Sci., **15**, 13, (1975), 219

12 G. Cappacio, T.A. Crompton and I.M. Ward, J. Polym. Sci., Polym Phys Ed., **18**, (1980), 301

13 S. Mitsuhashi, Bull. Text. Res. Inst., **66**, (1963),1

14 A.J. Pennings, A. Zwijnenburg, R. Lageveen, Kolloid Z. u. Z. Polymere, **251**, (1973), 500

15 A.J. Pennings, J. Polym. Sci. Polym. Symp., **59**, (1977), 55

16 A. Zwijnenburg and A.J. Pennings, Coll. and Polym. Sci., **254**, (1976), 868

17 A.J. Pennings et al, Pure and Appl. Chem. **5**, (1983), 777

18 P. Smith et al, Polym. Bull., **1**, (1979), 733

19 P. Smith and P.J. Lemstra, Coll. and Polym. Sci, **258**, (1980), 891

20 P. Smith, P.J. Lemstra, H.C. Booij, J. Polym. Sci., Polym Phys. Ed., **19**, **(**1981), 877

21 UK patents, GB 204 2414 and 205 1667, (1979), (DSM)

22 N.J.A.M. van Aerle, Ph-D thesis Eindhoven University of Technology, (1989), ch. 2

23 P.J. Lemstra, R. Kirschbaum, Polymer, **26**, (1985), 1372

24 Allied Signal, Canadian patent (1984), 1,276,065

25 M. Mackley, MRS Bulletin (Elseviers), (1997), 47

26 R. Kirschbaum, H, Yasuda, E.H.M. van Gorp, Proc. Int. Chem. Fibres Congress, Dornbirn (1986), 229

27 S. Kavesh, D.C. Prevorsek, US Patent 4,413,110

28 M. Motooka, H. Mantoku, T. Ohno, European patent 115 192

29 R. Kirschbaum, Proc. Rolduc Polymer Meeting, (1987), Elseviers

30 Marketing Research DSM High Performance Fibres, (1999)

31 H. v.d. Werff, A.J. Pennings, Coll. Polym. Sci., **269**, (1991), 747

32 V.A. Marikhin, L.P. Myasnikova, D. Zenke, R. Hirte, P. Weigel, Polymer Bull., **12**, (1984), 287

33 Brochure Dyneema, DSM High Performance Fibres, (1997)

34 Brochures Spectra, Allied signal, (1990)

35 L.E. Govaert , C.W.M. Bastiaansen, P.J.R. Leblans. Polymer, **34**, 3, (1993), 534

36 L.E. Govaert and P.J. Lemstra, Coll. Polym. Sci., **270**, (1992), 455

37 J.P. Penning, H.E. Pras, A.J. Pennings, Colloid Polym. Sci., **272**, (1994), 664

38 J. Smook, Ph-D Thesis University of Groningen, (1984)

39 J. de Boer, A.J. Pennings, Polym. Bull., **5**, (1981), 309

40 P.G. Klein, D.W. Woods, I.M. Ward, J. Polym. Sci., B, Polym. Phys., **25**, (1987),1359

41 R. Hikmet, P.J. Lemstra and A. Keller, Coll. Polym. Sci., **265**, (1987), 185

42 D.J. Dijkstra and A.J. Pennings, Polymer Bulletin, **17**, (1987), 507

43 N.J.A.M. van Aerle, G. Crevecoeur, P.J. Lemstra, Polym. Comm., **29**, (1988), 128

44 D.J. Dijkstra and A.J. Pennings, Polymer Bulletin, **19**, (1988), 73

45 H. Nishigawa, JP 63-326 899, 1988, JP 63326 900, (1988)

46 J. de Boer, H.-J. van den Berg, and A.J. Pennings, Polymer, **25**, (1984), 515

47 Y.L. Chen and B. Rånby, J. Polym Sci, A, Polym Chem., **27**,(1989), 4051

48 Y. Ohta et al, J. Polym. Sci., B, Polym Phys., **32**, (1994), 261

49 Y. Ohta, H. Yasuda, A. Kaji, Polym. Preprints Japan, **43**, 9, (1994), 3143

50 K. Yagi, EP 0 290 141, (1988)

51 R. Steenbakkers-Menting, Ph-D Thesis Eindhoven University of Technology, (1995), ch. 6

52 Y. Termonia and P. Smith, High Modulus Polymers, Marcel Dekker New York, (1996), ch 11

53 Y. Termonia and P. Smith, High Modulus Polymers, Eds. R.S. Porter, H.H. Chuah, T. Kanamoto, , Marecel Dekker, New York, (1988), ch. 9, 259

54 R.S. Porter and T. Kanamoto, Polym. Eng. Sci, **34**, 4, (1994), 266

55 V.A. Marikhin, Makromol. Chem. Suppl., **7**, (1984), 147

56 A.J. Pennings, J. Smook, J. De Boer, S. Gogolewski, P.F. van Hutten, Pure Appl. Chem., **55**, 5, (1983), 777

57 D.C. Prevorsek, Synthetic fibre materials, (1990), ch. 10, High performance fibres, Section 2; High performance polyethylene fibres.

58 L. Berger, PH-D Thesis EPFL, (1997)

59 H.H. Kausch, L. Berger, C.J.G. Plummer, A. Bals, Proc. Int. Manmade Fibre Congress Dornbirn, (1996)

60 R.G.C Arridge, P.J. Barham, A. Keller, J. Polym. Sci., Polym. Phys., **15**, (1977), 389-401

61 A. Zachariades, T. Kanamoto, J. Appl. Polym. Sci., **35**, (1988), 1265

Chapter 2 Basic aspects and limiting properties of UHMW-PE fibres

2.1 Introduction

2.1.1 Chain-folding vs. chain-extension

Since the first scientific routes for the synthesis of high molar mass polymers were discovered by Carothers in the 30's of this century, polymer scientists have attempted to improve the mechanical properties by orienting the chain molecules. In fact, the prerequisites for actually producing 'useful fibres', viz. high modulus and high strength fibres, were already formulated by Hill and Carothers [1] in the early 1930s, viz. long chain molecules which should be in an extended chain conformation and in a parallel (crystalline) register with the fibre axis.

Estimates of the Young's modulus of polymeric chains were made as early as 1936 by Meyer and Lotmar. They showed that the Young's modulus could be calculated from IR spectroscopic data [2]. Later, Lyons [3] and notably Treloar [4] used and refined this method for calculating the modulus of polymer chains. Treloar published in 1960 a seminal paper, with calculations of the ultimate stiffness of an extended polymer (polyethylene and polyamide) chain. He calculated the Young's modulus of a single, extended polyethylene chain, to be 182 GPa!, to be compared with a Young's modulus < 2 GPa, see table 2.1, for isotropic PE. These relatively straight-forward calculations triggered studies to pursue chain orientation/extension in order to improve the mechanical and physical properties of polymer systems, viz. fibres and tapes.

Table 2.1 Stiffness (Young's modulus) of various materials (at ambient temperature)

Material	**Young's modulus [GPa]**
Rubbers	<0.1
Amorphous thermoplastics, T < Tg	3-4
Semi-crystalline thermoplastics	0.1-3
Wood (fibre direction)	15
Bone	20
Aluminium	70
Glass	70
Steel	200
Ceramics	500
Carbon fibre	500-800
Diamond	1200
Polyethylene Fibre (Dyneema®)	80–130
Aramid Fibres (Kevlar®, Twaron®)	100–150
PBO (Zylon®)	180–280
M-5 (Akzo Nobel)	300

2.1.2 Chain extension in the melt

In the literature various processes have been described to orient the chains directly in the molten state. The problem of chain-orientation and extension in the melt is that extensive relaxation processes occur, the chains resist deformation and retract back to a random coil conformation.

Lowering the extrusion-spinning temperature is not a real solution for this problem. It was shown already in 1967 by van der Vegt and Smit [5] that on lowering the extrusion temperature of polyethylene, and other crystallisable polymers, that elongational flow-induced crystallisation will occur and the solidified polymer will block the flow.

The conclusion is, that the ultimate fate of chain extension directly in the melt is flow-induced crystallisation in the processing equipment, notably in the die. Consequently, in order to obtain a high degree of chain-extension, drawing should be performed in a separate step, after processing/shaping and below the melting point, viz. in the (semi)-solid state.

2.1.3 Solid-state drawing

In the 70s, Ward et al. [6-9] started systematic studies concerning the drawability of linear polyethylenes in the solid state and they developed a technological route for optimised melt-spinning and subsequent solid-state drawing of linear polyethylenes. By optimising the polymer composition and process conditions, PE fibres could be produced possessing Young's moduli up to 75 GPa and a strength level up to 1.5 GPa. The process of melt-spinning/drawing is limited with respect to the molar mass of the polyethylenes. With increasing molar mass, both the spinnability decreases (a strong increase of melt-viscosity causes difficulties to produce homogeneous filaments) and the drawability in the solid-state decreases which sets an upper limit to melt-spinning of polyethylenes of typically 500 kDalton (kD). The relatively low maximum draw ratio of semi-crystalline polymers in the solid state will be discussed below in paragraph 2.3.1, and is often referred to as the natural draw ratio.

In conclusion, melt-spinning followed by drawing in the solid-state, encounters two major limitations:

a) *with increasing molar mass, melt-spinning/extrusion becomes more difficult related to the strong increase in melt-viscosity (the zero-shear viscosity scales with* $M_w^{3.4}$

and

b) *with increasing molar mass the drawability in the solid-state decreases, viz. the chains in the extruded and solidified filaments become more difficult to extend.*

2.1.4 Solution-processing

Solution-spinning

An obvious route to increase the spinnability of high molar mass polyethylenes is to use solvents to lower the viscosity. Jürgeleit filed [10] a patent in 1959 concerning solution-spinning and subsequently drawing of linear polyethylene but the results were not impressive, a strength level of <1.2 GPa was obtained, to be compared with approx. 1.5 GPa in the case of optimised melt-spinning. Solution-spinning of ultra-high molecular weight (UHMW)-polyethylene, M_w typically $>10^3$ kD, was performed by Zwick but no post-drawing nor fibre properties were mentioned in his patent application [11]. Blades and White (Du Pont) introduced their so-called flash spinning [12] technique of pressurised solutions of linear polyethylenes. The fibrillated strands were subjected to slow drawing. Maximum values for the tenacity and Young's modulus were 1.4 GPa and 20 GPa, respectively.

Chain-extension in dilute solutions

Mitsuhashi [13] was probably the first to attempt inducing chain extension in solution, using a Couette type apparatus, and he reported in 1963 the formation of fibrous 'string-like' polyethylene structures upon stirring. His work remained unnoticed until approx. 10 years later Pennings et al., using a similar apparatus, reported the so-called 'shish kebab' type morphology of polyethylene crystals [14].

Stirring polymer solutions to induce chain-extension is less obvious than might be anticipated at first sight. Simple shear flow is inadequate and in order to obtain full chain-extension, the flow has to possess elongational components [15]. The effect of elongational flow fields on the transformation from a random coil into an extended coil in dilute solutions has been experimentally investigated by Peterlin [16] and addressed theoretically by Franck [15] and de Gennes [17]. The conclusion is that an isolated chain will fully stretch out beyond a certain critical strain rate, $(d\varepsilon/dt)_{cr}$, which scales with $M^{-1.5}$ as determined experimentally for monodisperse samples by Odell and Keller [18]. This relationship implies that longer chains are more readily extensible.

Chain-extension in dilute solutions can be made permanent if extension is followed by crystallisation. Taking into account the experimental observations that with increasing molar mass the chains become more readily extensible, and given the fact that polymers such as polyethylene are usually poly-disperse, one can easily envisage, in retrospect, that in an elongational flow field only the high molar mass fraction becomes extended and crystallises into a fibrous structure ('shish'). The remaining part will stay in solution as random coils and upon subsequent cooling, nucleates and crystallises as folded-chain crystals, nucleating onto the fibrous structures ('kebab').

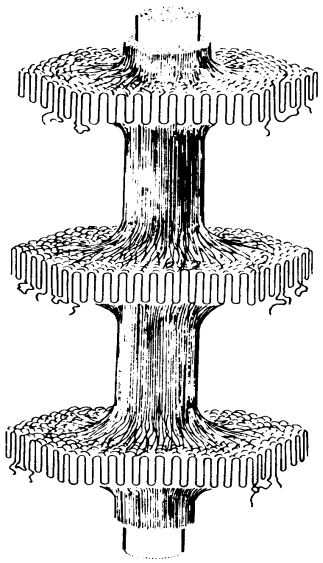

Figure 2.1 'Shish-Kebab' morphology with extended-chain (the core) and folded-chain crystals (the overgrowth)

The structure of shish-kebab type fibrous polyethylene is far from the ideal arrangement of PE macromolecules for optimum stiffness and strength. Due to the presence of lamellar overgrowth, the moduli of precipitated fibrous PE 'shish-kebab' fibrils were limited to up to about 25 GPa [19], to be compared with Young's moduli >50 GPa in the case of direct melt-spinning/drawing, as performed by Ward et al. In

fact, the ‘shish-kebab’ structure is only halfway between the folded-chain crystal and the extended chain crystal.

Fibrous structures without lamellar overgrowth were obtained by Zwijnenburg and Pennings [20,21] using their so-called surface growth technique, see figure 2.2. A seed fibre (polyethylene or even cotton) is immersed in a dilute solution of UHMW-PE and from the surface of the rotating inner-cylinder fibrous, tape-like, polyethylene structures could be withdrawn at low speeds. This pulling of fibres from the rotor is due, as was found out later after the discovery of the solution(gel)-spinning route, to the formation of a thin gel-layer on the rotor surface [22].

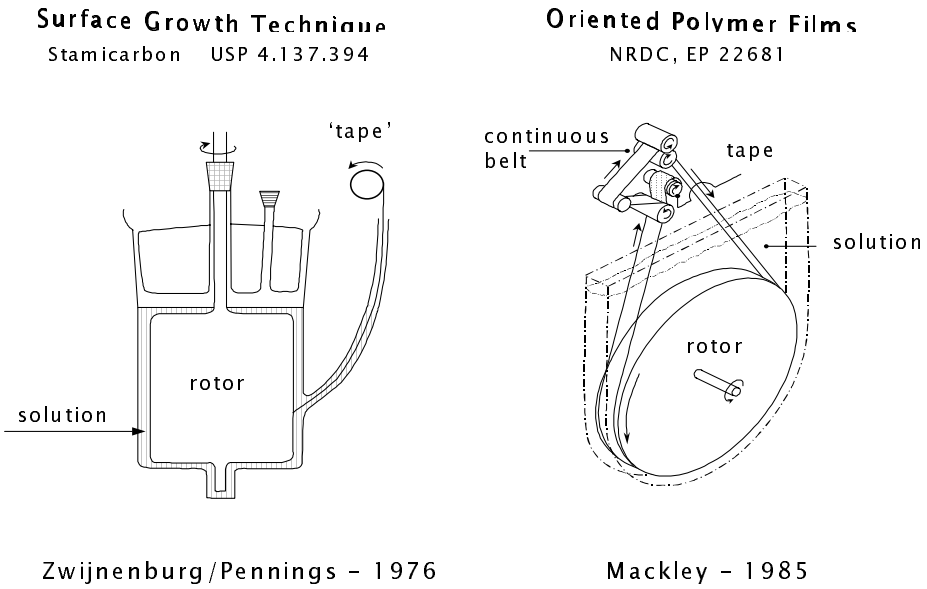

Figure 2.2 Surface growth techniques

Under optimised conditions, with respect to solution concentrations, temperatures and take up speeds, oriented UHMW-PE structures could be obtained possessing Young’s moduli over 100 GPa and strength values above 3 GPa. With increasing solution temperature, the lamellar overgrowth decreases and finally rather smooth oriented UHMW-PE structures could be obtained. The surface growth technique was another milestone on the route to high-performance UHMW-PE fibres and was, in

fact, the first experimental proof that high-modulus/high-strength structures could be made. The technique, however, possesses intrinsic draw backs such as very low production speeds, a non-uniform thickness of the tape-like structures which were pulled of from the rotor and the problem of scaling up this process. Attempts have been made to develop technologies for continuous production of UHMW-PE tapes, such as the rotor technique by M. Mackley [22], see figure 2.2. Supercooled UHMW-PE solutions were sheared and tape-like PE structures could be produced possessing stiffness values of approx. 60 GPa at take-up/roll-off speeds of several meters/min.

Gel-spinning (solution-spinning)

At the end of the seventies, solution(gel)-spinning of UHMW-PE was discovered at DSM [23-26]. In the solution(gel)-spinning technique, semi-dilute solutions are employed during spinning but the elongation of chains is performed by drawing in the semi-solid state, i.e. below the melting or dissolution temperature. Figure 2.3 shows schematically this process, now often referred to as solution(gel)-spinning.

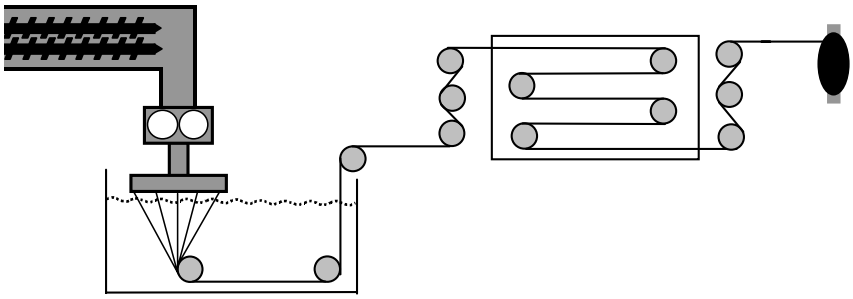

Figure 2.3 Solution(gel)-spinning of UHMW-PE

A solution of UHMW-PE with a low polymer concentration, typically of 1-2 %, was spun into water. Upon cooling a gelly filament is obtained consisting of a physical network, obtained by thermo-reversible gelation, containing a large amount of solvent. The as-spun/quenched filaments are mechanically sufficiently strong (gel-fibres) to be transported into an oven in which drawing is performed. At first glance, the ultra-drawability of these gel-fibres is not too surprising in view of the large amount of solvent which could act as a plasticiser during draw. The remarkable

feature, however, is that ultra-drawing is still possible after ***complete removal*** of the solvent ***prior*** to the drawing process. The solvent is necessary to facilitate processing of the rather intractable polymer UHMW-PE (melt-processing is impossible due to the excessively high melt-viscosity) and induces a favourable structure/morphology for ultra-drawing but the ***solvent is not essential*** during the drawing process.

Before discussing the actual drawing mechanisms (see section 2.3) involved in ultra-drawing UHMW-PE structures, first some fundamental aspects concerning stiffness and strength as documented in literature are addressed, in order to comprehend the following sections concerning drawability 2.3 and fibre properties 2.4.

2.2 The ultimate stiffness and strength of flexible polymers

2.2.1 The ultimate Young's modulus

In the previous section it was mentioned that Treloar calculated the Young's modulus of an extended polyethylene chain to be 182 GPa. Figure 1.1 (chapter 1) shows in fact that the Young's modulus of (experimental) polyethylene fibre grades surpasses the calculated limit of Treloar calculations. Using modern force field calculations, the ultimate Young's moduli are estimated in the range of 180–340 GPa [27,28].

Estimates of the ultimate Young's moduli of polyethylene and other polymer systems, can also be obtained from X-ray diffraction measurements on oriented fibres during mechanical loading [29,30]. Table 2.2 shows some representative data from the literature [31-36].

Table 2.2 Ultimate Young's moduli derived from X-Ray studies on oriented fibres

Material	X-ray modulus [GPa]
Polyethylene (PE)	235
Poly(vinyl alcohol) (PVAL)	230
Poly(ethylene terephthalate) (PETP)	175
Polyamide-6 (PA-6)	110
Polypropylene (i-PP)	40
Polyoxymethylene (POM	70

Generally, the Young's moduli derived from X-Ray data are lower in comparison with data derived from theoretical calculations. Nevertheless, all literature data show that the Young's modulus of polyethylene in the chain direction is extremely high, viz. >200 GPa.

2.2.2 The ultimate tensile strength

In the past, a variety of studies has been devoted to the theoretical tensile strength of oriented and chain extended structures, v.s. the breaking of chains upon loading [37,38]. The theoretical tensile strength of a single, extended, polymer chain can be calculated directly from the C-C bond energy. These calculations show that the theoretical tensile strengths are extremely high, in the order of 20-60 GPa. These values for the theoretical tensile strength are, in general, considered to represent the absolute upper limit of the theoretical tensile strength. The theoretical value of the tensile strength is generally calculated as the product of the Young's modulus and the strain for which the energy of the bonds is at a maximum. The values thus obtained are for absolute temperature (or infinite loading rate). Taking thermal vibrations into account, the strength levels decrease by 20-65% at ambient temperature [37,39]. Furthermore, in an array of chain extended polyethylene macromolecules, these theoretical values are approached only if all C-C bonds fracture simultaneously. This requires a defect-free, chain-extended structure and infinite polymer chains. In practice, however, we are dealing with finite chains and a completely different situation is encountered as will be addressed in the next section.

2.2.3 Infinite vs. finite chains

The theoretical estimates in sections 2.2.1. and 2.2.2 concerning the ultimate stiffness and strength of (extended) polymer chains were based on loading infinite chains or, alternatively, infinite chains in perfect crystals. In practice, however, we are dealing with finite chains and, consequently, notably the tensile strength is determined not only by the primary bonds but equally well by the intermolecular secondary bonds. Upon loading an array of perfectly aligned and extended finite polymer chains, the stress transfer in the system occurs via secondary, intermolecular, bonds. Chain overlap is needed in order to be able to transfer the load through the system, see figure 2.4b.

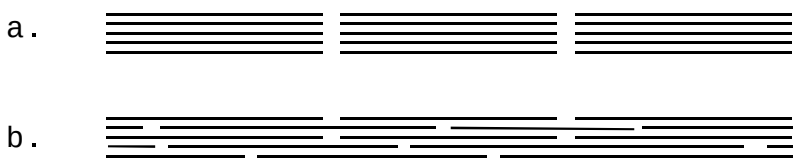

Figure 2.4 Chain overlap in arrays of extended chains of finite length. a: no chain overlap, zero strength, b: chain overlap determines strength

Qualitatively, one can easily envisage that the bonds in the main chains are only activated when the sum of the small secondary interactions, $\Sigma\varepsilon_i$, approaches E_i , the bond energy in the main chain. In this respect, one can distinguish between weak Van der Waals interactions, as is the case in polyethylene, or specific hydrogen bonds as encountered in the case of the polyamide or aramid fibres. Intuitively, one expects that in order to obtain high-strength structures in the case of polyethylene, a high molar mass is needed, in combination with a high degree of chain-extension, to build up sufficient intermolecular interactions along the chains.

Termonia and Smith [40,41,42] used a kinetic model to simulate the fracture behaviour of an array of aligned and extended *finite* polymer chains. Both chain slippage and chain rupture were considered by introducing a stress dependent activation barrier for rupture of inter- and intramolecular bonds. It was found that the molecular weight (or the number of chain ends) has a profound influence both on the

fracture mechanism and on the theoretical tensile strength of these hypothetical structures. It was shown that chain slippage prevails at a low molecular weight, as expected. Figure 2.5 shows the calculated stress-strain behaviour of polyethylene as a function of the molecular weight. In figure 2.6, polyethylene is compared with PPTA.

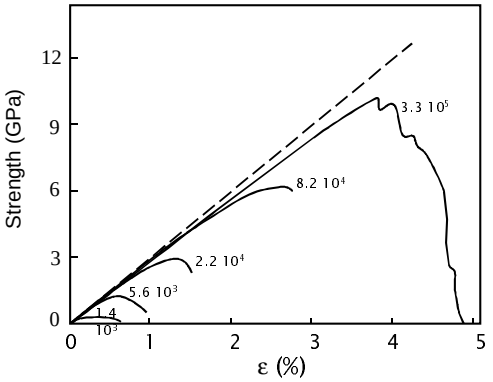

Figure 2.5 Calculated stress strain curves for polyethylenes of different chain length [42]

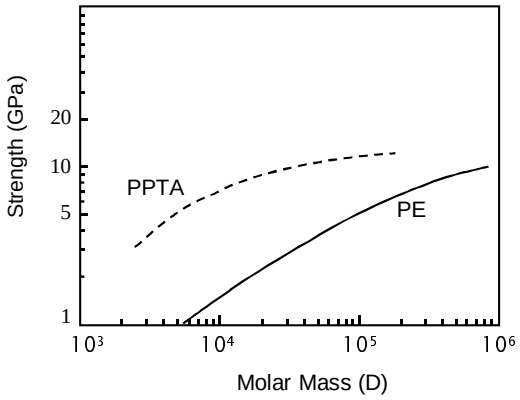

Figure 2.6 Calculated strength of polyethylene and PPTA as a function of molecular mass [42]

Figure 2.6 clearly demonstrates the influence of secondary interactions, viz. Van der Waals vs. hydrogen bonds. In order to obtain a strength level of 5 GPa, a molar mass of > 10^5 Dalton is needed for polyethylene whereas 10^4 Dalton is sufficient for PPTA. The conclusion is that polymers possessing strong secondary bonds require a smaller overlap length to obtain a high tenacity (in the case of perfectly aligned chains). This conclusion does not imply that any flexible polymer possessing hydrogen bonds, for example the conventional polyamides, is automatically an ideal candidate for obtaining high tenacity fibres. On the contrary, the hydrogen bonds also exist in the folded-chain crystals, which are formed upon solidification of the melt. These hydrogen bonds provide a barrier for ultra-drawing [43].

Figure 2.5 and 2.6 present calculated properties at ambient temperature and for relatively high strain rates (1/min). The limiting effects of the weak secondary Van der Waals bonds become even more pronounced when the mechanical properties are considered at higher temperatures and/or lower strain rates.

Figure 2.7 shows the effect of strain rate, and figure 2.8 the effect of temperature on the calculated stress strain curves.

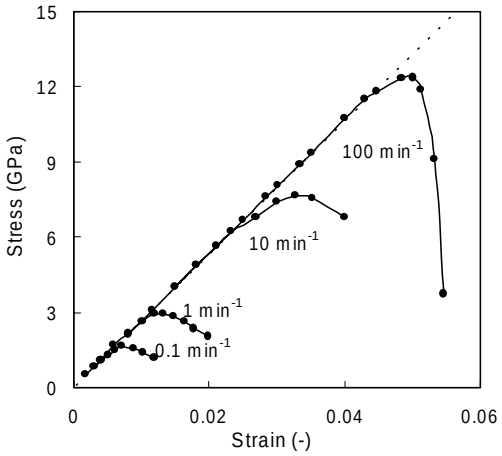

Figure 2.7 Calculated stress-strain curves for polyethylene with a molecular weight of $2.2*10^4$ Dalton for different strain rates, temperature 23°C [42]

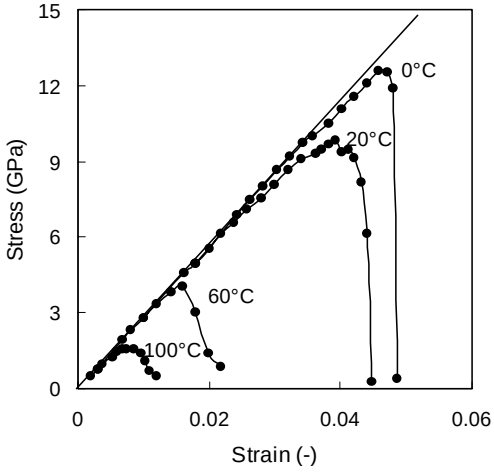

Figure 2.8 Calculated stress-strain curves for polyethylene with a molecular weight of $3.3*10^5$ Dalton for different temperatures, strain rate 1 min^{-1} [42]

Whereas at high strain rates and/or low temperatures, chain rupture is the dominating fracture mode, at low strain rate and at elevated temperature the mechanical properties are dominated by the secondary bonds, as will be discussed in chapter 2.4 (long term properties). The effect of the finite chain length is obvious at low strain rate and high temperature. At high strain rate (low temperature) high strength should be obtainable in principle even for low molecular weight.

2.3 Modelling of the drawing behaviour

2.3.1 Solid-state drawing of polyethylenes

Traditionally in the fibre industry, chain orientation and extension is generated in melt- and solution-spun fibres by two different methods: (i) applying a draw-down to the fibres during or immediately after spinning (in the molten state or super-cooled melt) and (ii) drawing of fibres at temperatures close to but below the melting- or dissolution temperature. Drawing in the (semi-)solid state, i.e. below the melting and/or dissolution temperature is usually much more effective, in terms of the development of the Young's modulus as a function of draw ratio, since relaxation processes are restricted since the chains are trapped into crystals, which act as physical network junctions.

In the case of polyethylenes, a well-known observation made by Ward et al. [8, 44] based on numerous *isothermal* drawing experiments, is that with increasing molar mass the maximum draw ratio decreases towards a limiting value of 4-5 at M_w values over 10^6 D, see figure 2.9. A limited drawability in the solid state is not unique for polyethylenes. Many other polymers demonstrate a limited drawability, for example polyamides, often referred to as the natural draw ratio.

To understand the drawing behaviour of polyethylenes in the solid-state, one automatically focuses on the role of crystallites, viz. the folded-chain crystals which are, in melt-crystallised samples, organised in more or less well-developed spherulites. There is, however, no direct correlation between crystal size or crystallinity and the maximum draw ratio as shown by numerous experimental observations. Slowly cooling from the melt can promote the solid-state drawability [45] but also can cause identical polyethylene samples to become brittle [46] in the case of very slow cooling operations. Hence, there is at first sight no apparent relationship between drawability and crystallinity/crystal structure in the case of polyethylenes.

Focussing on molecules rather than on crystalline structures, one can attempt to calculate the maximum draw ratio directly from the (assumed) chain dimensions. The topology and arrangement of molecules in melt-crystallised polymers, however, is

dependent on many parameters such as molar mass, crystallisation temperature, degree of supercooling etc. Taking the two extreme cases, respectively a) perfectly folded (single) crystals and b) the chains remain their random coil conformation upon solidification, one can calculate the maximum draw ratio as follows:

ad a) $\lambda_{max} = L / \delta$ 2. 1

ad b) $\lambda_{max} = N l_b \sin(\theta/2)/(C_\infty N l_b^{\,2})^{0.5} = 0.086 M^{0.5}$ 2. 2

In eq. 2.1 the maximum draw ratio is simply given by the ratio of the fold length L_f and the chain diameter δ. Taking typical values for the fold length L_f , 20 - 30 nm, and δ, 0.5 -0.7 nm, respectively, the maximum draw ratio for the case of well-stacked folded-chain lamellar crystals is between 30 - 60, independent of the molar mass.

In the extreme case of no folding at all, viz. the chain remains in the random-coil conformation upon solidification, the maximum draw ratio is simply related to full chain-extension of individual molecules. Assuming that no chain-slippage occurs during draw, the maximum draw ratio (λ_{max}) is given by the ratio of the contour length ($L = N l_b \sin(\theta/2)$, with l_b the bond length and θ the angle between two bonds) and the average unperturbed end-to-end distance $\langle r^2 \rangle_o$, and scales with the square root of M. In equation (2.2), N is the number of C-C bonds (M/14), (θ is the bond angle, 110° in the case of polyethylene) and C_∞ the characteristic chain stiffness (6.7 for polyethylene). λ_{max} for an isolated chain with $M = 10^6$ D, would therefore be 86.

It is clear, that both first approximation calculations predict a totally different maximum draw ratio than observed experimentally, see figure 2.9.

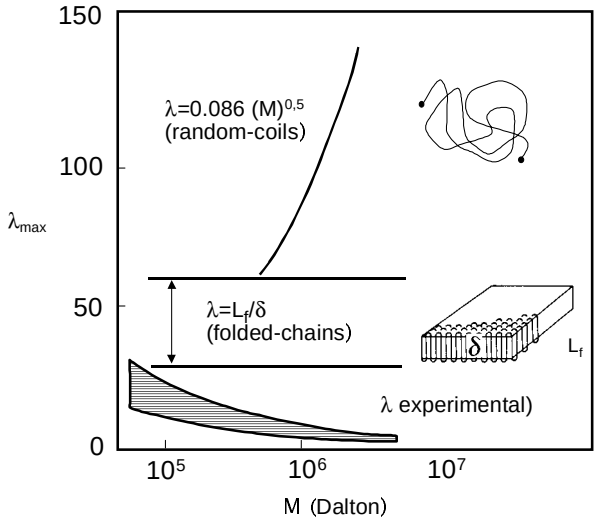

Figure 2.9 Predicted and experimentally observed (shaded area) maximum draw ratio of polyethylene

2.3.2 Solution (gel)-crystallised polyethylenes

As discussed in section 2.1. solution(gel)-spinning of UHMW-PE rendered as–spun/cast structures which are still ultra-drawable after *complete* removal of the solvent prior to the drawing process. The solvent is necessary to facilitate processing of the rather intractable polymer UHMW-PE (melt-processing is impossible due to the excessive high melt-viscosity) and induces a *favourable structure/morphology* for ultra-drawing but the *solvent is not essential* during the drawing process.

A very simple model for this enhanced drawability of solution-spun/cast UHMW-PE was put forward by Smith et al. [24] based on a network approach, ignoring completely the morphology and crystal structure, and the experimental observation that the maximum draw ratio scales with the inverse of the initial polymer concentration in solution: $\lambda_{max} \propto \varphi^{-0.5}$. In principle, this model is derived from classical rubber elasticity theory. It is assumed that entanglements are trapped in polyethylene upon crystallisation and act as semi-permanent crosslinks in a physical network upon solid state drawing. The maximum draw ratio, λ_{max}, scales with $M_e^{0.5}$, the ratio of the length of a fully stretched strand between two entanglement points (proportional to M_e), and the original distance, which is, based on Gaussian statistics,

proportional to $M_e^{0.5}$, hence $\lambda_{max} \propto M_e^{0.5}$. Upon dissolution, the entanglement density is reduced, about proportional to the inverse of the polymer volume fraction, and consequently the maximum attainable draw ratio in solution-crystallised samples is enhanced in comparison with melt-crystallised polyethylene, because the molar mass between entanglements, M_e, is increased by M_e/φ and $\lambda_{max} \propto (M_e/\varphi)^{0.5}$. On this basis, the experimentally observed dependence of the maximum attainable draw ratio on the initial polymer concentration in solution can be understood.

The entanglement model is remarkable versatile and can explain various phenomena, such as:

a) *the limited drawability of melt-crystallised UHMW-PE, λ_{max} 4-5, since the molar mass between entanglements, Me, of polyethylenes is approx. 2 kD and,*
b) *the dependence of λ_{max} at drawing in the solid-state after isothermal crystallisation at low supercoolings of UHMW-PE solutions, or from the melt in general, due to the fact that the chains are reeled in, viz. pulled out their entanglement network.*

One should notice that the simple entanglement network model, relating the maximum draw ratio solely to one single parameter, the initial polymer concentration in solution, should be used and applied with care. In the model it is tacitly assumed that the initial state has no preferential orientation, that entanglement slippage does not occur, and that the chain elements between entanglement loci are all fully stretched out.
Last but not least, the proposed ‘entanglement network’ model is not universally valid. It can be applied to apolar polymers such as polyethylenes and polypropylenes but not to polymers possessing relatively strong secondary interactions, such as hydrogen bonds. In the case of polyamids, the folded chain crystal resist deformation [43]

2.3.3 Solvent-free processing of UHMW-PE; Nascent Reactor Powders

The 'entanglement model' explains qualitatively the influence of the initial polymer concentration on the maximum draw ratio and also teaches that a relatively large amount of solvent is needed to remove entanglements prior to ultra-drawing. Especially in the beginning of the solution(gel)-spinning technique, only very low UHMW-PE concentrations could be handled, typically below 5%. Due to extensive development efforts and the use of efficient mixing equipment, such as twin screw extruders combined with temperature-gradient drawing processes, makes it nowadays feasible to handle more concentrated solutions but, nevertheless, solution(gel)-spinning requires a major amount of solvent which has to be recycled completely (in view of environmental legislation).

Solvent-free routes have been a challenge ever since the invention of the solution(gel)-spinning process and numerous attempts have been made to obtain disentangled precursors via different routes. The rationale behind this approach is that once disentangled UHMW-PE structures are obtained via some route, subsequent melt-processing should become feasible, at least one would expect a time-temperature window wherein disentangled UHMW-PE should possess a lower initial melt-viscosity in comparison with a standard equilibrium melt.
Additional arguments to this approach are the experimental observations that in UHMW-PE melts relaxation times over 10^4 seconds are present [47], even at 180°C. Moreover, it is well-established nowadays that it is virtually impossible to obtain homogeneous products by compression-moulding UHMW-PE powders [48,49], even at very long moulding times (>24 hrs). The very long chains do not cross boundaries between the powder particles. Consequently, chain diffusion/mobility in UHMW-PE melts is seemingly extremely slow and one expects a certain time scale for the transformation from a disentangled structure into a 'equilibrium' melt which could be used favourably.

To prepare disentangled UHMW-PE structures is feasible and rather straightforward. A rather obvious, but not very practical approach, is to collect precipitated single crystals grown from dilute solutions.

A much more elegant method is to make disentangled UHMW-PE directly in the reactor. Polymerisation conditions are known, viz. low temperature and rather low catalyst activity, which promote the formation of folded-chain crystals directly on the surface of the (supported) catalyst [50,51]. During low temperature polymerisation on (supported) Ziegler/Natta and/or metallocene-based catalysts, the growing chain on the catalyst surface will crystallise, since the temperature of the surrounding medium is below the dissolution temperature. In the limit of a low concentration of active sites on the catalyst (surface), one could expect that the individual growing chain will form a mono-molecular crystal. Summarising, the polymerisation technology is available to provide disentangled UHMW-PE directly from the reactor and can even be optimised to provide UHMW-PE powder particles possessing long polymer chains which *'have never "embraced" each other before the processing step*', viz. an extreme case of disentangling prior to processing .

Despite all efforts made to prepare specific disentangled UHMW-PE precursors for subsequent melt-spinning, the ultimate conclusion at this point in time is, that processing disentangled UHMW-PE with the aim to benefit from an initial lower melt-viscosity and to preserve the disentangled state to some extent during processing and prior to drawing, is not feasible at all. The salient feature is that disentangled UHMW-PE, either obtained by collecting precipitated single crystals or via specific low-temperature polymerisation shows [52]:

a) *the same high melt-viscosity (in shear) upon heating above the melting temperature as standard 'equilibrium' UHMW-PE melts. No memory effect from any previous polymerisation/crystallisation history can be depicted,* and moreover,
b) *upon re-crystallisation from the melt, the favourable drawing characteristics of disentangled UHMW-PE are lost completely and the drawing behaviour is indistinguishable from a standard melt-crystallised UHMW-PE sample.*

In view of the long relaxation times, mentioned above, corresponding to the tube renewal time, and the entanglement model, the absence of a pronounced memory effect is rather puzzling.

This problem has been addressed experimentally by Barham and Saddler and theoretically by De Gennes. It was shown by Barham and Sadler using neutron scattering techniques and deuterated polyethylenes [53] that upon melting of solution-crystallised polyethylenes the radius of gyration, which is rather low in the case of folded-chain crystals, 'jumps' to its equilibrium value corresponding to a Gaussian chain (random-coil). The authors introduced the term 'coil explosion' for this instantaneous coil expansion upon melting, which is independent of the molecular weight. The coil expansion process upon melting implies that the chain will expand very rapidly taking no notice of its neighbours, in contrast with the concept of the 'reptation' theory where the neighbouring chains play a dominant role by constituting a virtual tube that forces the chain to reptate along its own contour length.

In a recent note, De Gennes points to a way out of this dilemma [54]. He demonstrates that if a chain starts to melt, the free dangling end of the molten chain will create its own tube and moves much faster than anticipated from reptation theory. The effect is mainly independent of the molar mass, provided that the other end of the chain is still attached to the crystal.

The question remains, however, whether long chain molecules as present in UHMW-PE are capable of forming an (equilibrium) entanglement network on a short time scale based on inter-diffusion of complete chains.
Lemstra et al. [55] have proposed an alternative model for ultra-drawing which is based on local diffusion processes rather than the movement of complete chains. In a simplified view one could compare the formation of an entangled homogeneous melt with 'weaving of complete molecules' (the molecules have to penetrate fully into each other in order to form entanglements as depicted in figure 2.10). In this proposed alternative model, melting of folded-chain crystals is compared with 'knitting' of molecules, a localised process providing connectivity and loss of drawability as well. The entanglement model is based on topological constraints, entanglements, located *outside* the crystals in the amorphous zones.

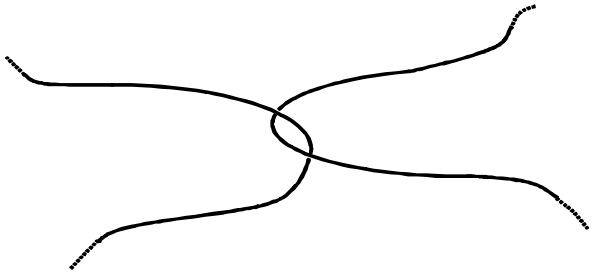

Figure 2.10 Schematic picture of a chain entanglement

The alternative model is based on stem arrangement *within* the crystals. This arrangement of molecular stems within the crystals determines the drawability.

Upon crystallisation from solution, the molecules fold usually along the 110 plane and the stems of a test chain (heavy dots) are shown in figure 2.11 without indicating the folds. For the sake of simplicity, it is assumed that adjacent re-entry occurs during crystallisation and that the chain is located within one crystal plane. Shearing and unfolding in the direction perpendicular to the chain and along the {110} plane is rather easy in view of the low shear moduli. Upon melting these crystals the chains will immediately adopt a random coil conformation as discussed before and stems of different molecules will interpenetrate in the 'coil explosion' process. Upon re-crystallisation, the stems of the test chain are now crystallised in a more random order within the crystal and shearing (slip) is more difficult, single-segment unfolding of crystals is no longer possible, unfolding of molecular chains require co-operation between many chain segments.

The schematic representation of stems within the crystals (see figure 2.11) is, of course, an oversimplification. In actual practice, superfolding will occur and crossover of stems belonging to one chain [56]. The presented model, however, only serves the purpose to demonstrate that adjacent re-entry and locality of molecules within a crystal facilitates the process of ultra-drawing which comprises fragmentation of lamellar crystals via shearing, tilting and subsequent unfolding of clusters.

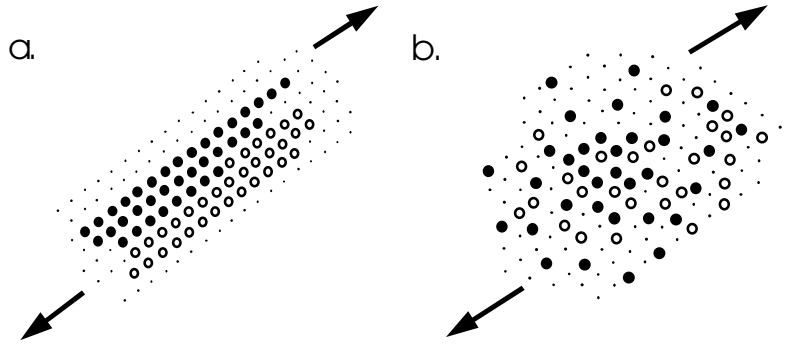

Figure 2.11 Adjacent (a) and random crystallisation (b) of chain segments

The instantaneous loss in drawability upon melting and re-crystallisation is due to re-arrangement and intermixing of stems involving only *local* chain motions rather than movement of the *complete* chain as proposed for self-diffusion in polymer melts

2.3.5 Solid-state processing

From the discussion in section 2.3.4. one might conclude that all attempts to prepare disentangled UHMW-PE structures by specific polymerisation conditions are in vain, since no advantage could be obtained in subsequent melt-processing. This conclusion is, in fact, not true. The only lesson to be learned is that the disentangled UHMW-PE precursors should never be heated above the melting temperature. Below the melting temperature, the non-entangled UHMW-PE reactor powders, so-called nascent or virgin powders, are remarkable ductile and can be processed via calandering or hot-compacting and subsequently drawn into tapes or fibrillated structures. The drawability of well-prepared nascent UHMW-PE powders is similar to solution-crystallised UHMW-PE samples. Processing of UHMW-PE reactor powders has been partly successful for making oriented tapes by sintering/compacting between rollers and subsequent drawing.

Kanamoto and Porter [57] developed a two-stage drawing process for reactor powders and they obtained Young's moduli over 100 GPa. Nippon Oil Company developed and patented several solid state processing routes for making strong UHMW-PE tapes. A process consisting of three stages: compaction, roll drawing and

tensile drawing, has been developed to pilot plant stage [58,59]. The products obtained by this process are characterised by a high Young's modulus (up to 120 GPa), but a moderate tensile strength (up to 1.9 GPa).

If fast molecular (stem) reorganisations occur at rather low temperatures, as envisaged in the case of nascent UHMW-PE reactor powders, the question arises how the drawability is preserved during compacting/sintering at temperatures below but close to the melting temperature. In section 2.3.3 it was stated that only small stem displacements are sufficient to destroy ultra-drawability.

Chain mobility below the melting temperature, in relation with drawability, has been studied on model systems of well-stacked UHMW-PE single crystals. Figure 2.12 shows stacked UHMW-PE lamellar crystals obtained by sedimentation from dilute solutions.

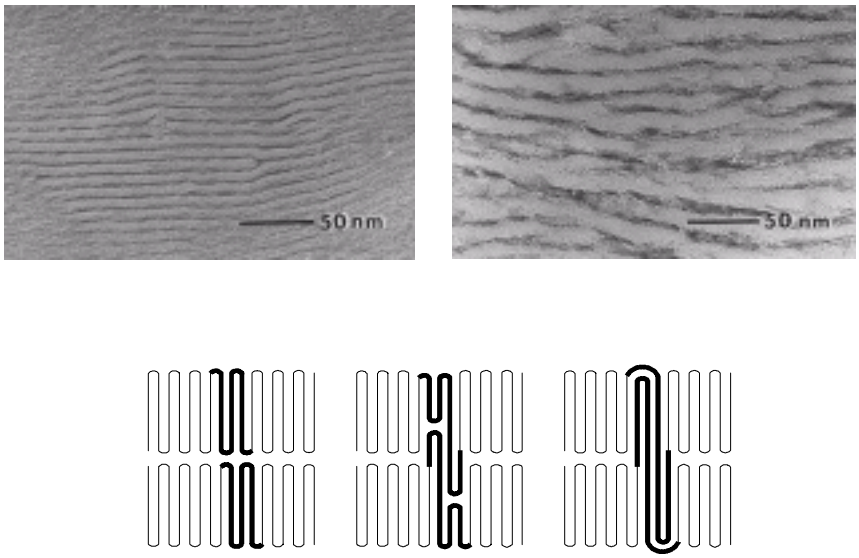

Figure 2.12 Doubling of the lamellar thickness, due to stem diffusion across the crystal interfaces

Upon heating, these (dried) solution-cast films above approx. 110 °C , it is observed that the lamellar thickness increases to twice its initial value, from 12.5 to 25 nm. Detailed in-situ synchrotron X-ray measurements combined with laser-Raman

demonstrate that this jump in thickness is related to stem diffusion [61,62] across the crystal interfaces as shown schematically in figure 2.12. Chain diffusion across crystal interfaces provides adhesion between crystals, a prerequisite for ultra-drawing an ensemble of individual single crystals of UHMW-PE, but the drawability is preserved since stem diffusion does not take place perpendicular to the chain direction, viz. across the crystal planes.

In conclusion, solid state processing of disentangled UHMW-PE structures is a possible route to produce high-modulus (split) fibres and tapes.

2.3.6 Processing via the hexagonal phase

As discussed before, UHMW-PE is an intractable polymer due to its excessive high melt-viscosity related to the high molar mass, typically > 10^6 D (according to ASTM definitions M > 3. 10^6 D). If one would attempt to process (extrude) UHMW-PE one would chose intuitively a processing temperature as high as possible within the limits of thermal decomposition. The result is that the extruded UHMW-PE strands show extensive melt-fracture. It was observed in the early 80s that upon lowering the processing temperature, the extruded strands became rather homogeneous around temperatures as low as 150 °C [63]. Figure 2.13 shows the extrusion characteristics of UHMW-PE in the three characteristic temperatures domains.

At temperatures < 135 °C, region-1, normal extrusion is impossible because insufficient sintering of individual powder particles occurs. Processing requires a special processing step that results in powder fusion in the solid state, see section 2.3.5.

At high temperatures, region-3, extrusion is not feasible, in this case due to extensive melt-fracture.

In the temperature range between 135 °C < $T_{extr.}$ < 155 °C, , region-2, strands could be extruded which look rather homogeneous upon visual inspection. This extrusion behaviour was independent of the initial crystallisation or polymerisation history. Since the extruded strands in temperature region 2 showed no enhanced drawability, starting from nascent reactor powder or solution-crystallised flakes, the topic of melt-extrusion in this specific temperature region was not pursued.

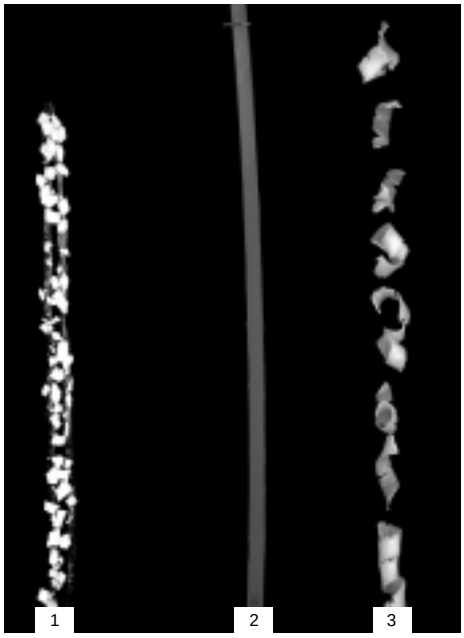

Figure 2.13 Extruded UHMW-PE 1: $T_{extr.}$ < 135 °C; 2: 135 °C < $T_{extr.}$ < 155 °C, 3: T_{extr} > 155 °C.

Recently, Keller and Kolnaar [64,65] revisited this topic and they were able to show that the hexagonal phase plays a role in the extrusion process in region 2. During extrusion, the UHMW-PE powder is in contact with the cylinder and die walls and orientation is induced, in particular at the interface polymer/metal. At this interface, the 'mobile' hexagonal phase could occur at temperatures around 155°C, and this 'mobile' hexagonal interface lubricates the extrusion process of UHMW-PE strands. The core of the strands consists of compacted UHMW-PE powder particles which are just melted and poorly sintered/fused. The extruded strands, consequently, demonstrate a drawability in the solid state which is at most similar to standard melt-crystallised UHMW-PE samples, but usually the maximum drawability is lower due to poor fusion/welding of the individual UHMW-PE particles, see below. Nevertheless, the occurrence of the hexagonal phase in polyethylene is a subject, which deserves more future attention, however not especially related to strong fibre production.

2.3.7 Summary drawing characteristics

Summarising the results concerning the drawing behaviour of ultra-high molecular weight polyethylene, one can make the following conclusions for **isothermal drawing** experiments, see figure 2.14.

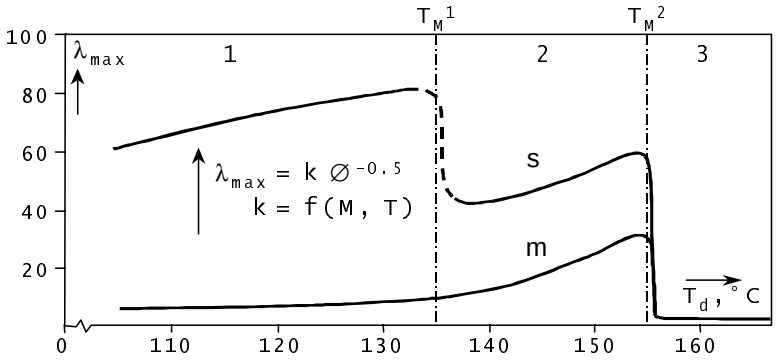

Figure 2.14 Drawing characteristics of UHMW-PE [65a]

Figure 2.14 summarises the drawing characteristics of UHMW-PE in the three temperature domains discussed above, for standard melt-crystallised and solution-crystallised samples, respectively (The drawing characteristics of nascent reactor powders are not depicted since they are similar to the solution-crystallised samples).

In region-1, below the melting temperature of folded-chain crystals Tm^1, a large difference is observed between melt-crystallised (m) vs. solution-crystallised (s) samples. Solution-crystallised samples become ultra-drawable and the drawability is dependent on the molar mass and initial polymer concentration, the maximum draw ratio, λ_{max} scales with $M^{-0.5}$ [24].

In region-2, $Tm^1 < T_{draw} < Tm^2$ (155 °C) there is often a noticeable difference in drawing behaviour between melt-crystallised samples, obtained via compression moulding, and solution-crystallised samples. These differences are not related to a difference in entanglement network structures, but related to macroscopic effects like poor sintering in the case of melt-crystallised samples. Solution-crystallised samples are somewhat better drawable (no grain boundaries) but in both cases the drawing

efficiency, in terms of the development of the Young's modulus as a function of the draw ratio is low. In region-2 chain slippage and relaxation processes occurs and the drawing is less effective.

In region-3, T_{draw} > 155 °C, drawing is not possible due to the onset of the hexagonal phase.

2.3.8 Drawing behaviour of other flexible polymer systems

The success of solution(gel)-spinning of ultra-high molecular weight polyethylene stimulated the research activities concerning the drawing behaviour of other linear polymers, notably polypropylene, polyoxymethylene and the aliphatic polyamides, nylon 6 and nylon 6.6. The prime motivation for using these polymers, and to attempt to obtain high modulus and high strength fibres, is their higher melting temperature in comparison with linear polyethylenes.

In this respect, it has to be noted that a fundamental difference exists between the drawability of apolar polymers such as polyethylene and polypropylene on the one hand and polar polymers such as the polyamides, on the other hand. The ultimate properties of solution(gel)-spun polypropylene fibres are, of course, limited intrinsically due to the fact that the polypropylene chain possesses a 3_1 helix conformation in the solid state, and consequently the upper limit of the Young's modulus is below 50 GPa. Nevertheless, also in the case of i-polypropylene the theoretical limits are approached.

Much more interesting would be to produce fibres from polar polymers such as the polyamides, see table-2.2 The high melting temperatures, compared with polyethylene, and the presence of hydrogen bonds, which could reduce the creep, see below, make the polyamides attractive candidates. An extensive research effort has been performed to produce high modulus and strength fibres based on aliphatic polyamides. These attempts have failed however despite major efforts in industry. It was demonstrated by Smith et al. [66] that the hydrogen bonds in lamellar, solution(gel)-crystallised polyamides, are essentially static up to the melting temperature and act as barriers prohibiting drawing.

Another polymer of interest is poly(vinyl alcohol), PVAL, which is commercially available in its atactic form. The small –OH group does not prevent atactic PVAL to crystallise, and the combination of a small side group and a orthorhombic crystal structure, like polyethylene, renders a high theoretical stiffness value, see table 2.2. The intermediate character in terms of polarity of PVAL, more polar than polyethylene but less directed hydrogen bonds (atactic) compared with polyamides, results in an drawability in between both extremes. The major difference with drawing of polyethylene is that in the case of PVAL the alpha-relaxation temperature increases with the draw ratio. In the case of polyethylene, the alpha relaxation temperature remains essentially constant upon drawing, in other words the crystals remain ductile, even in a highly oriented/extended structure. This property is favourable for ultra-drawing but also is responsible for creep upon static loading, see below. In the case of PVAL, the alpha-relaxation temperature increases upon draw and fibre fracture occurs as soon as the alpha-relaxation temperature approaches the melting and/or drawing temperature [67].

The above described observations diminish, to a certain extent, the need for a high maximum attainable draw ratio and a high molecular weight to obtain high strength fibres based on polymers with an intermediate polarity (cohesive energy density) such as PVAL. Poly(vinyl alcohol) fibres with a Young's modulus and tensile strength of respectively 100 GPa and 3 GPa can be made [68].

Similar observations were reported recently concerning another polymer with intermediate polarity, the polyketone fibres (PECO). Fibres, based on alternating copolymers of ethylene and carbon monoxide, possessing a Young's modulus and tensile strength of respectively ~50 GPa and 3.5 GPa were produced by Lommerts [69].

Lommerts proposed that the maximum attainable draw ratio of semi-crystalline polymers is related to their cohesive energy density which, in principle, represents the total energy of all intermolecular interactions in a polymer. The experimentally observed relationship between maximum attainable draw ratio of semi-crystalline polymers and cohesive energy density further illustrates that enhanced intermolecular interactions in 'polar' polymers dominate their solid state drawing behaviour.

Research concerning drawing of polymers possessing an intermediate polarity is still going on. For example, the drawability of high molecular weight polyesters (PETP) has been studied extensively by Ito and Kanamoto. Moduli up to approx. 35 GPa and tensile strength's up to about 2 GPa could be obtained [70].

2.4 Properties of Polyethylene Fibres

2.4.1 Axial properties (1-D)

Tensile strength

Until the late seventies, the maximum tensile strength of textile and technical yarns based on flexible macromolecules was limited to approximately 1 GPa. This situation was changed with the discovery of solution(gel)-spinning of UHMW-PE fibres.

Presently, UHMW-PE fibres possessing tensile strength's of 3-4 GPa are produced commercially, for example Dyneema® by DSM and Spectra® by its licencee Allied Signal. Figure 2.15 shows the properties of these high-performance polyethylene fibres in comparison with other advanced and classical (steel, glass) yarns.

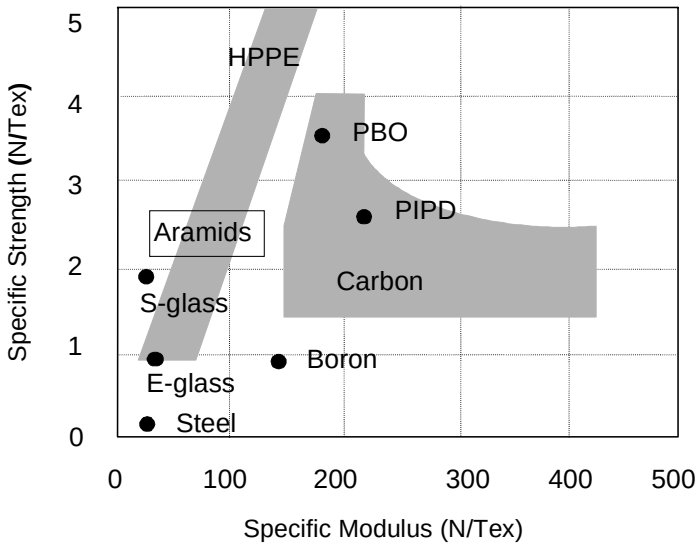

Figure 2.15 Specific mechanical properties of organic and inorganic fibres

Due to its low density, the specific value for the maximum strength of polyethylene fibres is currently superior, at least at ambient temperatures. On a laboratory scale, fibres with a strength level up to 6-8 GPa can be made by optimised drawing procedures.

It is obvious that the experimental values for the maximum tensile strength of solution-spun, ultra-drawn UHMW-PE fibres (6-8 GPa) are still low in comparison with the theoretical values, viz. > 20 GPa, for an extended polyethylene chain with an infinite molecular weight. In the past, different approaches were used to describe and to interpret the origin(s) of this discrepancy between experimental and theoretical values. One aspect of this discrepancy has already been addressed in section 2.2.3, the difference between finite and infinite chains. In the case of finite chains, the overlap of and the secondary forces between the chains are of utmost importance. The molar mass distribution and in particular the number average molecular weight (chain ends) are important parameters.

The influence of the weight average molar mass on the tensile strength of melt- and gel-spun, ultra-drawn polyethylene fibres, was systematically investigated by Smith and Lemstra [71]. In these studies, the tensile strength of fibres was compared at a fixed Young's modulus to eliminate the influence of degree of orientation and chain extension on the tensile strength. It was shown that the tensile strength of drawn fibres increases with increasing molecular weight and an empirical relationship between the tensile strength, Young's modulus, and the molecular weight was derived:

$$\sigma \propto M_w^{0.5} E^{0.8} \qquad 2.3$$

Smith and Termonia [40-42] have addressed the issue of finite chains theoretically and they have developed a kinetic model. The influence of the molar mass and the effect of chain-end segregation on the theoretical tensile strength of polyethylene and aromatic polyamides were investigated by Smith and Termonia using their kinetic model. For a molar mass in the order of 10^6 D, the theoretical tensile strength (at a strain rate of 1/min) is estimated to be approximately 10 GPa.

The tensile strength of UHMW-PE fibres, obtained via optimised laboratory experiments, 6-8 GPa, is rather close to this value. There however remains a gap between the strength of commercial and the predicted ultimate values. This gap is

most pronounced at relative high strain rate. The strength predicted by Termonia and Smith at high strain rate is approx. 25 GPa, and the strength of commercial fibres is maximum 4 GPa. This strength is only a weak function of the strain rate [73], see figure 2.16.

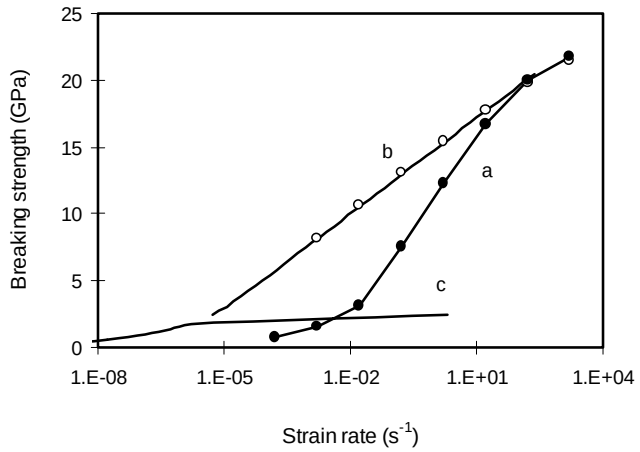

Figure 2.16 Calculated and experimental breaking stress as a function of the deformation rate, a: calculated, M = 2.2 10^4, b: calculated M = 3.3 10^5, c: experimental, Mw ≅ 2 10^6 (M_n ≅ 4 10^5).

Tensile modulus

The maximum tensile modulus of reported for gel-spun fibres is about 200 GPa. This is near the calculated modulus of the extended chain (220-340 GPa). In the model elaborated by Termonia and Smith the modulus was constant (and assumed to be 300 GPa independent of loading rate and of temperature). Polyethylene fibres, including gel-spun polyethylene fibres however creep under load. This is true even for a perfect model fibre consisting of finite chains.

For actual gel-spun fibres the chain extension is not perfect. As a consequence there is a (reversible) deformation (due to the tensioning of non extended, non-crystalline, chain segments). The compliance (and modulus) of a fibre is therefore a function of time. Furthermore it is a function of load and of temperature, see figure 2.17.

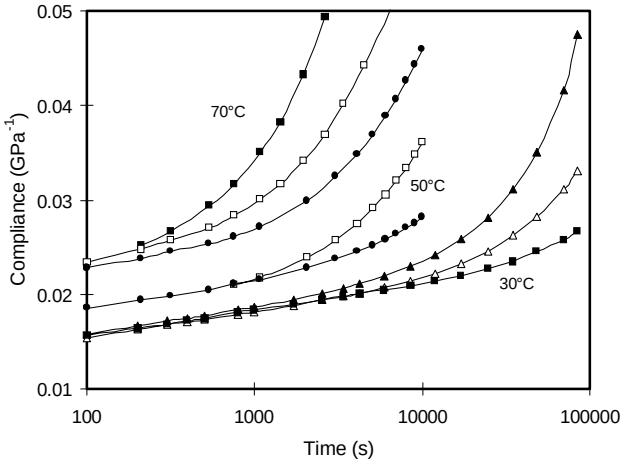

Figure 2.17 Compliance of a gel-spun fibre as a function of time, load and temperature

2.4.2 Properties (3-D)

All experimental studies concerning the tensile strength of polyethylene fibres were, of course, focused on achieving the maximum values for strength and stiffness in the fibre direction, a typically 1-D(imensional) problem. However, the 3-dimensional aspects of the fibre properties become obvious when UHMW-PE fibres are used in composite applications.

Polyethylene fibres are highly anisotropic structures. The favourable characteristics in the fibre (chain) direction in terms of stiffness and strength, are not matched at all in off-axis properties. This behaviour can be understood from the stiffness (C_{ij}) and the compliance (S_{ij}) tensor of polyethylene.

$$
C_{ij} = \begin{vmatrix} 7.99 & 3.28 & 1.13 & 0 & 0 & 0 \\ 3.28 & 9.92 & 2.14 & 0 & 0 & 0 \\ 1.13 & 2.14 & 316 & 0 & 0 & 0 \\ 0 & 0 & 0 & 3.19 & 0 & 0 \\ 0 & 0 & 0 & 0 & 1.62 & 0 \\ 0 & 0 & 0 & 0 & 0 & 3.62 \end{vmatrix} \text{ GPa}
$$

$$
\text{Sij} = \begin{vmatrix} 14.5 & -478 & -0.019 & 0 & 0 & 0 \\ -4.78 & 11.7 & -0.062 & 0 & 0 & 0 \\ -0.019 & -0.062 & 0.31 & 0 & 0 & 0 \\ 0 & 0 & 0 & 31.4 & 0 & 0 \\ 0 & 0 & 0 & 0 & 61.7 & 0 \\ 0 & 0 & 0 & 0 & 0 & 27.6 \end{vmatrix} \quad 10^{-2}\ \text{GPa}^{-1}
$$

The complete stiffness matrix Cij and the compliance matrix Sij of perfect polyethylene (single) crystals, were calculated by Tashiro et al. [27].
With these tensors the stiffness and compliance in an arbitrary load direction can be calculated. For example, when the b-axis of the crystal is oriented perpendicular to the uniaxial drawing direction, the Young's modulus as a function of the angle between the test and the chain direction is given by: [72]

$$
S_{33}(\theta) = S_{11}\sin^4\theta + S_{33}\cos^4\theta + (2S_{13}+S_{55})\cos^2\theta\sin^2\theta - 2S_{35}\cos^3\theta\sin\theta - S_{15}\cos\theta\sin^3\theta \qquad \textit{2. 4}
$$

From equation (2.4), the Young 's modulus E((θ) = S_{33}^{-1}(θ) can be calculated to be 312 GPa.
Figure 2.18 shows the E-modulus as a function of θ and demonstrates the highly anisotropic character of the orthorhombic polyethylene crystal. The dramatic drop in the E-modulus, even at small angles with the chain direction, is mainly caused by the low shear moduli of polyethylene, an advantage for ultra-drawing, but detrimental for off-axis properties of oriented polyethylene fibres. For comparison, the orientation dependence of graphite and PPTA is also plotted and last but not least of glass (isotropic) [73].

The low transverse and shear moduli of polyethylene are due to the absence of specific interactions along the chain (only weak van der Waals bonding), a major drawback in structural composite applications. It was shown by several authors et al [73,74] that the interlaminar shear strength of composites, is limited by the poor shear and compressive properties of polyethylene fibres.

2.5 Conclusions

This chapter provides an overview of the research on highly oriented structures made from polyethylene. By the gel-spinning process UHMW-PE fibres can be made possessing impressive strength and stiffness values, especially when their specific values are taken into account (see figure 2.15). The short term specific strength has not been matched by any other fibre, and the stiffness not by any fibre based on flexible polymer molecules. Polyethylene is the 'primus inter pares', thanks to the availability of high molar mass base material, the enhanced drawability after removing the constraints limiting drawability, the absence of specific interactions, such as hydrogen bonds, and the small cross-sectional area of the PE chain.

The penalty one has to pay for these beneficial characteristics is that the mechanical properties of polyethylene fibres are extremely anisotropic and that the fibres are prone to creep. Creep and stress rupture are seriously limiting the load that can be sustained for a prolonged period of time. Consequently, UHMW-PE fibres are not suitable for applications that require a high load level for prolonged periods of time, such as static cables, and for applications where off-axis loading is relevant, such as structural composites.

It was demonstrated that the long term properties of an array of fully extended polyethylene chains of finite length are limited by the weak interactions between the chains. In a perfect crystalline array the only way to increase the interactions is to increase the chain length. In actual fibres there are more possibilities for influencing the interaction between chains and thus to influence the long term mechanical properties especially the creep behaviour. The subject of the following chapters is to describe the creep of actual gel-spun UHMW-PE fibres, and a systematic research into the possibilities for improving these properties.

2.6 References

1 W. Carothers, J.W.Hill, J.Am.Chem.Soc., **54**, (1932), 1586

2 K.H. Meyer, W. Lotmar, Helv. Chim. Acta, **19**, (1936), 68

3 W. Lyons, J. Appl. Physics, **29**, (1958),1429

4 L.R.G. Treloar, Polymer, **95**, (1960), 95

5 A.K. van der Vegt, P.P.A. Smith, Adv. Polym. Sci. Monograph., **26**, (1967), 313

6 J.M. Andrews, I.M. Ward, J. Mater, Sci., **5**, (1970), 411

7 G. Capaccio, I.M. Ward, Polymer **15**, (1974), 233

8 G. Capaccio, I.M Ward., Polymer **16**, (1975), 243

9 G. Capaccio, A.G. Gibson, I.M. Ward, Ultra-High Modulus Polymers, A. Ciferri, and I.M. Ward, (Eds.), Elseviers Applied Sci., London, (1979), ch. 1

10 W. Jürgeleit, US patent 3,048,465,(1956)

11 M. Zwick, Patent Application NL 6501248, (1965)

12 H. Blades, J.R. White, US patent 3,081,519, (1963)

13 S. Mitsuhashi, Bull. Text. Res. Inst. (J), **66**, (1963), 1

14 A.J. Pennings, A.M. Kiel, Kolloid Z.Z. Polymere, **205**, (1965), 160

15 F.C. Franck, Proc. Roy., Soc., London, sec A, **319**, (1970), 127

16 A.J. Peterlin, Polym. Sci. **B4**, (1966), 287

17 P.G. De Gennes, J. Chem. Phys. **60**, (1974), 15

18 A. Keller, J.A. Odell, Colloid Polym. Sci. **263**, (1985), 181

19 A.J. Pennings, J. Polym. Sci. Polym. Symp. **59**, (1977), 55

20 A. Zwijnenburg, Ph-D Thesis University of Groningen, (1978)

21 DSM/Stamicarbon, U.S.Patent 4,137,394

22 M. Mackley, NRDC Eur. Patent 22681

23 P. Smith, P.J. Lemstra, UK Patents 2 040 414, 2 051 661, (1979)

24 P. Smith, P.J. Lemstra, Makrom. Chem. **180**, (1979), 2983

25 P. Smith, P.J. Lemstra, H.C. Booij, J. Polym. Sci., Phys. Ed. **20,** 1982), 2229

26 P. Smith, P.J. Lemstra, J. Mater. Sci. **15**, (1980), 505

27 K. Tashiro, M. Kobayashi, H. Tadakoro, Macromolecules, **13**, (1978), 914

28 A. Odajima, T. J. Madea, Polym. Sci. **C34**, (1966), 55

29 E.K, Nakamae, T., Nishino, Advances in X-Ray analysis, **35**, (1992), 545

30 T.Nishino, H.Ohkubo, K.J., Nakamae, Macromol. Sci.-Phys., **B31**, (1992),191

31 K. Nakamae, T. Nishino, H. Ohkubo, J. Macromol. Phys., **B30**, (1991),1

32 K. Nakamae, T. Nishino, H. Ohkubo, S. Matsuzawa, K. Yamura, Polymer **33**, (1992), 2281

33 K. Nakamae, T. Nishino, F. Yokoyama, T. Matsumoto, J. Macrom. Sci.-Phys., **B27**, 4, (1988), 404

34 I. Sakurada, T. Ito, K. Nakamae, Bull. Inst. Chem. Res. Kyoto Univ., **44**, (1966), 77

35 K. Nakamae, T. Nishino, K. Hata, Kobunshi Ronbonshu, **42**, (1985), 241

36 K. Nakamae, T. Nishino, Y. Shimiizu, K. Hat, Polymer, **31**, (1990), 1909

37 T. He, Polymer, **27**, (1986), 253

38 A. Kelly, N.H. Macmillan, Strong Solids, Clarendon Press, Oxford, (1986)

39 S.N. Zhurkov, Int. J. of Fracture Mechanics, **1**, (1965), 311

40 Y. Termonia, P. Smith, Macromolecules, **21,** (1987), 835

41 Y. Termonia, P. Smith, Polymer, **27**, (1986), 1845

42 Y. Termonia, P. Smith, High Modulus Polymers, A.E. Zachariades, and R.S. Porter, Eds., Marcel Dekker, New York, (1996), ch 11

43 A.R. Postma, P. Smith, A.D. English, Polymer Comm., (1990), 444

44 G. Capaccio, T.A. Crompton, I.M. Ward, J. Polym. Sci., Phys. Ed., **14**, (1976), 1641

45 I.M. Ward, Developments in Oriented Polymers, Elseviers, New York, 1988

46 P.J. Lemstra, Personal Communication

47 J.R. Leblans, C.W.M. Bastiaansen, Macromolecules, **22**, (1989), 3312

48 S. Rastogi,. L. Kurelec, P.J. Lemstra, Macromolecules, **31**, (1998), 5022

49 S. Rastogi, P. Koets, P.J. Lemstra, patent appl. NL 98/00093

50 H.D. Chanzy, R.H. Marchessault, Polmer, **8**, (1967), 567

51 Y.M.T. Engelen, P.J. Lemstra, Polym. Comm., 32, (1991), 343

52 C.W.M. Bastiaansen, Ph-D Thesis Eindhoven University of Technology, (1991)

53 D.M. Sadler, P.J. Barham, Polymer, **31**, (1990), 36

54 P.G. De Gennes, C.R. Acad. Sci. Paris, **t 312/II**, (1995), 363

55 P.J. Lemstra, N.A.M.J. van Aerle, C.W.M. Bastiaansen, Polymer Journal, **19**, (1987), 97

56 A. Keller, Faraday Discussions of the Chemical Society, **68,** (1979), 145

57 T. Kanamoto, T. Ohama, K. Tanaka, M. Takeda, R.S. Porter, Polymer, **28,** (1987), 1517

58 O. Otsu, S. Yoshida, T. Kanamoto, R.S. Porter, Proceedings PPS Conference, Yokohama, July (1998)

59 EP 376 423, and EP 425 947

61 S Rastogi, L. Kurelec, P.J. Lemstra, Macromolecules, **31**, (1988), 5022

62 S. Rastogi , A.B. Spoelstra, J.G.P. Goossens, P.J. Lemstra, Macromolecules, **30**, (1997), 7880

63 I.M. Ward, in Integration of Fundamental Polymer Science and Technology, L.A. Kleintjens, P.J.Lemstra, eds., Appl. Scio. Publ., London 1986

64 J.W.H. Kolnaar, Ph-D. Thesis University of Bristol, (1993)

65 J.W.H. Kolnaar, A. Keller, Polymer, **36**, (1995), 821

65a P.J. Lemstra, C.W.M. Bastiaansen, H.E.H Meier, Angew. Macromol. Chem., **145/146**, (1986), 343

66 A.R. Postma, P. Smith, A.D. English, Polymer Comm., (1990), 444

67 P.D. Garrett, D.T. Grubb, J. Polym. Sci., Polym. Phys., B, **26**, (1988), 2509

68 K. Yamaura, T. Tanigami, N. Hayashi, K.I. Kosuda, S. Matsuzawa, J. Appl. Polym. Sci., **40**, (1990). 905

69 B.J. Lommerts , Ph-D Thesis, University of Groningen, (1994)

70 M. Ito, K. Takahashi, T. Kanamoto, Journal of Appl. Polym. Sci., **40**, (1990), 1257

71 P. Smith and P.L. Lemstra, J.P.L. Pijpers, J. Polym. Scio, Polym. Phys. Ed., **20**, (1983), 2229

72 Nye, I.M. Ward, Physical Properties of Crystals, Cambridge University Press

73 A.A.J.M. Peijs, Ph-D Thesis Eindhoven University of Technology, (1993),ch. 3

74 Lacroix , Ph-D Thesis University of Hamburg/Harburg, (1998)

Chapter 3 Creep of highly oriented polyethylene fibres

3.1 Introduction

In the previous chapter an overview of the processing of polyethylene and the limiting properties of fibres based on polyethylene has been presented. Whereas gel-spinning enables the large scale production of strong fibres based on UHMW-PE, melt-spinning of polyethylene is limited to polyethylenes of a lower molecular weight (M_w up to about 300.000 Dalton).

Melt- and gel-spun, ultra-drawn polyethylene fibres are, of course, dissimilar with respect to the base materials, the processing conditions and the ultimate properties, see chapter 2. The maximum tensile strength of melt-spun and gel-spun polyethylene fibres is approximately 1.5 GPa and 7 GPa respectively. This difference originates from the enhanced drawability and higher molecular weight of the gel-spun fibres in comparison with melt-spun fibres. Despite these differences between melt- and gel-spun polyethylene fibres there are, however, also many similarities, especially from a phenomenological point of view. In both academic and industrial research centres, a substantial research effort has been devoted to elucidate the physical origin of the creep processes, and to model and predict the creep properties [1-15]. Moreover, numerous efforts have been performed to improve the creep resistance of both melt-spun and gel-spun fibres [10,11,16-29].

The aim of this chapter is to establish a basis for describing and comparing the creep behaviour both for melt-spun as well as gel-spun fibres, and for analysing the changes in the creep behaviour resulting from the modification of a fibre.

For meeting these aims, previous studies concerning the modelling and prediction of long term creep will be reviewed. The current status of the research in this area and the different approaches used, will be discussed and evaluated. The usual existing creep descriptions are of a phenomenological nature. As a relation is sought between molecular parameters and modifications on a molecular scale and the creep behaviour, the description of the creep is extended to the molecular level.

In the first part of this chapter (par. 3.2), general experimental phenomena related to the creep of melt- and gel-spun polyethylene fibres will be presented. Subsequently, the mathematical models used to model and predict the long-term properties of these fibres will be discussed (par. 3.3). The final part is dedicated to the molecular origin of the creep of highly oriented polyethylene fibres (par. 3.4).

3.2 Experimentally observed creep characteristics of polyethylene fibres.

Polymeric materials, including fibres, show creep under static loading conditions. In thermoplastic polymers, such as polyethylene, creep can be very extensive, both for non-oriented material as well as for highly oriented fibres. Figure 3.1 shows a typical creep curve of a polyethylene fibre, viz. the elongation of a fibre is plotted as a function of time under constant load.

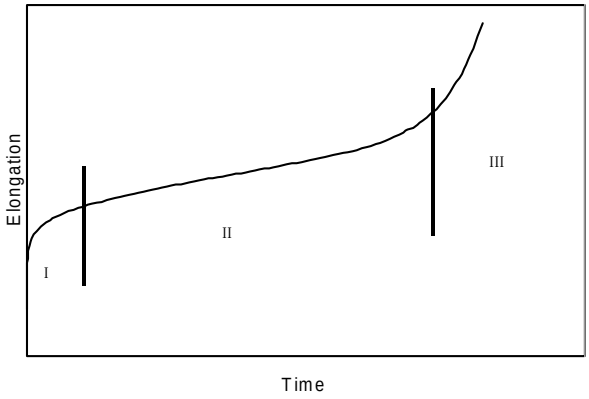

Figure 3.1 Elongation of a polyethylene fibre as a function of time

In such an elongation vs. time curve, that is also observed in many metals [30], three regimes can be distinguished characterised by a different behaviour of the creep rate, viz. the slope of the curve in figure 3.1.

- Regime I, the creep rate decreases with increasing elongation (primary creep).
- Regime II, the creep rate is approximately constant (secondary creep).
- Regime III, the creep rate increases again, signalling imminent failure (tertiary creep).

In polyethylene fibres, all three regimes can be observed, the secondary creep is especially pronounced. The elongation caused by primary and secondary creep is important for the applications of the fibre, and the present discussion focuses on these two regimes.

In figure 3.2, experimental creep curves are shown for a gel-spun polyethylene fibre as a function of the applied load [12], and in figure 3.3 as a function of the temperature.

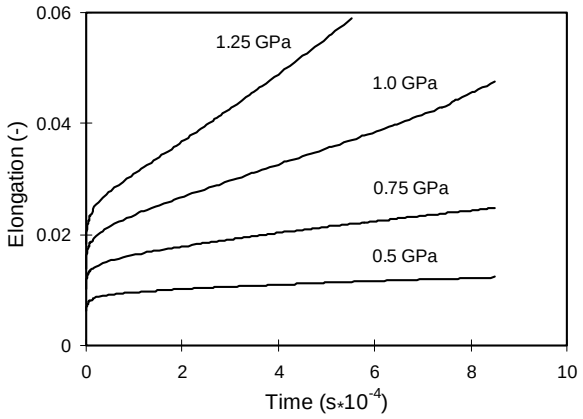

Figure 3.2 Creep of a commercial gel-spun fibre with an E-modulus of 100 GPa (Dyneema SK66) for various loads at a temperature of 30°C [12]

Figures 3.2 and 3.3 illustrate the typical creep behaviour of gel-spun and ultra-drawn polyethylene fibres. The fibres exhibit a linear increase in elongation upon prolonged exposure to static loading conditions (secondary creep in figure 3.1). It is also evident that the creep rate of the fibres strongly depends on the stress level and on the temperature.

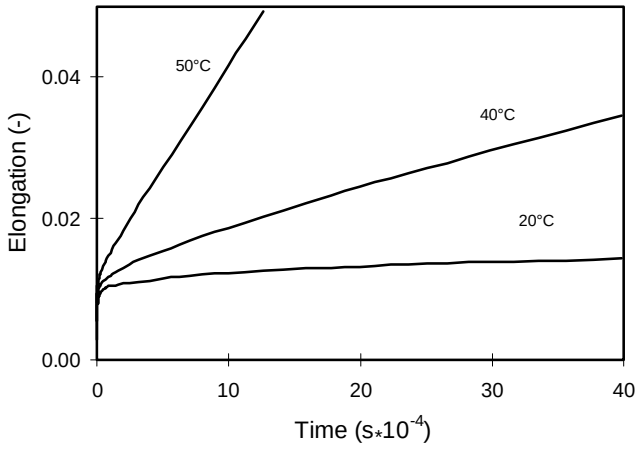

Figure 3.3 *Creep of a gel-spun PE fibre with a Young's modulus of 110 GPa at various temperatures, stress: 0.6 GPa [12].*

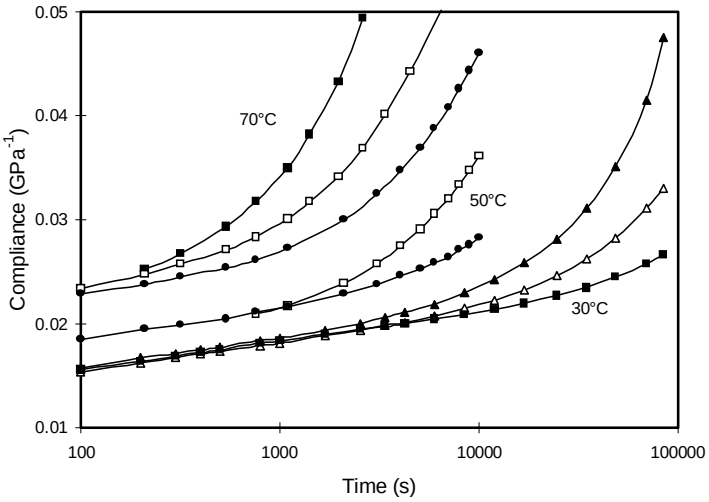

Figure 3.4 *Creep compliance of a Dyneema SK66 fibre at different temperatures and stresses (replotted from ref. 25). ●: 0.25 GPa, □: 0.4 GPa, ■: 0.5 GPa, ∆: 0.75 GPa, ▲: 1 GPa.*

Figure 3.4 shows the creep behaviour of a Dyneema SK66 fibre as a function of stress and temperature in a different way. In this figure the compliance ($E^{-1}= \varepsilon/\sigma$) is plotted vs. the logarithm of time.

In the first part, in fact region I of figure 3.1, the elongation varies linearly with the logarithm of time. Region II (secondary creep) is characterised by a constant creep rate, and appears in this logarithmic representation by an increasing slope of the graph at longer loading time.

Several more quantitative conclusions can be drawn from figure 3.4. The slope of the initial part of the graphs appears to be independent of the temperature. In this regime the compliance is also independent of the stress, i.e. the process is linear visco-elastic. At longer loading times, secondary creep becomes important. At long loading time the creep process is not linear visco-elastic anymore, as can be inferred from the diverging graphs.

Sherby and Dorn introduced a new method for analysing deformation data, by plotting the strain rate versus the strain [31]. Wilding and Ward showed that such a plot, which they called a Sherby and Dorn plot, is a valuable way for evaluating the creep behaviour at longer loading times [1,5].

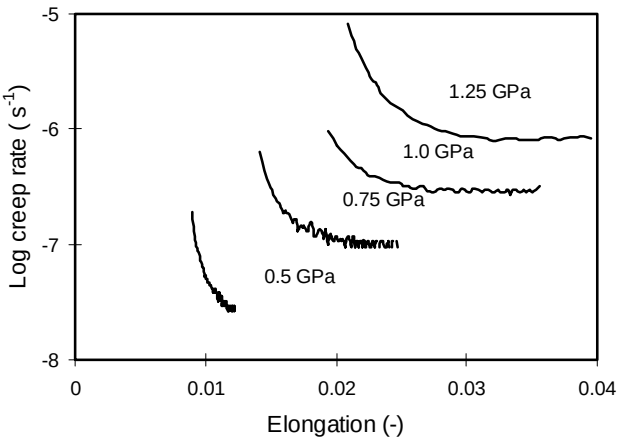

Figure 3.5 Sherby-Dorn plot for the creep data of figure 3.2, Dyneema SK66 fibre, reproduced from ref. 25

In figure 3.5, the data of figure 3.2 are replotted using a Sherby and Dorn plot. Figure 3.5 demonstrates that initially the creep rate is high, but decreases with increasing elongation, and levels off at an elongation of a few percent. At higher stresses the creep rate for the fibre attains a constant value, which is referred to as the plateau creep rate. At low stress, it takes a long time for the creep rate to become constant. For a load of 0.5 GPa the duration of the experiment (24 hours) was not sufficient for the creep rate to become constant.

Creep recovery experiments, wherein the elongation is measured after the load has been removed, show that part of the elongation is reversible [4,9,10,12]. Govaert et al [9] investigated the separation of the total elongation of a gel-spun polyethylene fibre in a reversible and an irreversible creep contribution quantitatively, the result is shown in figure 3.6.

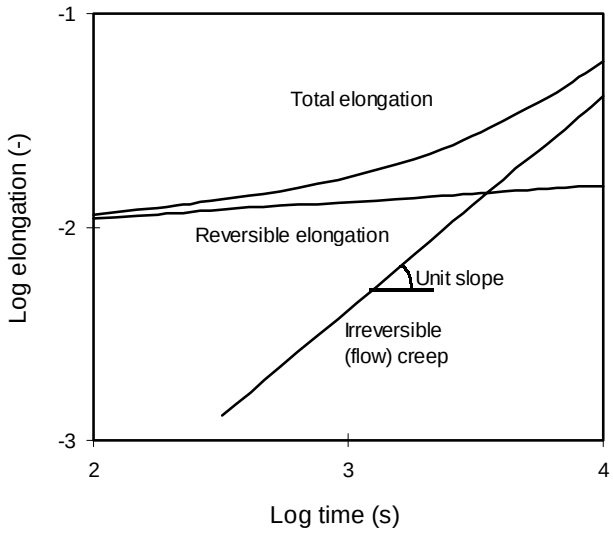

Figure 3.6 Reversible and irreversible contributions to the elongation of a fibre

In figure 3.6 the total strain is decomposed in two contributions, both well represented by a straight line on a double logarithmic scale. A straight line in such a plot demonstrates that the relation is given by a power law function (eq. 3.1);

$$\varepsilon(t) = ct^n \qquad 3.1$$

with the exponent n equal to the slope of the line.

The first contribution, with a small slope (approx. 0.07), represents the reversible creep; i.e. upon unloading the fibre this part of the elongation is completely reversed [9]. The second contribution is represented by a line with a slope unity, which shows that this part of the elongation increases proportional to the loading time. The elongation that remains after unloading the fibre, was shown to be identical to the latter contribution. The irreversible or flow creep is therefore proportional to the loading time and is characterised by a constant creep rate (the plateau creep rate in figure 3.5). The irreversible creep therefore behaves as a flow process; in this thesis it is therefore also referred to as the flow creep. The conclusions only apply when tertiary creep has not yet occurred.

The reversible and irreversible creep processes occur simultaneously. The definition of these is therefore different from that of primary creep and secondary creep, as mentioned in figure 3.1, that occur, by definition, sequentially.

It is however true that in region I (primary creep) reversible creep is the dominant contribution, and the irreversible creep is small. In region II (secondary creep) the situation is reversed, here the irreversible creep is the dominant contribution.

In conclusion:

- Polyethylene fibres exhibit creep that is strongly dependent on load and temperature.
- The elongation is the sum of a reversible and an irreversible contribution.
- The reversible creep process is to good approximation a linear visco-elastic process.
- The irreversible creep is a strongly non-linear process; because the flow creep rate is a non-linear function of the stress (except for very low stress).
- The irreversible elongation is determined by a single creep rate (the plateau creep rate), which is a function of the stress and of the temperature.

3.3 Mathematical description of the creep behaviour.

The mathematical description of the creep behaviour gives the effect of stress and temperature on the elongation for short and for long loading time, and takes into account the separation of the total elongation in a part that is reversible and one that is irreversible.

3.3.1 Stress-strain relations

The total creep elongation, ε_{tot}, is the sum of two contributions:

$$\varepsilon_{tot} = \varepsilon_{rev.} + \varepsilon_{irrev.} \qquad 3.2$$

wherein the reversible contribution, ε_{rev}, is well described by a linear visco-elastic process, and the irreversible creep, ε_{irrev}, is a non-linear visco-elastic process as shown above.

Linear visco-elastic material behaviour can be described fully by either a time dependent stress relaxation modulus, E(t), or a time dependent creep compliance, D(t) [32]. The stress relaxation modulus is defined by the stress response, $\varepsilon(t)$, to an elongation step: $\varepsilon(t) = 0$ for $t < 0$, and $\varepsilon(t) = \varepsilon_0$ for $t \geq 0$.

$$E(t) = \sigma(t) / \varepsilon_0 \qquad 3.3$$

The creep compliance, D(t), is defined as the elongation response, $\varepsilon(t)$, to a stress step (σ_0)

$$D(t) = \varepsilon(t) / \sigma_0 \text{ or } \varepsilon(t) = D(t).\sigma_0 \qquad 3.4$$

E(t) and D(t) are related, the reversible mechanical behaviour is fully characterised by one of them. For creep experiments, the description using the creep compliance is more appropriate because D(t) is proportional to the elongation.

The effect of the temperature is accounted for by the introduction of an effective time, $\psi(T(t))$, or for isothermal experiments by a variable a(T), that is a function of temperature only.

$$\varepsilon_{rev}(t) = D(\psi).\sigma_0 \qquad 3.5$$

Equation 3.5 holds for an arbitrary temperature history. Creep experiments are usually performed at constant temperature; and for such experiments equation 3.5 simplifies to:

$$\varepsilon_{rev}(t) = D(\frac{t}{a(T)}).\sigma_0 \qquad 3.6$$

The reversible elongation for an arbitrary stress history (isothermal experiment) is given by:

$$\varepsilon_{rev}(t) = \int_0^t D(\frac{t-\tau}{a(T)}).\dot{\sigma}(\tau)d\tau \qquad 3.7$$

The irreversible elongation is determined by the plateau creep rate, $\dot{\varepsilon}(\tau)$; for an isothermal and constant stress experiment:

$$\varepsilon_{irrev.}(t) = \int_0^t \dot{\varepsilon}_{pl}(\sigma(\tau),T)d\tau \qquad 3.8$$

The total, reversible plus irreversible, elongation for an arbitrary isothermal experiment then becomes:

$$\varepsilon(t) = \int_0^t \{D(\frac{t-\tau}{a(T)}).\dot{\sigma}(\tau) + \dot{\varepsilon}_{pl}(\sigma(\tau),T)\}d\tau \qquad 3.9$$

This model provides the framework for the description of the elongation and creep of polyethylene fibres used in this thesis. The creep behaviour of a fibre is thus described by the functions E(t) or D(t) and the plateau creep rate.
Experimental data allow to estimate these functions with a certain accuracy. In the following section it will be discussed which relations have been used for fitting the observed creep data.

3.3.1 Characteristic functions

Reversible creep

Compliance functions reported to give a good description for the creep behaviour of polyethylene fibres for a certain range of experimental conditions are power law functions [9-12]:

$$D(t) = D_0 (t / t_0)^n \qquad 3.10$$

and logarithmic functions [17]:

$$D(t) = D_0 + c.\log(t / t_0),\ t > t_0 \qquad 3.11$$

In equations 3.10 and 3.11, D_0 represents the integrated effect of relaxation times shorter than assessed experimentally.

Govaert et al. [9-12] described the reversible elongation behaviour of a commercial gel-spun fibre, over a wide range of experimental conditions, by a time dependent modulus:

$$E(t) = E_\infty + \int_{\tau_{min}}^{\tau_{max}} H(\tau) e^{\frac{-t}{\tau}} d\ln(\tau) \qquad 3.12$$

The limiting modulus E_∞ in equation 3. 12 represents the integrated effect of relaxation times larger than experimentally assessed. The relaxation time spectrum, H(t), and temperature shift factor, a(T), were determined using mechanical dynamic mechanical analysis. A broad relaxation time distribution was required to fit the data. Figure 3.7 gives the distribution obtained for Dyneema SK 66 fibre.

While the distribution $H(\tau)$ determined by Govaert describes the reversible deformation behaviour of a fibre to uni-axial loading over a wide range of experimental conditions, equations 3.10 and 3.11 fit the experimentally observed reversible creep in a certain, more limited, range of conditions.

Equations 3.10 and 3.11 imply certain relaxation time distributions. These distributions can be calculated [32] using the experimentally observed Young's modulus (100 GPa) and the exponent for power law creep (n = 0.062) or the coefficient (c) for logarithmic creep (2.510^{-12}/Pa/dec.):

$$\ln H(\tau) = -\frac{d\varepsilon(t)}{d\ln t}(t = \tau) \qquad 3.13$$

The resulting distributions are also plotted in figure 3.7.

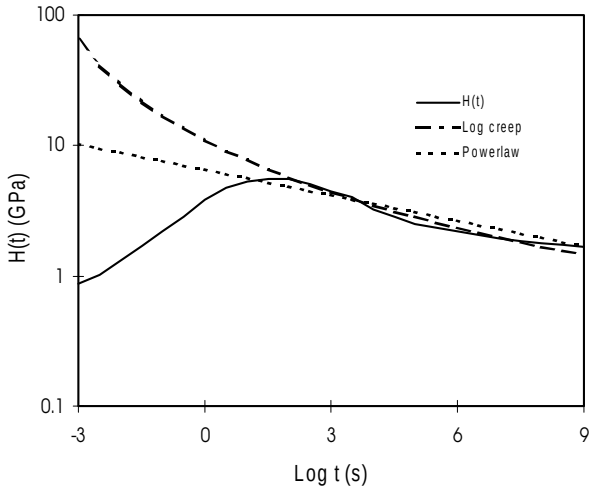

Figure 3.7 Relaxation-time spectrum for Dyneema SK 66 fibre, reference temperature 30°C [9]

The (calculated) relaxation time distributions, implied by equations 3.10 and 3.11, diverge at small loading time; the distributions are obviously in error for a loading time less than a few seconds. For relaxation times larger than 10 seconds both equation 3.10 (power law) and 3.11 (logarithmic function) give reasonably accurate results. For long loading time the distributions are comparable to the distribution determined by dynamic mechanical analysis.

Though both equations 3.10 and 3.11 give reasonable fits to creep data when data for very short loading times are not considered [3, 9-12], equation 3.11 fits the data over many decades [19, this thesis chapter 4]. In this thesis the reversible creep will be fit by equation 3.11, for convenience, it will be referred to as *logarithmic creep*.

Govaert showed that the temperature dependence of the reversible mechanical response upon uni-axial loading can be described reasonably well by an horizontal (time/temperature) shift factor a(T) only; a(T) being a temperature dependent multiplication factor for all relaxation times [12]. This implies that the coefficient (c) of the logarithmic creep does not depend on the temperature. The effect of the

temperature on the reversible elongation is fully accounted for by the iso-chronous compliance at a certain (small) reference time, see also figure 3.3.

Irreversible or flow creep

The irreversible creep elongation of a polyethylene fibre is proportional to the loading time; $\varepsilon(t) = \dot{\varepsilon}_{pl}.t$, Therefore not the elongation itself, but the elongation rate (the flow creep rate) has been modelled. The flow creep rate of many, amorphous and semi-crystalline, polymers is well described by thermally activated processes, over a wide range of experimental conditions [33]. Also the plateau creep rate of polyethylene fibres has almost universally been described by the concept of thermally activated processes [4,5].

If the flow creep rate of a fibre can be described by a single activated process, then the relation between the strain rate and the stress is given by:

$$\dot{\varepsilon}_{pl} = \dot{\varepsilon}_0 . e^{\frac{-U}{kT}} . \sinh\left(\frac{\sigma v}{kT}\right) = \dot{\varepsilon}_0 . e^{\frac{-U}{kT}} 0.5\{e^{\frac{+\sigma v}{kT}} - e^{\frac{-\sigma v}{kT}}\} \qquad 3.14$$

A thermally activated process is characterised by three parameters: the activation energy (U), the activation volume (v), and the pre-exponential rate factor ($\dot{\varepsilon}_0$). Equation 3.14 shows that the net strain rate is the sum of a positive rate contribution (forward flow) and a negative one (back flow). At zero stress both contributions are equal (and therefore the net strain rate is zero), at high stress the back flow is negligible.
Figure 3.8 gives a plot of the strain rate as a function of the stress for a single activated process (equation 3.14).

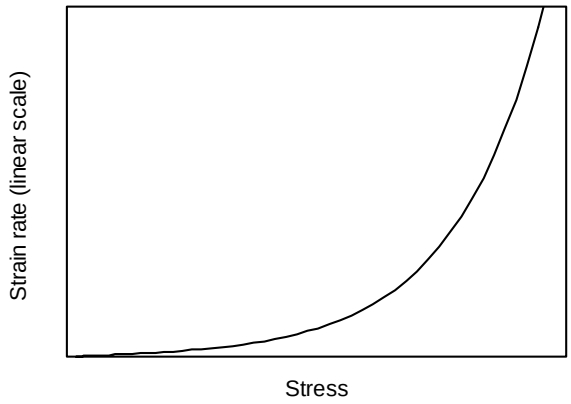

Figure 3.8 Strain rate as a function of stress for a single activated process

Figure 3.9 gives the same relation as figure 3.8, but on a semi-logarithmic plot.

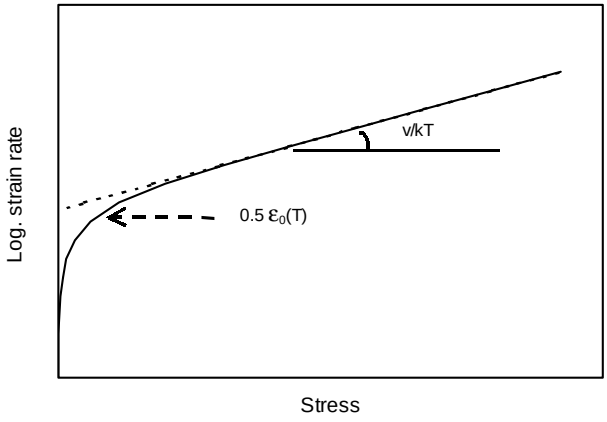

Figure 3.9 Strain rate as a function of stress for a single activated process, semi-logarithmic plot

At high stress, when the back flow can be neglected, the strain rate is an exponential function of the stress; viz. the graph of the logarithm of the strain rate versus stress is a straight line (see figure 3.9). The intercept of this line with the y-(strain rate) axis

is the value of the thermally induced forward, and backward, flow rate at zero stress The slope of the graph is v/kT; where v is the activation volume of the process.
The thermally induced flow rate is a function of the temperature, in the following a shorthand notation is used (eq. 3.15).

$$\dot{\varepsilon}_0(T) = \dot{\varepsilon}_0 . e^{\frac{U}{kT}} \qquad 3.15$$

For low stress ($\sigma v/kT<1$), equation 3.14 can be approximated by:

$$\dot{\varepsilon} = \dot{\varepsilon}_0(T) . \frac{v}{kT} . \sigma \qquad 3.16.$$

At low stress the strain rate is therefore proportional to the stress, in this regime the process behaves as a Newtonian fluid. The 'viscosity' is an Arrhenius function of the temperature. At higher stress, the slip becomes 'activated' by the stress.
Equation 3.16 can be rewritten such that it gives the stress in a thermally activated process as a function of the strain rate; the relation is given in equation 3.17.

$$\sigma = \frac{kT}{v} . \sinh^{-1}(\dot{\varepsilon} / \dot{\varepsilon}_0(T)) \qquad 3.17$$

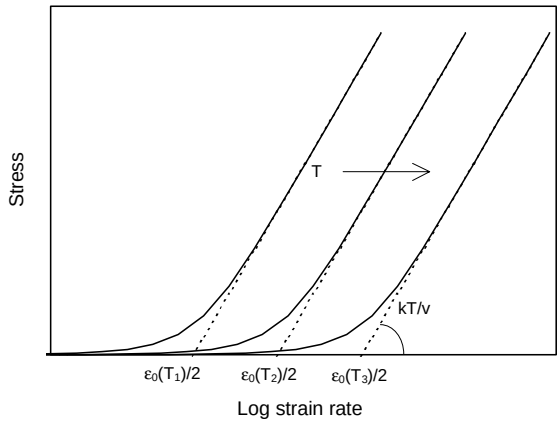

Figure 3.10 Stress a function of strain rate for a single activated process at different temperatures

In figure 3.10, the stress in a thermally activated process is plotted as function of the strain rate (viz. the same as figure 3.9 but with axes reversed) for three different temperatures.

For a deformation process, described by a single thermally activated process, there is a temperature dependent critical strain rate ($0.5\dot{\varepsilon}_0(T)$) indicating the linear–non linear transition, where the process becomes activated by the stress.

In practice the plateau creep rate of polyethylene fibres cannot be described over the range of accessible experimental conditions by a single thermally activated process.

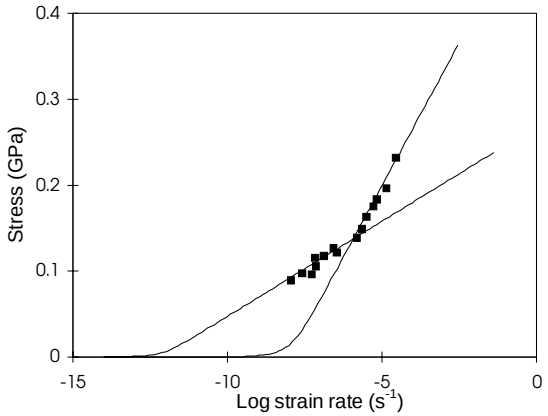

Figure 3.11 Stress as function of strain rate. Attempted fits by a single activated process. Data points from ref. 20.

Figure 3.11 shows creep rate data reported by Ward et al. [4] with attempted fits by a single activated process. A satisfying fit is only possible for part of the data.

Figure 3.12 shows that the data of figure 3.11 can be described satisfactorily by the sum of two activated processes. The contribution of the individual processes is also shown in figure 3.12.

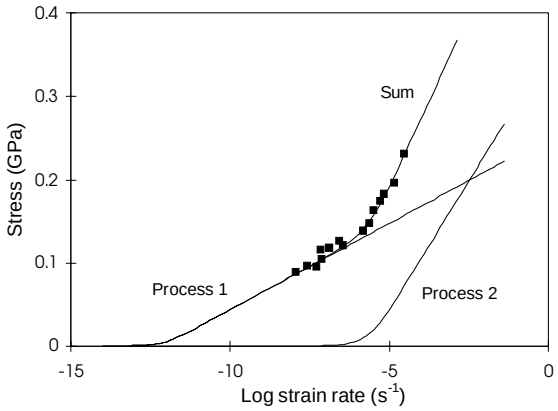

Figure 3.12 Stress as function of strain rate. Fit by two parallel processes. Data as for figure 3.11

Experimental data on the flow creep of melt- and gel-spun polyethylene fibres can in many cases be described by two activated processes acting in parallel [4,5]. Earlier this model had been shown to describe the yield stress versus strain rate behaviour of non-oriented high density polyethylene [34,35].

The stress on the fibre is shared by the two processes, each characterised by its own activation volume (slope), and (pre-exponential) rate constant. The first process dominates at low strain rate; at a higher strain rate both processes contribute to the total stress. In the example of figures 3.11 and 3.12 the contribution of the second process is negligible for strain rates up to 10^{-6} s^{-1}.

The stress is the sum of the stresses acting on each process, the relation between strain rate and stress is given by equation 3.18:

$$\sigma = \frac{kT}{v_1}\sinh^{-1}(\dot{\varepsilon}/\dot{\varepsilon}_{01}(T)) + \frac{kT}{v_2}\sinh^{-1}(\dot{\varepsilon}/\dot{\varepsilon}_{02}(T)) \qquad 3.18$$

$$\dot{\varepsilon}_{0i}(T) = \dot{\varepsilon}_{0i}\, e^{\frac{-U_i}{kT}} \qquad 3.19$$

where (i = 1,2).

At low strain rates, $<10^{-6}$ s^{-1}, the relative contribution of the second process is extremely small. At very low strain rates ($<10^{-12}$ s^{-1}) the stress carried by the second

process is 10^{-6} of that carried by the first process. The second process follows the overall elongation, without contributing significantly to the stress on the fibre.
At higher strain rate the contribution of the second process increases. When the strain rate is sufficiently high, the second process generally dominates the flow creep of polyethylene fibres. The second process will dominate at sufficiently high strain rates, if the activation volume of this process is smaller than that of the first process. In the example shown in figure 3.12, this is the case for strain rates larger than 10^{-2} s^{-1}.

Figure 3.12 suggests that there exists a critical strain rate for each process, below which the process does not carry any significant load. The semi-logarithmic plot is however misleading. At low strain rates the stress carried by each process increases proportional to the strain rate (but much faster for the first process).

As long as both processes are linear the first process dominates, and the relative contributions do not change. When $\sigma v/kT$ becomes of the order of unity the process becomes activated by the stress, the 'viscosity' of the process falls. For the first process this is the case already at a low strain rate, because the 'viscosity' of the process is high, and because the activation volume is large. From a certain strain rate the relative contribution of the first process begins to decrease. As the activation volume of the second process is smaller than that of the first process, the second process will become dominant at high strain rate.

The two flow processes are parallel, viz. the strain rate is the same for both processes, and the stress is the sum of the contributions of both processes. Schematically the model can be represented by figure 3. 13

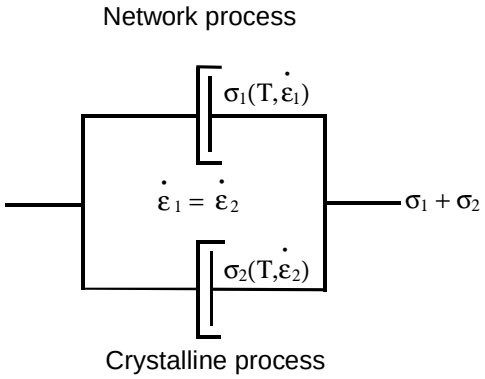

Figure 3.13 Two thermally activated process model for irreversible creep

Remark: whereas many experimental data show that at least two processes are required for describing the data, it cannot be excluded that more thermally activated processes are active. Due to experimental limitations the plateau creep rate cannot be determined for low stress (limit approximately 10^{-10} s^{-1}). It cannot be ruled out that at a lower stress further processes are active, or that a threshold stress exists below which the flow creep rate is zero as has been proposed [12,37]. At a higher strain rate a new process may become noticeable.

3.4 Molecular processes responsible for creep

In the previous sections, it was shown that the elongation is partly reversible and partly irreversible. First, the molecular interpretation of the irreversible creep will be discussed.

3.4.1 Irreversible creep

It is assumed that the flow creep is caused by chain slip, enabled by the diffusion of small, Reneker type, defects [2-5,11,25,36]. Here it is further assumed, that the resistance of the chains against slippage can be different for different chain segments. This is in line with Ward [2], who proposed two molecular flow processes, each described by a single activated process. The stress of the first process is carried by the entanglement network, and is therefore called the *network process*. This process is characterised by a small rate constant and a large activation volume.

The second process is attributed to slip of crystalline chains, and is called the *crystalline process*. The structural model is the crystalline bridge model as proposed by Gibson et al. [37,38], for accommodating the network process an amorphous entanglement network is added [1]. This process has a small rate factor and a small activation volume.

Usually the following physical interpretation is given to the parameters of the activated processes. The activation energy is the energy that has to be overcome in the slip process considered. The rate constant is proportional to the number of slip sites available. Finally the activation volume is related to the size of the volume surrounding a slip site from which stored elastic energy can be dissipated in the slip process [36].

Creep data that have been analysed using the model of two parallel activated processes, show that the parameters of the process depend systematically on draw ratio [39], molecular weight [4], branching [19,40,41], and crosslinking [16,18,20]; more details are given in a following chapter. Such results can be understood more easily with the interpretation of the physical parameters of activated processes given below.

The flow creep process observed macroscopically is the combined effect of a large number of slip processes on a molecular scale. It will be assumed, that also on the molecular scale the processes are parallel. The stress carried by a process is the sum of the stresses acting on the chain segments contributing to the process. The reason that two processes are being observed, is that there exist two populations of chain segments, that have a different resistance against slip. Figure 3.14 shows a schematic picture of this model.

Chain slip through the crystalline phase is enabled by the diffusion of defects. Boyd suggested a short twist (~12 CH_2 units) as the most likely mechanism [42]. The bold lines represent chain segments with a large resistance against slip (the first or network process), the thin lines chain segments with a lower resistance (the second or crystalline process).

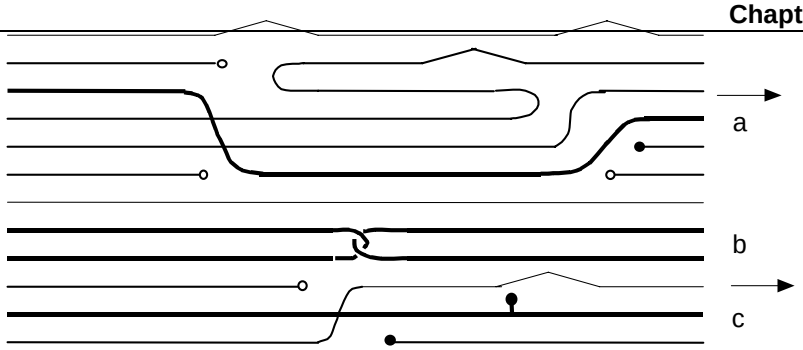

Figure 3.14 Molecular structure with chains with different slip resistance.a: chain with register switches, b: entangled chains, c: chain with a side group twist region (Boyd/Reneker) in chain, ○: chain leaving plane of drawing, ●: chain end, —● : sidegroup

Several candidate mechanisms, that cause a high slip resistance of a chain segment are shown, chain segments that change register (a), entangled chains (b), or chain segments with a side group (c). Chain segments of the second process are crystalline chain segments with a typical extended segment length. Such segments terminate in a fold, in a lax non-crystalline segment (loop), or in a chain end. The typical length of an extended crystalline chain segment is much smaller (tens of nanometers) than that of a molecule (several microns), implying that the number of chain ends is small compared to the number of segments, and depending on the draw ratio also with the number of loops and folds.

Summarising: (i) chain segments with a high slip resistance contribute to the first, or network, process, (ii) chain segments with an average resistance are responsible for the second process, (iii) the elementary (molecular) slip events are also thermally and stress activated processes.

Only part of the chains contribute to the first (and second) process. Let f be the fraction of the cross-section occupied by chains contributing to one of the activated processes, then of course, f is proportional to the number of contributing chains per unit area. The stress on an elementary process is then intensified by a factor $\beta = 1/f$.

β is different for the two types of chains. The parameters of an elementary process are U_e, $\dot{\varepsilon}_{0e}$, and v_e respectively.

Equations 3.13 and 3.15 transform to:

$$\dot{\varepsilon} = \dot{\varepsilon}_{0e} . e^{\frac{-U}{kT}} . \sinh\left(\frac{\beta\sigma v_e}{kT}\right) \qquad 3.20$$

and

$$\sigma_e = \beta\sigma = \frac{kT}{v_e} . \sinh^{-1}\left(\dot{\varepsilon} / \dot{\varepsilon}_{0e}(T)\right) \qquad 3.21$$

In equation 3.19 and 3. 20 the parameters of an elementary process, U_e, $\dot{\varepsilon}_{0e}$, and v_e have the same meaning as for the macroscopically observed process.

The activation energy (U_e) is the energy barrier that has to be overcome in an elementary slip process. The activation energy furthermore determines the fraction of the processes that are activated at any time (at room temperature and zero stress, this fraction is very small, $\approx 10^{-20}$).

The relation between the parameters of an elementary process and those of the macroscopically observed process is:

$$U = U_e,\ \dot{\varepsilon}_{0e} = \dot{\varepsilon}_0 / \beta \text{, and } v = \beta v_e \qquad 3.22$$

As f is (much) smaller than 1, therefore β is (much) larger than 1, the rate constant for an elementary process is larger than that for the macroscopic process, the activation volume is smaller.

The most important difference between the elementary processes is the average spontaneous diffusion rate (at a certain temperature) of a typical chain segment involved in the process.

The sum of the fractions, f_1 and f_2, of chains contributing to the two observed processes may well be (and in most cases is) smaller that 1, implying that also chains are present that do not contribute to the stress of any of the two processes.

The observed change in the activation volume of the macroscopically observed activated processes (for instance the effect of drawing) can be understood by

change of the fraction f (or the factor β) only. The elementary processes are invariant, they are characterised by constant activation energy U and volume v (it will be shown in chapter 4, that this holds for the effect of drawing).

The behaviour of activated processes can be understood as resulting from the thermally activated chain mobility. In polyethylene the mobility of even crystalline chains is high, as is demonstrated by solid state ^{13}C NMR [43,44], chain segments move forward and back, and enter and leave the crystalline and amorphous phase. In absence of an external load the net deformation rate is zero, as there is no preferred direction of the movement of the individual chains. The presence of a stress causes the forward flow processes to be favoured and the back flow processes to be suppressed, and thus results in net chain movement.

The analysis given above explains two important aspects, in a different way than usually is done.
The first aspect: the differences in the rate factor of a macroscopically observed activated process for different fibres are mainly caused by differences in the temperature activated diffusion rate (at zero load) of the chain segments involved, and not (only) by differences in the number of possible slip sites.
The second aspect: the macroscopically observed activation volume of a process is inversely proportional to the number of chains that contribute to that process. Variations in the, macroscopically observed, activation volume of a process are caused by variations in the number of contributing chains, whereas the activation volume of the elementary processes is constant. As the network and crystalline processes are different, it is likely that the activation volumes (as well as the activation energies) are different.

The interpretation given above implies that the ‘network’ contribution to the stress is carried by a small fraction of highly loaded chains that resist slip more strongly than the average chain does. At low strain rate, typical crystalline chain segments can slip freely through the crystalline phase, without contributing to the load on the fibre. At high strain rate, the contribution of the crystalline segments to the load becomes dominant, because of their larger number.

3.4.2 Reversible creep

The reversible creep of (gel-spun) polyethylene fibres is a linear visco-elastic process, characterised by deformation processes that require a wide distribution of relaxation times.

A few studies have been devoted to the physical origin of the reversible creep in ultra-drawn polyethylene fibres. Govaert and Lemstra [10,12] attribute the (delayed) reversible creep to the tensioning and retraction of (non-crystalline) chain segments that are out of register. The reversibility is a consequence of the fact that chains cannot cross, and that the segments will remain out of register whatever the deformation is. Figure 3.15 (reproduced from ref. 26) demonstrates the basic idea.

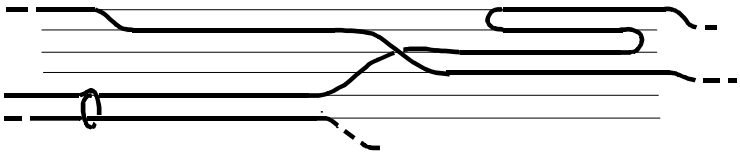

Figure 3.15 Structure of PE fibres with chain segments that are out of register for explaining the reversible creep of a polyethylene fibre redrawn from ref. 26

The explanation of the reversible creep behaviour of highly drawn polyethylene fibres, reported by Govaert and Lemstra, is based on three major assumptions

- Reversible deformation is not compatible with defect diffusion within crystals.
- The reversible deformation is due to tensioning and retraction ("entropic contribution") of non-crystalline chain segments.
- The non-removable, non-crystalline chain segments are exclusively identified with out-of-register chain segments.

It should be noted, however, that the arguments mentioned above do not take into account the large mobility of polyethylene chain segments in the crystalline phase as demonstrated by:

- Chain diffusion through the crystalline phase, a spontaneous, thermally activated, process with no directional bias [42-45]. Schmidt-Rohr and Spiess [43,44] inferred, from 2-dimensional solid state ^{13}C-NMR, jump rates from 30 s^{-1} at 45°C to

10^4 s^{-1} at 100°C in non-oriented linear polyethylene, and predict a jump rate of chain segments in the order of 1 s^{-1} at room temperature.

- Annealing (at temperatures of 100°C-140°C) results in increased primary (mostly reversible) creep (this thesis chapter 7). It is assumed that this is caused by the increased relaxation of typical non-crystalline chains
- At room temperature, a slow annealing process can occur in highly crystalline polyethylene fibres. Kudasheva et al. [46] reported a decrease of the E-Modulus of polyethylene fibres (produced by orientational crystallisation and drawing) by 40% after one year storage. This long time scale indicates that chain diffusion in crystalline areas is involved.

Thermally activated diffusion of chain segments in the crystalline phase is, at least in polyethylene, a well-established process that occurs spontaneously. Chain diffusion should be taken into account to understand reversible creep. The extend of the reversible creep depends on how far the non-crystalline segments can be tautened and will relax due to entropic effects. Any non-crystalline chain segment is subjected to entropic effects.

Figure 3.16 shows the essential aspects of the process of diffusion of crystalline chain segments related to reversible creep.

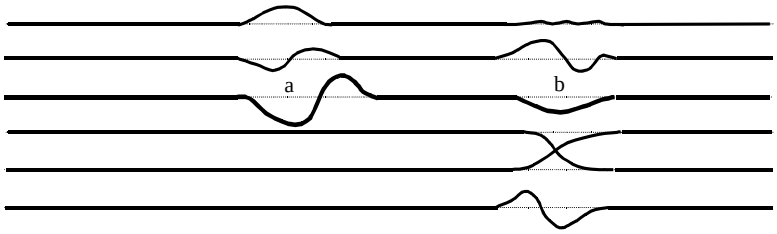

Figure 3.16 Effect of chain diffusion on non-crystalline chain segments, a and b are non-crystalline segments of a single polymer chain.

Upon loading a fibre, the non-crystalline segments are tautened. Initially, non-crystalline chain segments in nearby chains will have a certain length distribution. Some of the segments will be taut sooner after the application of the load than other segments. This results in stress differences between neighbouring non-crystalline segments of a single chain. Due to the high chain mobility a stress difference cannot

persist between such segments of a single chain. Chain diffusion will change the length distribution of the non-crystalline segments along the fibre direction, and the stresses will be equalised. In figure 3.16, a chain with two adjacent non-crystalline segments of a single chain, a and b, is indicated, segment b will become taut before segment a will do. Chain diffusion will make segment a shorter and segment b longer, in order to make the stress in both approximately equal. This process is repeated many times, and will change the length distribution of the non-crystalline chains. Upon unloading, the length distribution returns to its original statistical equilibrium value for, again, entropic reasons.

For the analysis given above, it is not required that the chains are in constant register. In the presence of register switches along the chain, the same mechanism occurs.

In the beginning of the chapter it was shown that the total elongation can be separated in a reversible and an irreversible contribution. The analysis presented above assumes a close relation between the reversible and irreversible elongation processes. Both reversible and irreversible creep processes require slip of chain segments through the crystalline phase. Slip (or diffusion) of a chain segment through the crystalline phase as such does therefore not necessarily imply that the process is irreversible. Slip of a complete chain is obviously an irreversible process.

The description of the molecular processes involved in the (reversible) deformation process, is in line with the generally accepted mechanism of the mechanical relaxation processes, especially the α-relaxation in semi-crystalline polymers, as reviewed by Boyd [42,45]. The α-relaxation in polyethylene requires the presence of both a non-crystalline phase and a crystalline phase, and the possibility for chains to move from the one phase to the other. The rate of chain diffusion, is a function of the length of the crystalline chain segment [45]. It is therefore inferred that the creep resistance increases with length of a typical crystalline chain segment.

3.5 Conclusions

The creep behaviour of melt-spun and solution (gel)-spun polyethylene fibres is qualitatively the same, and can be described by the same model.

The total creep can be separated in a linear visco-elastic and *reversible* contribution, and a non-linear, thermally and stress-activated *irreversible* part.

The reversible creep is in good approximation proportional to log time. The reversible deformation is due to tautening and recoiling of non-crystalline chain segments. Tautening and recoiling require slip of chain segments through the crystalline phase.

The irreversible elongation is proportional to the loading time and can be described well by two parallel thermally activated Eyring processes, related to respectively a crystalline and a network process.

On a molecular scale, the two processes are related to two populations of chains with a different flow resistance. The chain segments contributing to the network process possess a high flow resistance related to their entangled, non-register or branched nature. At low loads, and consequently low strain rates, the crystalline process does not contribute to the load, because of the high, thermally activated mobility, of crystalline chain segments.

Each process involves only a fraction (β) of the chains crossing a section of the fibre; the ratio between the macroscopically observed activation volume and pre-exponential rate constant depend on the fraction β.

3.6 References

1 M.A. Wilding and I.M. Ward, Polymer, **19**, (1978), 969-976

2 M.A. Wilding and I.M. Ward, Polymer, **22**, (1981), 870

3 M.A. Wilding and I.M. Ward, Plastics and Rubber Proc. and Appl., **1**, (1981), 167

4 I.M. Ward and M.A. Wilding, J. Polym. Sci., Polym. Phys., **22**, (1984), 561

5 I. M. Ward, Polym. Eng. Sci., 24, **10**, (1984), 724

6 I.M. Ward, Progress Coll. Polym. Sci., **92**, (1993), 103

7 I.M. Ward, Macromol. Symp., **98**, (1995), 1029

8 Y. Termonia, P. Meakin, P. Smith, Macromol., **18**, (1985), 2246

9 L.E. Govaert , C.W.M. Bastiaansen, P.J.R. Leblans. Polymer, **34**, 3, (1993), 534

10 L.E. Govaert and P.J. Lemstra, Coll. Polym. Sci., **270**, (1992), 455

11 P.J.R. Leblans, C.W.M. Bastiaansen, L.E. Govaert, J. Polym. Sci., B, Polym. **27**, (1989), 1009

12 L.E Govaert, PH-D Thesis Eindhoven University of Technology, (1990), chapters 2-4

13 B. Dessain, O. Moulart, R. Keunings and A.R. Bunsell, J. Mater. Sci., **27**, (1992), 4515

14 M.J.N. Jacobs, M. Segers, DSM Internal report (1995)

15 N.N. Peschanskaya, P.N Yakushev, L.P. Myasnikova, V.A. Marikhin, A.B. Sinani, M. Jacobs, Solid State Phys., **38**, 8, (1996), 2582

16 D.W. Woods, W.K. Busfield, I.M. Ward, Polym. Comm. **25**, (1984), 298

17 D.W. Woods, W.K. Busfield, Plastics Rubber, Proc. Appl., **5**, (1985), 157

18 P.G. Klein, N.H. Ladizeski, I.M. Ward, J. Polym. Sci., B, Polym. Phys., **24**, (1986), 1093

19 P.G. Klein, D.W. Woods, I.M Ward, J. Polym. Sci., B, Polym Phys., **25**, (1987), 1359

20 D.W. Woods, W.K. Busfield, I.M. Ward, Plastics and Rubber Proc. Appl., **9**, (1988), 155

21 J. Rasburn, P.G. Klein, and I.M. Ward, J. Polym. Sci., B, Polym Phys., **32**, (1994), 1329

22 P.G. Klein, J.A. Gonzalez-Orozco, I.M. Ward, Polymer, **35**, 10, (1994), 2044

23 Y.M.T. Engelen C.W.M. Bastiaansen, P.J. Lemstra, Polymer, **35**, 4, (1994), 729

24 H. van der Werff, PH-D Thesis, University of Groningen, (1991), 31

25 D.J. Dijkstra and A.J. Pennings, Polymer Bulletin, **19**, (1988), 73

26 J.P. Penning, H.E. Pras, A.J. Pennings, Colloid Polym. Sci., **272**, (1994), 664

27 J.P. Penning, Thesis University of Groningen, (1988), chapter 6

28 R. Hikmet, P.J. Lemstra, A. Keller, Coll. Polym. Sci., **265**, (1987), 185

29 Y.L. Chen, B. Rånby, Polym. Adv. Technology., **1**, (1990), 103

30 W. R. Cannon, T.G. Langdon, J. Mater. Sci., **18**, (1983), 1

31 O.D. Sherby, and J.E. Dorn, J. Mech. Phys. Solids, **6**, (1958), 146

32 J.D. Ferry Visco-elastic properties of polymers, John Wiley and Sons, New York (1980)

33 A.S. Kraus, H. Eyring, Deformation kinetics, J. Wiley an Sons, New York (1975)

34 J.A. Roetling, Polymer, **6**, (1965), 311

35 C. Bauwens-Crouwet, et al, J. Polym. Sci., **2**, 7, (1969), 735

36 D.C. Prevorsek, Synthetic fibre materials, Part 2, High Performance Fibres ,Ed. H. Brady, Series: Polymer Science Technology. Chapter 10, (1994), 263

37 A.G. Gibson, G.R. Davies, I.M. Ward, Polymer, **19**, (1978), 683

38 A.G. Gibson, G.R. Davies, I.M. Ward, Polym. Eng. Sci., **20**,14, (1980), 941

39 W. Hoogsteen, R.J. van Hooft, A.R. Postema, A.J. Pennings, J. Mater. Sci., **23**, (1988), 3459

40 Y. Ohta, H. Yasuda, A. Kaji, Polym. Pre-prints Japan, **43** ,9, (1994), 3143

41 Y. Ohta, Y. Sugiyama, H. Yasuda, J. Polym. Phys. B, Polym. Phys., **32**, (1994), 261

42 R.H. Boyd, Polymer, **26**, (1985), 1123

43 K. Schmidt-Rohr, H.W. Spiess, Macromol., **24**, (1991), 5288

44 K. Schmidt-Rohr, H.W. Spiess, Multidimensional solid state NMR and Polymers, Academic Press, (1994), 271

45 R.H. Boyd, Polymer, **26**, (1985), 323

46 V.V. Kudasheva, G.K. Elyashevich., Conference orientational effects in polymers, Prague (1998)

Chapter 4 Influence of the molecular weight and the draw ratio on the creep properties of polyethylene fibres

4.1 Introduction

In chapter 3 a framework was presented for describing the creep of highly oriented polyethylene fibres. In the present chapter this framework will be used to analyse the creep behaviour of melt-spun and gel-spun polyethylene fibres and the influence of important process and feedstock parameters.

The creep characteristics of polyethylene fibres depend on a large number of variables, notably the draw ratio [1], the molecular weight distribution of the polymer, [2,3], the drawing temperature [4,5] and drawing conditions [6]. Drawing and (flow) creep are thought to be essentially the same processes, albeit at a different temperature and time scale; “easy draw, easy creep” [7]. It can, therefore, be expected that the parameters which determine the drawability also influence the creep behaviour. For gel-spun fibres additional parameters are the polymer concentration during spinning [4,8,9] and the type of solvent [10].

In this chapter the effect of the molecular weight, the draw ratio, and the polymer concentration of the solution will be considered. The drawing and creep behaviour can also be influenced by modification of the polymer or the fibre such as: branching and crosslinking. The effect of such modifications will be considered in chapter 5.

In the first part of this chapter the literature data on the flow creep of highly drawn, melt-spun as well as gel-spun, polyethylene fibres will be analysed. In the second part the influence of the draw ratio on the creep properties of gel-spun fibres will be reported. In the third part, an analysis will be presented on the possibilities for improving the creep of gel-spun fibres using variations of the main parameters.
Both the creep of gel-spun polyethylene fibres and that of highly drawn melt-spun polyethylene fibres is evaluated. A good database is available for melt-spun fibres; such fibres were studied in detail by Ward et al. [1,10-22], while for gel-spun fibres relatively few data are available [8,23-36].

4.2 Literature data on creep

4.2.1 Melt-spun polyethylene fibres

The creep deformation of (melt-spun) polyethylene fibres is partially reversible and partially irreversible, however mostly only the more important irreversible deformation has been studied in detail. The first part is therefore limited to the irreversible or flow creep.

Ward et al. [1,14,15,17,20,22] analysed their irreversible creep, or flow creep, data of melt-spun fibres by the two-process model as presented in chapter 3. Each of these processes is characterised by three parameters: the activation energy, a rate constant, and an activation volume.
The activation energy for the high stress (crystalline) process is approximately 30 kcal/mol (126 kJ/mol) [1,14,20,22]. This activation energy does not seem to depend on the molecular weight or on process variables such as the draw ratio. For polyethylene containing small side branches the activation energy of the crystalline process is higher and increases with the number of branches [31]. Also the activation energy for the low stress, or network, process is high: Klein et al. [20] reported a value of 43 kcal/mol (180 kJ/mol). The higher activation energy for the crystalline process in branched polyethylene and for the network process suggests a higher slip resistance of the molecular chains involved. It will be assumed that the activation energy for the crystalline process (in linear polyethylene) is 30 kcal/mol (126 kJ/mol) and for the network process 43 kcal/mol (180 kJ/mol).

Typical data of Wilding and Ward on the influence of the draw ratio on the flow creep of melt-spun fibres are presented in figure 4.1 [1].
The creep rate as a function for stress is well described by two thermally activated processes. The change in slope for the three graphs is at approximately the same creep rate (2.10^{-6}/s), indicated in figure 4.1 by a dotted line. This implies that the second process starts to contribute to the stress at that strain rate.

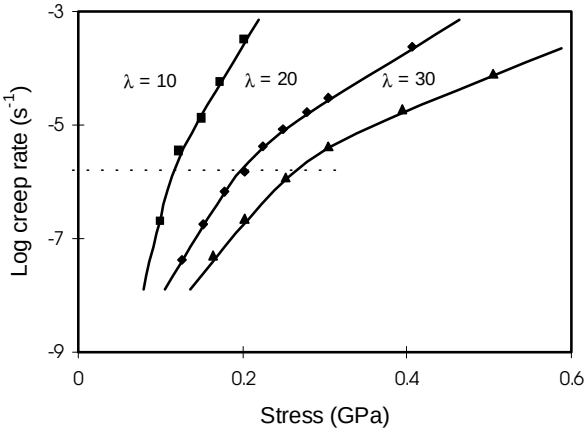

Figure 4.1 Flow creep for melt-spun fibres of different draw ratio [1]

The slope of the graphs of log creep rate vs. stress decreases with increasing draw ratio over the full stress range, implying that the activation volumes of both processes decrease with increasing draw ratio (see table 4.1).

Wilding and Ward also reported on the influence of the molecular weight of melt-spun fibres (λ =15), in figure 4.2 a selection of their data is replotted.

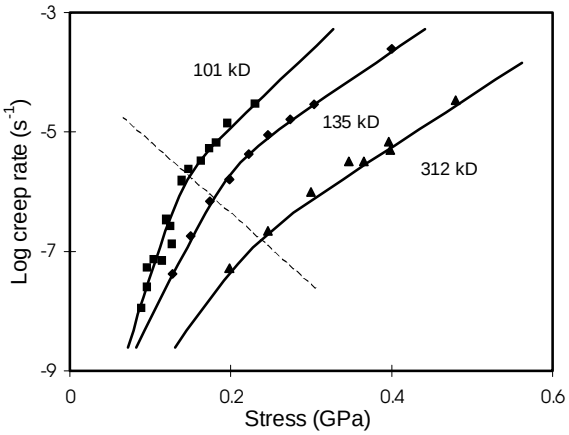

Figure 4.2 Flow creep for melt-spun fibres of different molecular weight. [1]

With increasing M_w the strain rate at which the second process starts to contribute seems to shift to lower strain rate. Furthermore the slope of the first part increases more strongly with molecular weight than that of the second part.

The data presented above have been analysed using the two-process model. The fit parameters of the data of figures 4.1 and 4.2 are given in table 4.1. Table 4.1 gives also data on the creep of a commercially melt-spun fibre (Technora).

Wilding and Ward [1] fitted mostly data with a constant v_1. However as can be seen in figures 4.1 and 4.2, a constant activation volume does not describe well the effect of draw ratio for the data shown. For this reason the data have been fitted with 4 parameters, for each process an activation volume ,v_1 and v_2, and a temperature dependent rate constant, $[\dot{\varepsilon}(T)_0]_1$ and $[\dot{\varepsilon}\ (T)_0]_2$. The parameters for the second, crystalline process are well constrained. This is less so for the first process. Conclusions on the parameters of the first process are therefore less solid than that of the second.

Table 4. 1 Two-process parameters for creep of melt-spun fibres of different draw ratio and different molecular weight.

Fibre	**M_w*10^{-3}**	**E**	**v_1**	**$[\dot{\varepsilon}(T)_0]_1$**	**v_2**	**$[\dot{\varepsilon}\ (T)_0]_2$**	**Ref.**
	D	GPa	nm^3	s^{-1}	nm^3	s^{-1}	
BP 006-60, λ=10	135	7	0.58	3.0x10^{-13}	0.370	4x10^{-6}	13
BP 006-60, λ=20	135	18	0.23	6.0x10^{-11}	0.130	7x10^{-6}	13
BP 006-60, λ=30	135	45	0.17	8.0x10^{-11}	0.080	6x10^{-6}	13
Technora, λ=30	61	-	0.33	7.2x10^{-11}	0.031	9.4x10^{-5}	19
Rigidex 50, λ=20	101	20	0.50	1.5x10^{-13}	0.150	3.0x10^{-6}	13
BP 006-60, λ=20	135	18	0.37	2.4x10^{-13}	0.123	1.5x10^{-6}	13
BP H020-54, λ=20	312	33	0.26	1.1x10^{-13}	0.106	3.1x10^{-7}	13

The data in table 4.1 show that the activation volume decreases with increasing draw ratio. In contrast, the rate factor for both processes does depend little on drawing. An exception is the rate factor of the first (network) process for the fibre with $\lambda = 10$. The difference is however not significant, the data are compatible with constant rate parameters. The change in creep of melt-spun fibres as function of draw ratio can therefore be described by a change in the activation volumes only.

With increasing molecular weight the rate factor decreases, most significantly for that of the second process. The effect of M_w on the activation volumes is relatively small, and may even be absent. The lower activation volumes observed for the fibre with M_w = 312 kD can be explained by its higher modulus (implying more efficient drawing).

4.2.2 Gel-spun fibres

Few systematic studies were performed on the creep of gel-spun fibres of different quality. Govaert reported on the creep of a commercial fibre (Dyneema SK66) [23-26]. Peijs et al [27] compared these data with those for Dyneema SK60 and Spectra 1000 fibres (figure 4.3).

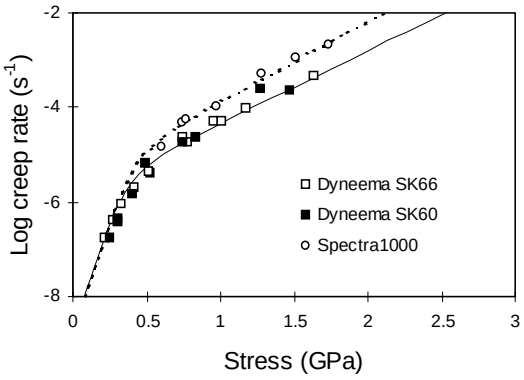

Figure 4.3 Two-process fit for flow creep of gel-spun Dyneema and Spectra fibres, temperature 70°C [ref. 26]

The data were described using a single, modified, activated process, with an activation energy of about 30 kcal/mol, and a power law stress dependence. The data have been reanalysed using the two-process model; see figure 4.3.
Further two-process data on the flow creep of gel-spun fibres were reported by Ward and Wilding [15], for a Hostalen Gur fibre produced by Pennings, by Prevorsek on a Spectra fibre produced by Allied Signal [28], and by Dijkstra [30] and Penning [31] on a fibre produced from a Hifax 1900 polymer.

The available two process parameters are given in table 4.2. The rate factors reported by Peijs [26] for 70°C are recalculated to room temperature using activation energies of 43 kcal/mol and of 30 kcal/mol for the network and crystalline process respectively. The activation volumes are small and rate constants are low in comparison with that of melt-spun fibres, implying that the creep rate of gel-spun fibres is much smaller than that of melt-spun fibres.

Table 4. 2 Two-process data for creep of gel-spun PE fibres

Fibre	M_w*10^{-3}	**E**	v_1	$[\dot{\varepsilon}(T)_0]_1$	v_2	$[\dot{\varepsilon}(T)_0]_2$	**Ref.**
	D	GPa	nm^3	1/s	nm^3	1/s	
Host. Gur*	3.500	35	0.31	$1.5x10^{-10}$	0.015	$1.0x10^{-7}$	14
Spectra (Allied	2.220	-	0.25	$7.2x10^{-15}$	0.010	$1.8X10^{-9}$	26
Dyneema SK60	2500	100	0.10	$8.4x10^{-14}$	0.020	$5.3x10^{-9}$	25a
Dyneema SK66	2500	100	0.10	$8.4x10^{-14}$	0.020	$5.3x10^{-9}$	25a
Spectra 1000	-	100	0.10	$8.4x10^{-14}$	0.023	$1.3x10^{-8}$	25a
Hifax 1900	4000	140	0.03	$3.4x10^{-10}$	0.015	$3.0x10^{-6}$	29

The results of Ward et al. [15] on a Hostalen Gur fibre, and that of Penning et al. [32] on a Hifax 1900 fibre are at variance with the general trend. For the data of the Hifax 1900, this is due to a different assignment of the activated processes, see annexe 4.1. The model parameters for the creep of the Hostalen Gur fibre seem to be a mix

of those for melt-spun and for gel-spun fibres, notably high rate factors (as for melt-spun fibres), and small activation volumes (as for solution spin fibres). The modulus of the Hostalen Gur fibre was relatively low, 35 GPa. Ward already noted the very small contribution of the network for this fibre and the small activation volume for the crystalline process. Table 4.2 shows furthermore that the rate factors are high as for a melt-spun fibre of a much lower molecular weight. The results suggest that the creep rate is not determined by the full chain length but only by part of it. Such could be the case if many chain folds are present. The chain extension is relatively low for this fibre. This is consistent with the relatively low modulus of the fibre. The small activation volume however is typical for that of a high modulus fibre. It implies that the load is shared by many chains, suggesting a very regular structure. The low network contribution can be the result of the processing conditions for instance a low polymer concentration, details are however not available.

4.2.3 Summary literature creep data melt-spun and gel-spun fibres

While the creep of melt-spun and gel-spun fibres is qualitatively the same, there are quantitative differences in the flow creep of melt-spun and gel-spun fibres. The rate of irreversible creep of gel-spun fibres is significantly lower than that of melt-spun fibres, when measured at the same temperature and stress level. Comparing the results of melt-spun and gel-spun fibres, i.e. figures 4.1, 4.2, with figure 4.3 and the table 4.1 with 4.2, important differences can be identified: the creep of gel-spun fibres is characterised by smaller activation volumes and smaller rate constants for both processes.

For melt-spun fibres the stress sensitivity (activation volume) of both processes decreases with increasing draw ratio (modulus). For gel-spun fibres, that have a still higher modulus, the activation volume at least for the crystalline process, is indeed very small, in line with the trend seen for melt-spun fibres. The results from the analysis are summarised in table 4.3

Table 4.3 Summary influence of λ and M_w on the parameters of the two process creep model, ↓: decreases, ≈: no large change, if any, =: no change

	v_1	$\dot{\varepsilon}_{01}$	U_1	v_2	$\dot{\varepsilon}_{02}$	U_2
$\lambda \uparrow$	↓	-	≈	↓	=	=
$M_w \uparrow$	≈	↓	≈	≈	↓	=

The combined data suggest that the parameters, that describe the flow creep of melt-spun as well as that of gel-spun fibres follow the same trends. The range of the variables covered by the data, is however very small for the gel-spun fibres. More data on the creep properties of gel-spun fibres are required for drawing more solid conclusions.

4.3 Creep of gel-spun UHMW-PE fibres as a function of draw ratio

4.3.1 Experimental

Fibres

A precursor fibre was obtained by spinning UHMW-PE (Stamylan UH of DSM, $M_w \approx 2.5 \times 10^6$) from a solution in Decalin and drying this fibre. From this precursor fibre, fibres of different draw ratio (modulus) were produced. The fibres were multifilament yarns, each consisting of about 100 filaments.

Tensile properties

The tensile properties were determined using a Zwick 1474 universal tester, with pneumatic fibre grips (Orientec). The specimen length was 300 mm, the test speed 150 mm/min. The fibre cross-section was determined from the weight of a unit length of fibre assuming a density of 970 kg/m^3.

Creep

The creep properties were determined using a temperature controlled dead load creep rig. An optical displacement gauge with a resolution of 30 micron and a range of 100 mm was used for measuring the elongation of the fibre. The load was applied by a computer-controlled table, allowing loading without overshoot within a few

tenths of a second. The free sample length was 500 ± 2 mm. Creep experiments were done at constant temperature (40±1^{0}C) and various loads; between 0.2 and 1 GPa; or at a constant stress 0.6 GPa and at temperatures of 20°C, 40°C and 70°C.

4.3.2 Results

Short term mechanical properties

The mechanical properties of the fibres of different draw ratio (PE1-PE5) are given in Table 4.4.

Table 4.4 Fibre properties

	Yarn count	**Elongational rigidity**	**Breaking load**	**Modulus**	**Breaking stress**	**Elongation at rupture**
	tex*	kN	N	GPa	GPa	%
PE1	58.0	2.27±0.03	102±5	38±0.5	1.7±0.09	5.7
PE2	43.4	2.82±0.03	103±4	63±0.7	2.3±0.10	4.5
PE3	33.9	3.00±0.06	98±4	86±1.6	2.8±0.12	3.9
PE4	25.2	2.88±0.06	84±5	111±2.3	3.2±0.20	3.4
PE5	21.3	2.87±0.08	72±8	131±3.8	3.3±0.35	3.0

*tex: mass in g/1000m

Table 4.4 shows that while the Young ‘s modulus and breaking stress increase with increasing draw ratio, the elongational rigidity of the fibre (equal to the product of the Young ‘s modulus and the cross section) is essentially independent of the draw ratio, for PE2-PE5. The table also shows that the breaking load of the fibre decreases with increasing draw ratio, especially at high draw ratio.

Creep

Typical creep curves for PE4 at 40^0C are given in figure 4.4.

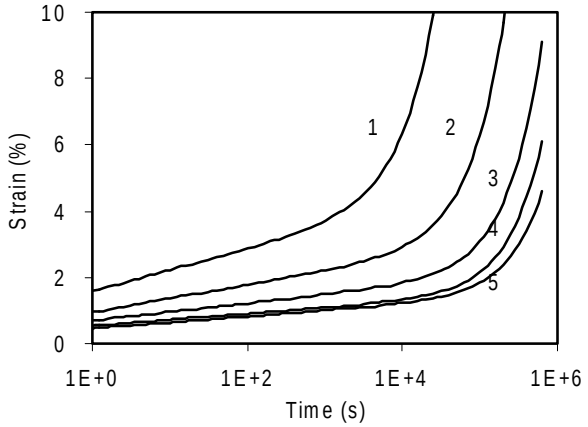

Figure 4.4 Creep PE1-PE5, temperature 40°C, stress 0.6 GPa

The strain is analysed according the description given in chapter 3, viz. by eq. 4.1:

$$\varepsilon_{tot} = \frac{\sigma}{E} + c\sigma \log\frac{t}{t_0} + \dot{\varepsilon}_{plateau}\, t \qquad 4.1$$

Irreversible creep

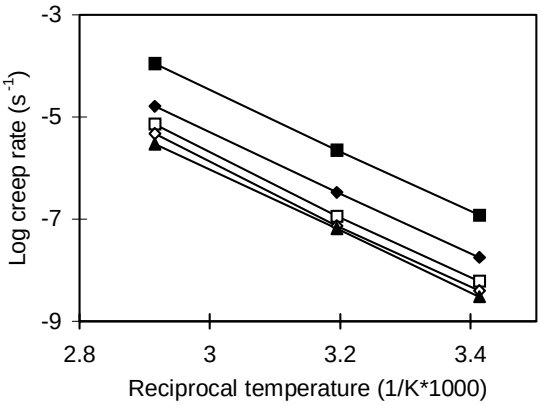

Figure 4.5 Creep PE4, temperature 40°C, ■: 0.2 GPa, ◆: 0.4 GPa, □: 0.6 GPa, ◇: 0.8 GPa, ▲: 1 GPa

Figure 4.5 shows the plateau creep rate as a function of temperature at a stress of 0.6 GPa. Figure 4.5 shows that the creep rate (at a stress of 0.6 GPa) is well described by a constant activation energy. The activation energy is calculated using equation 4.2:

$$dU = k\frac{d\ln\dot{\varepsilon}_{pl}}{d(1/T)} + \sigma v \qquad 4.2$$

Wherein v is given by equation 4.3, viz. the slope of the graphs in figure 4.6 (for stresses >0.5 GPa).

$$v = kT\frac{d\ln\dot{\varepsilon}}{d(\sigma)} \qquad 4.3$$

The effective activation energy is within experimental accuracy (123-132 kJ/mol), independent of draw ratio. This result is well in line with literature data [23-26].
Figure 4.6 gives the creep rate as a function of stress at a temperature of 40°C.

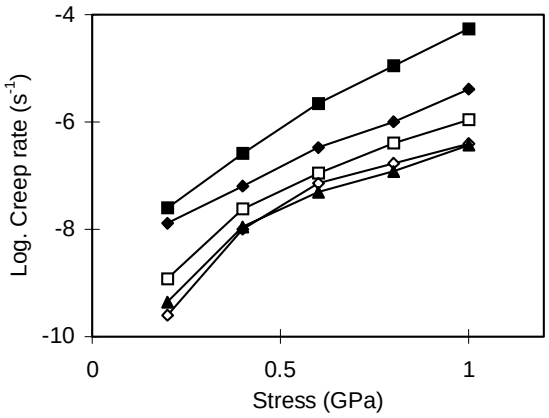

Figure 4.6 Plateau creep rate, temperature 40° C, ■: PE1, ◆: PE2, □: PE3, ◊: PE4, ▲: PE5

In stead of analysing the data for each fibre individually using the concept of stress dependent thermally activated processes, which gives a result analogous to that given in figure 4.1 and table 4.1 for melt-spun fibres, the data for PE1-PE5 are combined. In figure 4.7, the plateau creep rate is plotted as a function of load on the fibres.

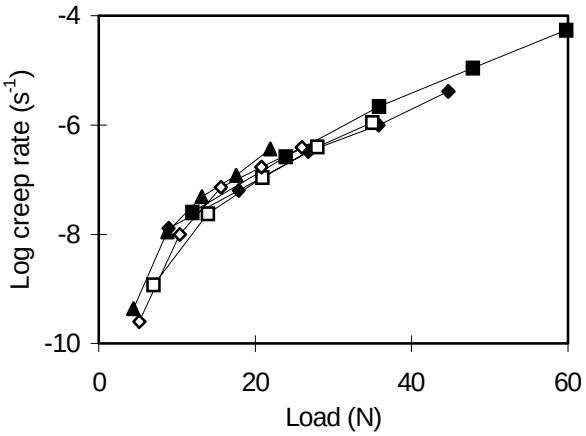

Figure 4.7 Plateau creep rate PE1-PE5 against load on the fibre, ■: PE1, ◆: PE2, □: PE3, ◊: PE4, ▲:PE5

The data fit a single line to a reasonable accuracy. *This implies that the creep rate for fibres that carry the same load does not depend on the draw ratio*.

The result obtained above can be translated back to the more usual stress related description. For this all loads are converted back to stresses, using the cross-section of each fibre. In figure 4.8, the result is given for PE5. The line gives a two process fit of the data

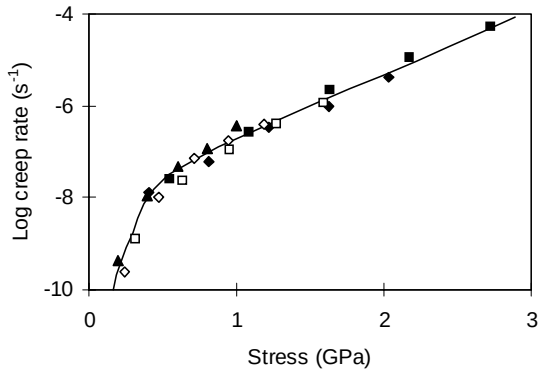

Figure 4.8 Plateau creep rate PE1-PE5 fibres, load converted to stress using cross-section of PE5, ■: PE1, ◆: PE2, □: PE3, ◇: PE4, ▲:PE5–: two-process model fit

Equivalent plots can be made for PE1-PE4, by scaling the x-axis. Table 4.5 gives the calculated two process parameters for the plateau creep rate for PE1-PE5.

Table 4.5 Two-process parameters for flow creep rate, of PE1-PE5, T = 40°C

Fibre	$\dot{\varepsilon}_{01}$	v_1	$\dot{\varepsilon}_{02}$	v_2
	1/s	nm^3	1/s	nm^3
PE1		0.272		0.044
PE2		0.204		0.033
PE3	$1.0x10^{-12}$	0.159	$6.0x10^{-8}$	0.025
PE4		0.118		0.019
PE5		0.100		0.016

As the actual fibre cross-section is apparently not relevant for the creep behaviour (for fibres carrying the same load), v_1 and v_2 (related to the stress) are proportional to the cross-section. Furthermore the rate constants are the same for PE1-PE5, independent of the draw ratio.

Reversible creep

The reversible creep is reasonable well characterised by logarithmic creep. In the stress related description, the creep is determined by the coefficient c:

$$\varepsilon_{rev} = c\sigma \log(\frac{t}{t_0}) \qquad 4.4$$

As for the irreversible creep, the data for the reversible creep can also be analysed as a function of the load on the fibres. Equation 4.4 then becomes:

$$\varepsilon_{rev} = c_L P \log(\frac{t}{t_0}) \qquad 4.5$$

wherein c_L is the creep coefficient and P the load. As 1 tex is equivalent to a cross-section of $1.03*10^{-9}\ m^2$, the parameter c_L can be calculated as:

$$c_L = c / 103 * 10^{-9} * \text{yarncount (tex)} \qquad 4.6$$

The result is given in table 4.6.

Table 4.6 Coefficients c and c_L for reversible creep

	PE1	**PE2**	**PE3**	**PE4**	**PE5**
c ($*10^{-12}$) 1/dec./Pa	10.6±2.4	6.8±2.4	4.3±1.1	3.0±0.7	3.0±1.1
c_L ($*10^{-4}$) 1/dec./N	1.8	1.5	1.2	1.2	1.4

The coefficient c decreases with increasing draw ratio. No significant trend is observed for c as function of stress (expected for linear visco-elastic behaviour) nor of temperature. In table 4.5 the average value for each fibre is given. The coefficient, c_L is essentially independent of the draw ratio for PE2-PE5, only for PE1 the factor is somewhat larger.

The result implies, that also the reversible creep is, to a fair approximation, independent of the draw ratio, for fibres that carry the same load.

4.3.4 Summary

Both the short term elongation as well as the long term elongation (reversible creep and irreversible creep) of gel-spun fibres, that carry the same load, are essentially independent of the draw ratio.

The first observation reflects the well known fact that (for the range of draw ratios studied) the Young 's modulus of the fibres is proportional to the draw ratio. The second implies that the coefficient of reversible creep and the activation volumes for the two process model for flow creep are proportional to the inverse of the draw ratio, i.e. are proportional to the fibre cross section. The rate factors for the flow creep do not depend on draw ratio.

Following the interpretation proposed in chapter 3, it is concluded that the number of load carrying chains in the cross-section of a fibre does not depend on the draw ratio, and that the resistance against slip of the load carrying chains is constant.

4.4 Possibilities for improving the creep of gel-spun fibres by variation of M_w, λ, and the polymer concentration

By combining the data for melt-spun and gel-spun fibres better conclusions can be drawn on the influence of the major parameters: M_w, λ, and concentration, on the creep behaviour.

Effect of molecular weight

The rate factors of both processes are a function of the molecular weight. A large range of the molecular weight is available when the results of melt-spun and gel-spun fibres are combined. Doing so, differences in the morphology of the fibres are ignored. This may not be fully justified, however as the rate constants do not depend on draw ratio, the effect of processing differences s probably small. In figure 4.9 the rate factors for melt-spun and gel-spun fibres found in the literature and those obtained for PE1-PE5 are plotted against molecular weight.

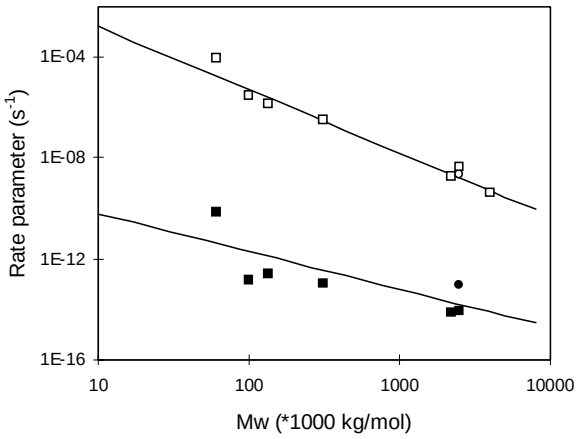

Figure 4.9 Creep rate parameters as a function of molecular weight, ■: $\dot{\varepsilon}_{01}$, □: $\dot{\varepsilon}_{02}$ (●, ○ : PE1-PE5)

Figure 4.9 shows that the rate factors scale approximately with $M_w^{-1.5}$ (network process) and $M_w^{-2.5}$ (crystalline process).

The result can be compared with a relation claimed by Dunbar [6]: $\dot{\varepsilon} \propto M_w^{-2}$. (In fact a relation between creep rate and intrinsic viscosity was claimed: $\dot{\varepsilon} \propto IV^{-2.78}$, while $Mw \propto IV^{1.39}$ [42]).

The rate constant, especially that for the crystalline process, is a strong function of the molecular weight. This suggests, that the average diffusion rate of a typical crystalline chain segment, depends strongly on the molecular weight. The length of a typical extended chain segment (typically 50 nm), however is only a small fraction of the total chain length (>1 μm). For the slip of a complete chain, the combined effect of the slip of many segments in a single chain must be involved, the number of the segments being proportional to the length of the chain. A further factor that can be expected to contribute is the length of the crystalline segment itself. The length of a typical extended chain segment is larger in gel-spun fibres than in melt-spun fibres, typically 20 nm and 70 nm respectively [43]. The dependence of the rate of diffusion

of a chain segment on its length is a well-known fact. For instance the position of the α-loss peak [44, 45] and the crystalline spin-lattice relaxation time T_1 as observed by ^{13}C-NMR, are dependent on the stem length [46].

Effect of draw ratio

There is no or only a small influence of the draw ratio on the rate factors.
The activation volumes decrease with increasing draw ratio, within a series fibres the activation volumes scale with $1/\lambda$. As the Young's modulus is to good approximation proportional to λ, the activation volumes scale approximately with 1/E, the product of Young's modulus and activation volume should be constant. In figure 4.10 the product of modulus and activation volumes for both melt-spun and gel-spun fibres, is plotted as function of the modulus.

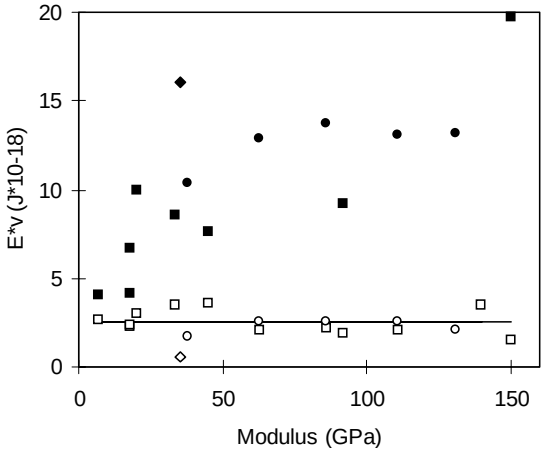

*Figure 4.10 Product of modulus and activation volume for melt-spun and gel-spun PE fibres as function of modulus, ■ : E*v$_1$, □ : E*v$_2$, (◆, ◊ : Hostalen Gur fibre, ●, ○ : PE1-PE5)*

For the crystalline process the product E*v is independent of the modulus, implying that the activation volume of this process is proportional to the inverse of the modulus. The relation is the same for gel-spun and melt-spun fibres.

For the network process the relation does not hold, generally E^*v_1 increases with modulus, implying that the activation volume v_1 does not decrease in proportion to the modulus. v_1 is relatively large for the highly drawn gel-spun fibres.
The large activation volume of the network process implies that only few chains contribute to the stress carried by this process (see chapter 3). The small contribution of the network process in gel-spun fibres can be attributed to the low entanglement network density in gel-spun fibres.

Effect of the concentration

Penning et al. [8] studied the creep of a fibre spun with a concentration of 1.5% in detail and added a few data points for fibres spun at a higher concentration. The data for the fibre spun from a solution of 1.5% can be described over this stress range by a single activated process, however a two-process fit is made with a weak network. The strength of the network is defined by choosing the rate constant equal to that of a typical gel-spun fibre, and the activation volume to a value (500 $Å^3$), representative for a weak network.

The observation that the relation between v_2 and E is the same for melt-spun and gel-spun fibres, shows that the concentration does not influence this aspect.
The concentration has a direct influence on the entanglement density, as is apparent from its strong influence on the viscosity of the solution, and from the fact that the maximum draw ratio scales with the square root of the concentration [38].

Several options can be considered for fitting the data points for the fibres spun from a higher concentration. An increase of the concentration is thought to result in increased resistance of the network process, because of a denser entanglement network, but not to strengthen the crystalline process. The creep improvement is therefore modelled by modifying the strength of the network process, either by adapting the activation volume of this process or by the rate factor of this process; The result is given in figure 4.11 (variation of activation volume only) and in table 4.7.

Table 4.7 Two process fit parameters for fibres spun from different concentration [data from ref. 8]

Conc.		$\mathbf{v_1}$	$\dot{\varepsilon}_{01}$	$\mathbf{v_2}$	$\dot{\varepsilon}_{02}$
		$Å^3$	s^{-1}	$Å^3$	s^{-1}
1.5%	Ref.	500	10^{-13}	27	10^{-09}
3.0%	v1	300	10^{-13}	27	10^{-09}
5.0%	v1	170	10^{-13}	27	10^{-09}
3.0%	ε'_{01}	500	10^{-18}	27	10^{-09}
5.0%	ε'_{01}	500	10^{-26}	27	10^{-09}

The increased contribution of the network process is reflected in the smaller activation volume or a very much smaller rate factor for the fibres spun with a higher concentration.

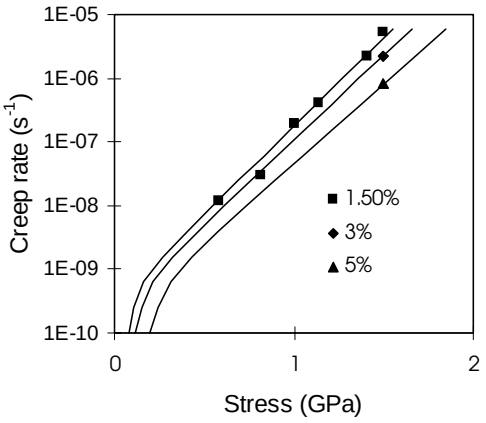

Figure 4.11 Creep of fibres spun from different concentration. The lines are two-process fits with different strength of the network process (table 4.7)

The most simple interpretation is that the increased strength of the network process is due to an increased number of chains contributing to this process. In the example given by a factor 1.7 (3%) respectively 3 (5%). The numbers depend on the

parameters chosen for the fibre spun with a concentration of 1.5%; however the conclusion that the increased network contribution is caused by a small increase of the number of contributing chains, will remain unchanged.

The strength of the network process can also be fit by adapting the rate factor of the network process. A reduction of this factor by several decades is required, see table 4.7. Either the slip resistance of the chains involved should become much larger, or the number of slip sites that can be activated is reduced by that factor. Both explanations are highly unlikely.

It is concluded that the effect of increasing polymer concentration on the creep rate can be understood by an increase of the number of chains that contribute to the stress on the network process.

4.4.2 Improving the creep by variation of the processing parameters

The results described above enable to estimate the effect of variation of processing parameters on the creep properties of gel-spun fibres. Figures 4.12-4.14 are plotted with reversed axes, in order to emphasises the contribution the of the process to the stress on the fibre.

The influence molecular weight on the relation between stress and creep rate is calculated using the relations shown in figure 4.9; the result is shown in figure 4.12.

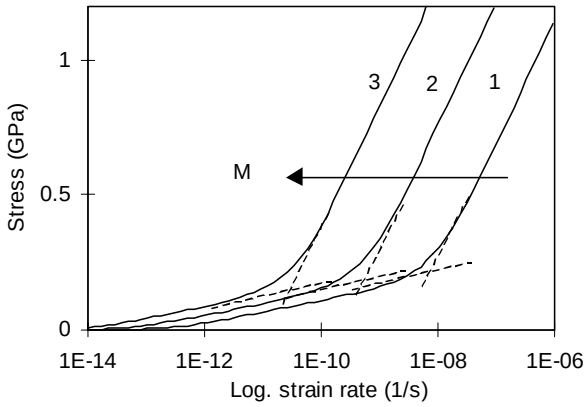

Figure 4.12 Calculated influence of a variation of molecular weight on the creep rate; 1: $M_w = 0.67*10^6$ D, 2: $M_w = 2*10^6$ D, 3: $M_w = 6*10^6$ D

With increasing molecular weight the graph of stress vs. strain rate shifts to lower strain rate, (to higher stress at equal strain rate). Also the strain rate at which the crystalline process begins to contribute to the stress shifts to lower strain rate.

The effect of increasing the draw ratio is a decrease of the activation volumes. The calculated effect of a variation of draw ratio is given in figure 4.13; the activation volumes of both processes are scaled with the inverse of the draw ratio, the rate constants kept constant. The reference fibre is a moderately drawn UHMW-PE fibre with a modulus of 80 GPa (estimated draw ratio 40).

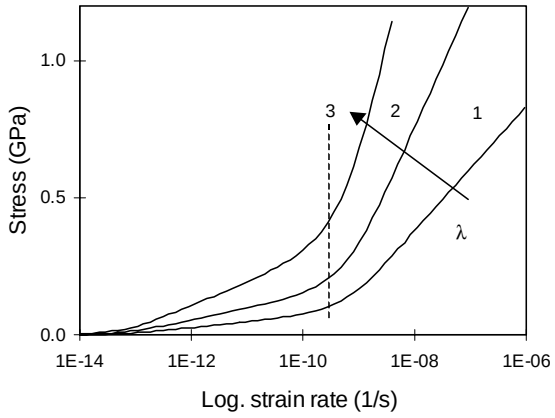

Figure 4.13 Calculated influence of the draw ratio on the creep rate; 1: λ=20, 2: λ=40, 3:λ= 80

The transition where the crystalline process starts to contribute remains at the same strain rate. At low strain rates the increased contribution of the network process results in higher stress. A decrease of the creep rate by one decade (at high load) requires doubling the draw ratio. It is obviously no route for improving the creep properties of the present commercial fibres to a large extend. For intermediate loads the improvement is somewhat larger (1.5 decades for a factor 2 increase in λ).

As discussed, above the influence of the polymer concentration can be understood as an enhancement of the network contribution only.

Figure 4.11 gives the effect for a concentration from 1.5 to 5%. It is shown that the network resistance (the inverse of the activation volume) is about proportional to the concentration. This enables to predict the effect of a higher concentration. In figure 4.14 the influence of the polymer concentration up to 10% is shown.

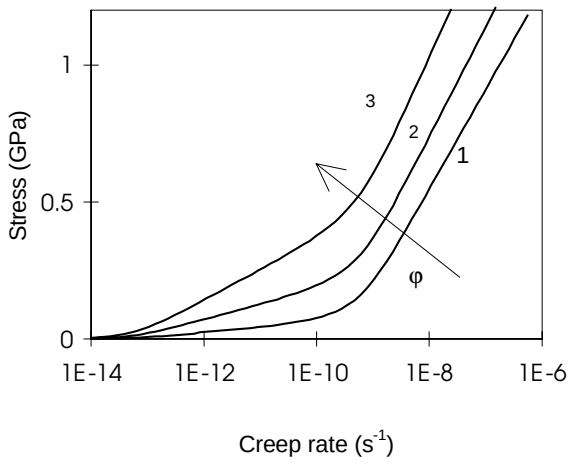

Figure 4.14 Calculated influence of the polymer concentration (network strength) on the plateau creep rate; 1: φ = 1.5 %. 2: φ = 5 % 3: φ = 10%

By increasing the density of the entanglement network the creep improvement is most pronounced at intermediate stress. At high stress the improvement is moderate. The improvement at very low stress is also small, this is a consequence of the fact that only the number of contributing chains is increased, but not their resistance against slip.
For improving the creep resistance of polyethylene fibres, either the number of chains contributing to the stress or the resistance against slip of (a fraction of) the chains must be increased.

For the crystalline process the number of chains is already high (as is shown by the small activation volume), a further significant improvement is difficult to achieve in the present commercial processes. Furthermore only above the threshold strain rate for the crystalline process an improvement is possible. For improving the crystalline

process the resistance of crystalline chain segments must be enhanced. Options that have been considered are: the use of branched polyethylene or modified polyethylene [2,33,34]. Problems can be expected because of interference with the drawing process.

Improving the network strength is another option. The threshold creep rate for this process is very low, essentially zero for all practical purposes. Therefore any increase in the contribution of the network process improves the properties over the full range of strain rates. It is not possible to start with a strong network; a key feature of the gel-spin process is the creation of a low network density. Increasing the network before drawing interferes with the drawing process.

Increasing the network strength after drawing of the fibre seems therefore to be the most promising way for improving the creep resistance of gel-spun fibres. In chapters 6 and 7 the options of creating a network in gel-spun fibres after drawing of the fibre will be explored.

In chapter 5 a literature review is made of the efforts for improving the creep resistance of gel-spun fibres, including those by modification of the polymer or the fibre before, during, and after drawing.

4.5 Conclusions

The improvement of the creep properties of gel-spun as well as melt-spun fibres caused by drawing can be explained by a decreased stress dependence of the creep only, and is explained by an increased number of stress bearing chains per unit of cross-section.

A higher molecular weight results in an improved creep resistance because of a lower thermally activated creep rate of chain segments. It is proposed that this is partly caused by an increase of the length of a typical crystalline chain segment and partly by an increase of the number of segments involved.

Increasing the polymer concentration in the gel results in increased network strength, because of an increased number of contributing chains.

It is concluded that the best option for a further significant improvement of the creep properties of gel-spun fibres is strengthening of the network process after the fibre has been drawn.

Both the short-term as well as the long-term mechanical data show a remarkable invariance upon drawing. The data can be explained by assuming that the number of chains contributing to the stress in the fibre cross-section is constant and that the resistance against deformation is constant.

4.6 References

1 I. M. Ward and M.A. Wilding, J. Polym Sci., Polym. Phys., **22**, (1984), 561

2 P.Smith. P.J. Lemstra, J.P.L. Pijpers, J. Polym. Sci., B, Polym. Phys., **20**, (1982), 2229

3 P. Smith, P.J. Lemstra, J. Polym. Sci., Phys. Ed., **19**, (1981), 1007

4 P. Smith , P.J. Lemstra, H.C. Booij, J. Polym. Sci., B. Polym. Phys., **19**, (1981), 877

5 P.J. Lemstra, N.A.J.M. van Aerle, C.W.M. Bastiaansen, Polym. J., **19**, 1, (1987), 85

6 J.J. Dunbar et al. USA Patent, **745** 146, (1985)

7 J. Xue, Eindhoven University of Technology, Personal communication

8 J.P. Penning, H.E. Pras, A.J. Pennings, Colloid Polym. Sci., **272**, (1994), 664

9 C.W.M. Bastiaansen, Processing of Polymers, H.E.H. Meier Ed., Mater, Sci. Techn. **18**, (1997), 551

10 R. Kirschbaum, Proc. Rolduc Polymer Symposium, (1987)

11 M.A .Wilding and I.M. Ward, Polymer, **19**, (1978), 969

13 M.A. Wilding and I.M. Ward, Polymer, **22**, (1981), 870

14 M.A. Wilding and I.M. Ward, Plastics and Rubber Proc. and Appl., **1**, (1981), 167

15 I. M. Ward, Polym. Eng. Sci., **24**, 10, (1984), 724

16 I. M. Ward, Progress Polym. Sci., **92**, (1993), 103

17 I. M. Ward, Macromol. Symp., **98**, (1995), 1029

18 D.W. Woods, W.K. Busfield, I.M. Ward, Polym. Comm., **25**, (1984), 298

19 D.W. Woods, W.K. Busfield, I.M. Ward, Plast. Rubber Proc. Appl., **9**, (1988), 155

20 P.G. Klein, D.W. Woods, I.M Ward, J. Polym. Sci., B, Polym. Phys., **25**, (1987), 1359

21 I.M. Ward, Brit. Polym. J. **18**,4, (1986), 216

22 J. Rasburn, P.G. Klein, and I.M Ward, J. Polym. Sci., B, Polym Phys., **32**, (1994), 1329

23 P.J.R. Leblans, C.W.M. Bastiaansen, L.E. Govaert, J. Polym. Sci., B, Polym. Phys., **27**, (1989), 1009

24 L.E Govaert, PH-D Thesis Eindhoven University of Technology, (1990), ch. 3

25 L.E. Govaert and P.J. Lemstra, Coll. Polym. Sci., **270**, (1992), 455

26 L.E. Govaert , C.W.M. Bastiaansen, P.J.R. Leblans. Polymer, **34**, 3, (1993), 534

27 T. Peijs, E.A.M. Smets, L.E. Govaert, Appl. Comp. Mater., **1**, (1994), 35
28 D.C. Prevorsek, Synthetic fibre materials High Performance Fibers 2, ch.10, (1996) , 262
29 H . van der Werff, PH-D Thesis, University of Groningen, (1991), 31
30 D.J. Dijkstra and A.J. Pennings, Polymer Bulletin, **19**, (1988), 73
31 Y. Ohta, H. Sugiyama, H Yasuda, J. Polym. Sci., B, Polym Phys., **32**, (1994), 261
32 J.P. Penning, Ph-D Thesis University of Groningen, (1988), ch. 6
33 Y. Ohta, A. Kaji, H. Yasuda, Polym Pre-prints Japan, **43**, 9, (1994), 3143
34 Y. Ohta, H. Sugiyama, H. Yasuda, J. Polym. Sci., Polym. Phys., **32**, (1994), 261
35 J. Smook, W. Hamersma, A.J. Pennings, J. Mater, Sci., **19**, (1984), 1359
36 D.J. Dijkstra, J.C.M. Torfs, and A.J. Pennings, Colloid and Polym. Sci., **267**, (1989), 866
37 O.D. Sherby, and J.E. Dorn, J. Mech. Phys. Solids, **6**, (1958), 146
38 C.W.M. Bastiaansen, Ph-D Thesis Eindhoven University of Technology, (1991), ch. 3
39 W. Hoogsteen et al, J. Mater. Sci., **23**, (1988), 3459
40 N.A.J.M. van Aerle, PH-D Thesis Eindhoven University of Technology, (1989), ch. 3
41 P. Smith and P.J. Lemstra, Colloid Polym Sci., **258**, (1980), 891
42 ASTM D 2857
43 V.A. Marikhin, L.P. Myasnikova, Makromol Chem., Macromol. Symp., **41**, (1991), 209
44 C.R. Ashcroft, R. Boyd, J. Polym. Sci., Polym. Phys., **14**, (1976), 2153
45 R.H. Boyd, Polymer, **26**, (1985), 1123
46 D.F. Axelson, L. Mandelkern, R. Popli, P. Mathieu, J. Polym. Sci., Polym. Phys., **21**, (1983), 2319
47 N.A.J.M. van Aerle, PH-D Thesis Eindhoven University of Technology, (1989), ch. 3
48 N.A.J.M. van Aerle and C.W.M. Braam, J. Mater. Sci, **23**, (1988), 4429
49 Y. Termonia, P Smith, High Modulus Polymers, A. Zachariades, R.S. Porter, Marcel Dekker, N.Y., (1996), ch. 11, 321
50 D.J. Dijkstra, J.C.M. Torfs, A.J. Pennings, Colloid and Polym. Sci., **267**, (1989), 866

Annexe 4.1 Flow processes observed in an ultra-drawn Hifax 1900 fibre.

Penning [8,31] fitted the data of Dijkstra [30] for a Hifax 1900 fibre, using the two process model. Figure 2 of reference 30 is replotted as figure 4.1.1.

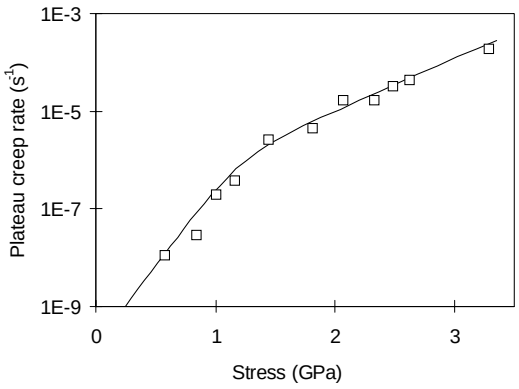

Figure 4.1.1 Plateau creep rate for a Hifax 1900 fibre at room temperature. The line is the two process fit by Penning et al. [31].

The first process was assumed to be the network process, the second the crystalline process. Remarkably are, a very low activation volume for the first process, and high rate constants for both processes, see table 4.2.

The network process can normally be observed only at low stress (<0.5 GPa), where no data are available. For this fibre a weak network should be expected, because the fibre was spun from a low (1.5 %) concentration. It is therefore assumed that the network process is not seen, because low stress data are not available.

The first process is therefore identified as the combination of the first and second process usually observed in gel-spun fibres. The result is then well in line with the results for other gel-spun fibres.

The values measured at high stress (> 1.5 GPa) are maximum stresses in a tensile test. At high stress the strain to failure is small, and the fibres do not show extensive plastic deformation, the maximum stress is determined by chain rupture. Figure 4.1.1 is equivalent to results reported by Peijs [27], reproduced in chapter 2, figure 2.16.

Chapter 5 Improvement of the creep of highly oriented polyethylene fibres; literature review.

5.1 Introduction

In the preceding chapters, it has been shown that polyethylene fibres, both melt-spun as well as gel-spun fibres, possess qualitatively the same creep characteristics. Although the creep rate of gel-spun fibres is much lower than that of melt-spun fibres, mainly due to the higher molecular weight and the higher degree of chain extension, the creep, especially the persistent flow creep, is still limiting for many of their present and anticipated applications f polyethylene fibres is caused by thermally activated diffusion of crystalline chain segments. Improving the creep resistance is possible by increasing the number of the fibres.
In chapter 3, is was argued that the creep o of chains that contribute to the load on a fibre, or by increasing the resistance against slip of at least a fraction of the molecular chains. In 1981 Ward described some possible routes for improving the creep behaviour [1], drawing, the use of high molecular weight polymer, the use of copolymers, and crosslinking. Subsequent research has been pursued along one or several of theses routes [2,3].

Many routes for improving the creep properties of oriented fibres are also effective for improving the stress resistance of non-oriented polyethylene in view of its use in (hot) water pipes. Special grades have been developed that have an improved lifetime, the parameters are: molecular weight, (butyl)side-groups [4,5], and crosslinking [6].

The creep behaviour of gel-spun fibres and the effect of molecular weight and draw ratio is reported in chapters 3 and 4. Already shortly after the first publication on the development of the gel-spinning process, research was done for improving the creep resistance of the gel-spun fibres [7-11]. Since that time, research in this field has been continued. In this chapter the literature data on improvements of the creep resistance of melt-spun and gel-spun polyethylene fibres are discussed, the limitations for improving the creep of polyolefin fibres are indicated and new routes for further improvement are identified.

The scope of this chapter is limited to linear polyolefin fibres, for this reason other polymers, as polyamide, poly-vinylalcohol, and polycetone, that have a creep resistance that is superior to that of polyethylene, are not considered.

5.2 Creep of melt-spun fibres

5.2.1 Effect of branching

The effect of branching was investigated by Ward et al [1] and Rasburn et al. [3]. The plateau creep rates of fibres produced from copolymers of ethylene and butene at a temperature of 22.5°C are shown in figure 5.1. The polymers used were Alathon 7030 (homo-polymer) and Rigidex 002-55 (0.4 C_2H_5 /1000 C atoms) , and Rigidex 002-47 (1.3 C_2H_5 /C atoms), more data in table 5.1.
In figure 5.1 the data of reference 3, figures 3 and 8 are replotted.

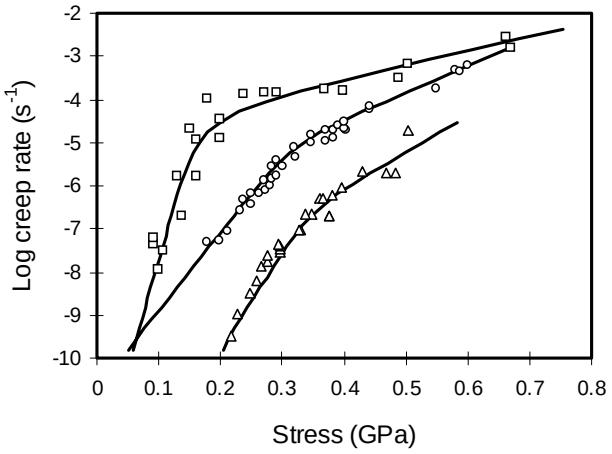

Figure 5. 1 Creep of drawn polyethylene fibres with different concentration of branches [3],□: homo-polymer, ○: 0.4 C_2H_5 /1000C, △ :1.3 C_2H_5 /1000C-atoms

The reduction in the creep rate, due to the presence of small side groups, is most pronounced at intermediate stresses (here 0.1–0.4 GPa). The data for Rigidex 002-47 (1.3 branches /1000 CH_2 groups) were measured partly at a temperature of

22.5°C and partly at 50°C. The results obtained at 50°C have been re-scaled to fit the data obtained at 22.5°C.

From the shift factor required (2.7 decades) an activation energy of 180 kJ/mol was calculated. This activation energy is high compared with that reported for non-branched polyethylene [12-14]. The value for the activation energy is the same as has been reported for the network process [15].

At low stress, the slope of log strain rate versus stress is smaller for the branched polymer than for the homopolymer, at high stress the slope is larger. In table 5.1 the two process fits for the data in figure 5.1 are shown.

Table 5. 1 Two process parameters for the flow creep rate of fibres spun from polymers with different degree of branching (butyl chains), λ=15

Sample [3]	**$M_{w^*}10^{-3}$**	**E**	**v_1**	**$[\dot{\varepsilon}(T)_0]_1$**	**v_2**	**$[\dot{\varepsilon}(T)_0]_2$**
Fibre (CH_3/1000 C atoms)	D	GPa	nm^3	1/s	nm^3	1/s
Alathon 7030 (-)	115	14	0.47	$3.3x10^{-13}$	0.033	$1.0x10^{-4}$
Rigidex 002-55 (0.4)	170	18	0.17	$3.7x10^{-11}$	0.086	$2.2x10^{-5}$
Rigidex 002-47 (1.3), 50°C	155	21	0.22	$2.5x10^{-12}$	0.125	$2.5x10^{-4}$
Rigidex 002-47 (1.3), 22°C	155	21	0.22	$5.0x10^{-15}$	0.125	$5.0x10^{-7}$

The reduction of the creep rate for Rigidex 002-55 (0.4 branches/ 1000 C-atoms) is only due to the smaller stress sensitivity (activation volume) of the first, or network, process. This can be explained by an increase of the number of chains contributing to the stress for this process. For Rigidex 002-47 the reduction of the creep rate is also due to stronger network process, however this is not due to a smaller activation volume only, also the rate constant is smaller. The results suggest the molecular mechanism is changed, namely the resistance of the chain segments against slip is also increased.

The activation volume for the second, or crystalline, process increases with degree of branching. The increased activation volume for the crystalline process is caused by a less favourable load distribution over the chains in the crystalline phase.

5.2.2 Crosslinking before drawing

Ward et al. [12] and Klein et al. [16] irradiated as spun fibres with γ-rays, and eliminated the radicals by sufficiently long storage in an inert atmosphere. The influence of the irradiation dose on the creep properties was reported by Klein et al [16], see figure 5.2. The maximum draw ratio decreases with increasing irradiation, however all fibres were tested at the same draw ratio (λ = 12), the maximum draw ratio of the fibre with the highest irradiation dose.
Some creep reduction was observed for doses below the gel-dose. This was attributed to the creation of branches [16].

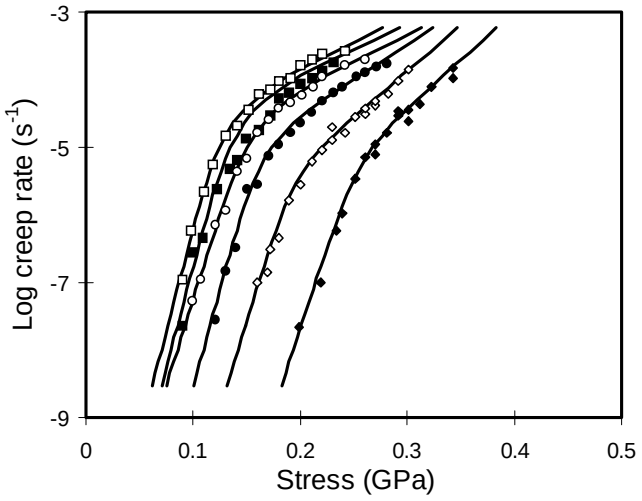

Figure 5. 2 Creep of melt-spun polyethylene fibres crosslinked before drawing (replotted from ref. 16, fig 12). Temperature 23°C. Radiation dose (kGy): □: 0, ■:70, ●: 130, ○: 240, ◊: 350, ♦: 600.

The treatment results in a horizontal shift of the log creep rate vs. stress curves, and a small increase of the slope of the graph at high stress levels. The shift is

proportional to the irradiation dose. The creep data can well be described by the two process model. The improvement of the creep resistance can be fully accounted for by an increase of the resistance of the low stress process only, and more specifically by a smaller rate constant. The authors suggested the following explanation for the increase of the resistance of the first process; the number of slip sites that can be activated is made smaller by the same factor as the creep rate (for the data in figure 5.2, by many decades).

The interpretation of the data by only two activated processes is unlikely. The interpretation proposed by the authors [16], implies that essentially all chains are blocked , and that the creep is caused by the slip of a very small fraction of chains. According the interpretation proposed in chapter 3, the constant activation volume for the network process suggests that the fraction of load due to the network process is carried by a constant number of load bearing chains, each with an increased resistance against slip. It is then however difficult to understand, that the number of network chains remains constant when the irradiation dose is varied.

The data of figure 5.2 suggest a different interpretation: the contribution of the two flow processes is essentially unchanged, but part of the load is carried by a third different load bearing structure. The irradiation results in a chemical network, in addition to the entanglement network initially present, and the density of this network is a function of the radiation dose. The new process can hardly be a flow process, because the chemical network will resist persistent flow, and fails due to chain rupture. The network will result in a threshold stress below which no flow creep occurs. The level of this stress should be a function of the network density, as is observed. The threshold stress increases in proportion (0.022 GPa/Mrad) to the radiation dose. This interpretation is supported by the shape of the Sherby and Dorn plots for the creep of the treated fibres [6]. For a stress higher than the threshold stress, the Sherby and Dorn plot, has the shape as in figure 3.5 with a well defined plateau region. For a stress below the threshold, the shape of the curve is initially the same, but at a certain deformation the creep rate starts to decrease again, and falls to an immeasurable value.

The effect of crosslinking of polyethylene for obtaining fibres of high strength and creep resistance was also performed at Raychem [17]. Fibres of a relatively high strength (1.4 GPa) and low modulus (8 GPa) were obtained, the creep properties were reported only at a low static load of 105 MPa. Crosslinking was done by e-beam irradiation in the presence of 0.5% an agent (tri-allyl-iso-cyanurate) that promotes chain reactions by bridging.

5.2.3 Crosslinking of the drawn fibre.

Perkins et al [18] irradiated, highly oriented, extruded and drawn fibres (Alathon 7050, M_w 60.000) with γ-ray doses up to 600 kGy. The fibres possessed a high modulus 43 GPa), but low strength (0,3 GPa). The low strength was attributed to a low degree of connectivity between the crystalline domains. The strength and elongation to failure increased, especially so (by a factor 2) when the samples were annealed prior to irradiation. It was proposed that the increase in mechanical properties was due to an increase of inter-lamellar tie molecules.
In 1983 a patent was filed by Ward for high energy radiation crosslinking of highly oriented melt-spun fibres, in vacuum or in a sensitising atmosphere [19]. It was claimed that the treatment was only effective for polyethylene with M_w <350.000. Sensitising media proposed are: acetylene, dienes, acrylic monomers, and sulphur-mono-chloride, with acetylene preferred. All data reported are on a low M_w polymer: Alathon 7050, M_w = 60.000.

Ward et al explored the possibilities of crosslinking highly oriented polyethylene fibres in inert (vacuum or nitrogen) or sensitising (C_2H_2) atmosphere (3, 15, 20-23] The fibres used were either produced by Celanese (Alathon 7050, M_w 60.000, λ = 30), or an equivalent fibre produced by Montedison. The crosslink efficiency is much larger in the presence of acetylene and at elevated temperature. Annealing after irradiation enhances the crosslink efficiency, especially if the annealing is done in acetylene atmosphere. Gamma ray irradiation is more effective than e-beam irradiation, due to the lower dose rate [15]. Highly efficient crosslink schemes were designed, requiring a dose of less than 100 kGy, thus limiting the effect of chain scission. In this way fibres were produced that exhibit no flow creep for a stress up to 0.4 GPa, the samples rupture in a brittle way [15]. For lower irradiation doses,

especially in acetylene, significant creep improvements were realised, while retaining ductility [21]. At very high doses flow creep was observed again, the plasticity being due to chain scission [22].

Klein et al. [15] analysed some data using the two process creep model. Insufficient data does not allow a two process analysis for some of these crosslinked fibres, in that case single process fits are reported, table 5.2 gives the results available.

Table 5. 2 Two process parameters for crosslinking melt-spun polyethylene fibres after drawing

Sample [ref.15]	M_w	v_1	$[\dot{\varepsilon}(T)_0]_1$	v_2	$[\dot{\varepsilon}(T)_0]_2$
	*1000	nm^3	1/s	nm^3	1/s
Alath. 7050, λ = 30	115	0.307	$7.2x10^{-11}$	0.031	$9.4x10^{-5}$
Alath. single process fit	115			0.028	$2.6x10^{-6}$
Alath. 9 MRad, vacuum	115x	-	-	0.064	$3.0x10^{-6}$
Alath. 0.27 MRad, C2H2	115x	-	-	0.083	$3.3x10^{-7}$
Alath. 0.7 MRad, C2H2	115x	-	-	0.070	$4.4x10^{-7}$
Rig. 002-55, λ = 15 [3]	170	0.169	$3.7x10^{-11}$	0.086	$2.2x10^{-5}$
Rig. 002-55,10 MRad/N2	170x	0.213	$3.5x10^{-12}$	0.066	$1.4x10^{-4}$
Rig. 002-55,0.5 MRad/ac.	170x	0.196	$3.4x10^{-13}$	0.074	$4.1x10^{-5}$

The improved creep resistance can be explained by a strengthening of the network process. At the same time the crystalline process is degraded, as is shown by the increase of the activation volume. This is most probably due to a less favourable load sharing between chains in the crystalline phase. At high dose, even in inert atmosphere, the rate factor decreases. It was concluded that the amorphous phase is crosslinked, and that (net] chain scission occurs in the crystalline phase.

At first sight, irradiation in an inert atmosphere followed by crosslinking in C_2H_2 environment is interesting because it has the advantage of avoiding the reactive atmosphere in the radiation chamber [23,24). However for this scheme to work, it is

required to prevent the decay of the radicals before impregnation with acetylene gas. This can be realised by cooling the samples to a low temperature, for instance by immersing in liquid nitrogen. While the creep resistance of melt-spun fibres made from non-branched polyethylene can be improved by crosslinking, it appears that this is more difficult for fibres made of branched chains [3]. Crosslinking in vacuum only results in an increase of the creep even at a dose of 2 MRad. Low dose irradiation in acetylene atmosphere (0.25 MRad) resulted in a moderate improvement. Table 5.2 gives the data for a Rigidex 002-55 fibre with 0.4 butyl side groups/1000C.

5.2.4 Summary of creep improvements of melt-spun fibres.

Various methods have been shown to be successful for improving the creep (the resistance against flow creep) of melt-spun fibres.
Drawing and increasing the molecular weight result in an overall improvement of the creep properties. Branching, crosslinking before drawing, and crosslinking of the drawn fibre however improve the creep mainly at low stress (0.1-0.3 GPa) because they only increase the strength of the network process. The crystalline process is weakened. The effect of crosslinking before drawing can be described by load sharing with a real chemical network. This is supported by the fact that the flow creep seems to be suppressed completely up to a certain stress level.

Crosslinking degrades the resistance of the crystalline process especially so at high draw ratio. This is mainly due to an increase of the stress sensitivity, the activation volume, is larger in treated fibres. The latter is due to a less favourable load distribution over the crystalline chains segments.

In improving the creep properties of melt-spun polyethylene fibres by using a branched polymer, or by crosslinking before drawing, a balance has to be made between the drawability and the creep improvement obtainable. Useful schemes for modifying the fibre after drawing require that chain scission is minimised.

5.3 Creep improvements gel-spun fibres

The possibilities for influencing the creep behaviour of gel-spun fibres by variation of the major process parameters: molecular weight, and draw ratio have been discussed in chapter 3. Here only creep improvements by modification of the polymer or fibre are reviewed.

5.3.1 Branching

Bastiaansen et al [25] and Ohta [13,14] studied the possibilities for producing high strength gel-spun fibres with improved creep properties using polymers containing short branches (up to 12.5 methyl groups/1000C) and of blends of this polymer with a polymer with low branch content. Side groups result in a lower maximum draw ratio and a lower modulus and strength. Optimum results were obtained with 5-10 -CH_3 groups/1000 C atoms. Figure 5.3 shows a typical series of data on branched fibres from references 13 and 25.

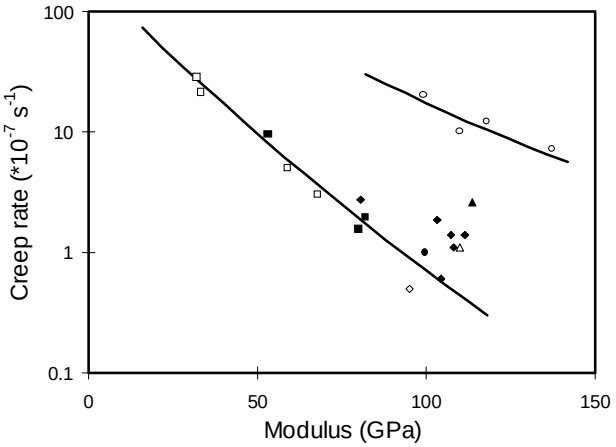

Figure 5. 3 Creep rate of fibres with different concentration of methyl side groups [14]. Temperature: 50°C, stress: 0.78 GPa. Number of CH_3 groups/1000C-atoms : ○*: 1 ,* ▲*: 2.3,* △*:4,* ◆*: 6.8,* ■*: 9.5,* ◊*:10,* ●*:11.4,* □*: 12.5*

A strong improvement of the creep properties for fibres of equal draw ratio was realised [13,14,25]. The effect of side groups on the creep has been analysed in more detail in order to separate the effect of branching and draw ratio. First it is assumed that the improvement only depends on the number of branches. The data in figure 5.3 suggest this. The data are shifted vertically in order to fit a single master curve of creep rate against modulus. The result, the logarithm of the calculated plateau creep rate vs. modulus of the fibre, is given in figure 5.4.

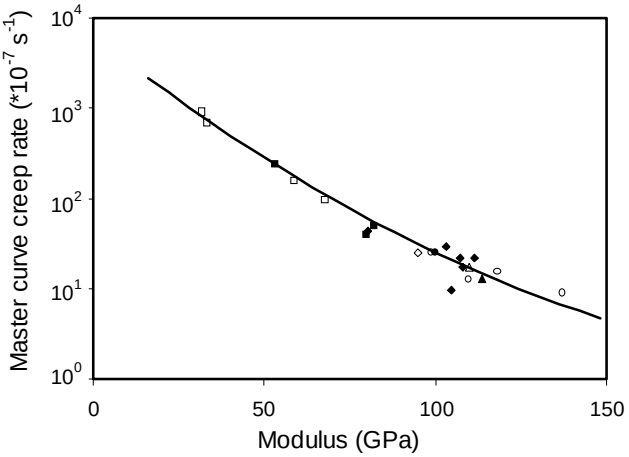

Figure 5. 4 Master curve for the creep rate of fibres of different branching ratio (reference zero branching). Temp 50°C, Stress 0.78 GPa, symbols as in figure 5.3.

Figure 5.4 shows that the effects of draw ratio and branching content can reasonable well be separated. The shift factor, the factor by which the creep rate of the branched fibre is smaller than that of the non-branched fibre, is shown in figure 5.5.

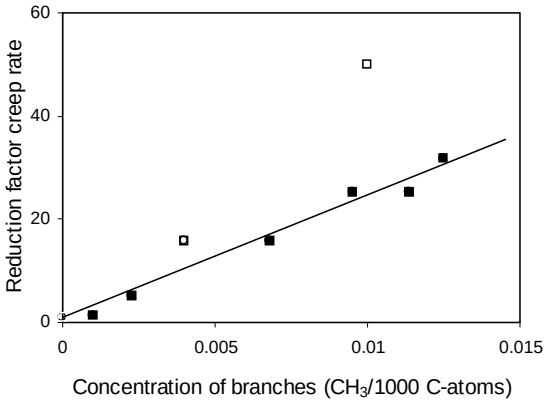

Figure 5. 5 Reduction factor for creep rate as a function of the concentration of CH_3 branches, ■: blend of polymers with 1 respectively 12.5 CH2 branches/1000 C atoms, □ : non blended polymers

For the fibres made from a blend of a non-branched and a branched (12.5 CH3 groups per 1000 C-atoms) the improvement of the creep is proportional to the number of branches. The reduction factor at a stress of 0.78 GPa and a temperature of 50°C is about a factor 20 for 1% of branches. The creep reduction in the fibres produced from non-blended branched polymers, is somewhat larger that for the blends with the same average branching ratio.

As the activation energy increases with the concentration of branches, for the data given above, from 140 to 240 kJ/mol [13], the temperature dependence of the creep rate is larger in fibres made from branched polymers. At room temperature, the creep rate of a fibre made from a polymer with 10 branches /1000 C-atoms will be reduced by a further factor 10, compared with a fibre made of a non-branched polymer.

For melt-spun fibres branching results in an increase of the resistance of the low stress, or network process, while the crystalline process is degraded. Ohta reported creep data on gel-spun fibres of different branch content. The data were evaluated with a single activated process [13], therefore only an effective activation volume was determined. It was found that the branch content has only a minor influence on this parameter. Changes, in either v_1 or v_2 are most probably small.

In the examples given above only the effect of methyl branches was considered. Polymers with many other type of branches have been described; alkyl- (ethyl-, propyl-, butyl- and hexyl-) groups [26], substitution with Cl atoms [27] and oxygen containing groups [28]. The effect of a chlorine atom is comparable to that of a methyl group. The larger groups can be used in a very small concentration only, typically 1 branch/1000 C-atoms, because of their strong influence on drawability. In all cases a creep improvement was claimed but the data are insufficient for comparing their merits.

5.3.2 Crosslinking before drawing

Hikmet et al [8] produced irradiated gel-cast films by e-beam irradiation, up to 15 MRad, before drawing. The ultimate draw ratio decreased significantly with increasing dose. Modulus and strength at constant draw ratio where essentially constant. Creep was determined on tapes with λ=60 at room temperature for loads between 0.4 and 0.65 GPa. At constant draw ratio a significant improvement of the creep was observed, mainly at the lowest stress. The maximum draw ratio was reduced significantly, no data were given of the creep at the maximum draw ratio for each fibre. The data could be described by a single activated process, this is not unexpected given the minimum load of 0.4 GPa for which data are available (table 5.3).

Table 5. 3 Two process creep parameters for crosslinked gel-cast fibres.

Sample [ref.]	M_w	**E**	v_{eff}	$\dot{\varepsilon}_{0eff}$
	*1000 D	GPa	nm^3	1/s
Host Gur 412, λ=60 [8] non-irradiated	2200	90	0.048	$1.3x10^{-9}$
Host Gur 412, irradiated, 5 MRad	x	83	0.055	$2.0x10^{-10}$
Host Gur 412, irradiated, 10 MRad	x	82	0.064	$8.8x10^{-12}$

The improvement of the creep resistance is due to a lower rate constant. The improvement can well be explained by the presence of an enhanced network process. When the high stress data on the creep of melt-spun fibres that are crosslinked before drawing are analysed by a single process, the same trends are found.

5.3.3 Crosslinking at intermediate draw ratio

5.3.3.1 Gamma/E-beam crosslinking

Van Aerle [29] studied crosslinking of UHMW-PE at an intermediate stage of drawing. The highest crosslink efficiency was at the draw ratio where the crystallinity was at its minimum. Crosslinking up to this stage improved the creep, at a later stage the properties were impaired. It was suggested that the decreasing efficiency was caused by a decrease of crosslinking efficiency at higher draw ratio and not by an increase in the chain scission. A small creep improvement was demonstrated. All samples were given the same irradiation dose (60 kGy). This dose is relatively high, and as the crosslink efficiency has a maximum at intermediate draw ratio ($\lambda = 5$), better results might have been obtained by optimising (lowering) the irradiation dose at this draw ratio.

Also Akay [30] reported on the effect of draw ratio on the crosslink efficiency of linear polyethylene subjected to γ-ray irradiation. Enhanced crosslinking is again observed at intermediate draw ratio ($\lambda = 9$). The enhanced crosslink efficiency is attributed to the presence of mobile (non strained) tie molecules; by further drawing the tie molecules become taut and the scission to crosslink ratio increases.
Burkhard [31] irradiated fibres between two drawing steps with e-beam irradiation in vacuum. Irradiation resulted in a higher maximum total draw ratio, the relation between draw ratio and (room temperature) mechanical properties did not change. Yield stress at 80°C was depressed significantly, implying a higher creep rate and increased ductility. Irradiated fibres could be drawn to a higher draw ratio. For some irradiated samples, drawn to the maximum draw ratio, an increase of the yield stress was observed. This suggests that a significant creep improvement can be realised in this way.

5.3.3.2 UV-crosslinking

Nishigawa et al. and Sakano et al. [32,33] impregnated gel-spun UHMW-PE fibres by adding UV crosslinking agent (benzophenone) to the bath used for solvent extraction. Drawing was performed in two steps, UV irradiation (1 min, 313 nm) was done between the first and second drawing steps. High strength fibres (4.5 GPa) were claimed. A slightly improved creep resistance was claimed, the creep rate being approximately 20% of that of the non-treated sample. Also Suwanda [34] claims a process for UV-crosslinking of polyethylene using two step drawing and UV irradiation during the second drawing step. Benzophenone is used as initiator, tri-allyl-cyanurate as crosslink promoter. The polymer is UHMW-PE (Hizex 145M), however the reported strength and modulus are low (0.5 GPa and 10 GPa respectively).

5.3.4 Crosslinking of the drawn fibre.

5.3.4.1 Gamma/E-beam irradiation.

Klein et al. [15] irradiated a gel-spun UHMW-PE fibre produced by DSM (M_w 1.63 $*10^6$ D) by gamma irradiation in vacuum and in an acetylene atmosphere. The crosslink efficiency is much larger in the presence of acetylene. The gel fraction was about 95% already at the lowest irradiation dose (70 kGy), decreasing to approx. 80% at high dose. Only a fibre with a relatively high dose (900 kGy) has been evaluated. The creep properties were degraded for all loads tested (0.2-1.7 GPa). It is claimed that a weak chemical network is formed. The data however show, that the network contribution to the load dos not increase. The creep is higher especially because of the higher activation volume of the crystalline process. Regrettably no data are available for fibres that received a lower dose, and had an even higher gel fraction. As a crosslink network is already formed at a low dose, and as chain scission certainly would be lower, better results could have been expected. An aspect that was not considered, is the distribution of the acetylene gas in the fibre. As the sample holder was filled only 30 minutes before starting the irradiation, and as the diffusion constant decreases strongly with increasing draw ratio [35], it may well be that only the surface of the fibre is impregnated and crosslinked effectively.

Crosslinking of gel-spun fibres with high energy radiation was also studied by de Boer et al. [36,37] and Dijkstra et al. [38-41]. for realising improved thermal and creep resistance. However only a strong deterioration of the mechanical properties, including the creep, was observed.

High sensitivity of gel-spun fibres to low dose e-beam irradiation was also shown by Burkhard [31]. Both a decrease in the breaking strength and yield stress (indicating a lower creep resistance) were observed.

Engelen [42] studied the possibility of using trans-1,4-polybutadiene (tr-PB) as a crosslink promoter for improving the creep and thermal properties of UHMW-PE. The crosslink efficiency did not depend very strongly on the presence of tr-PB. E-beam irradiation resulted in an impairment of the creep resistance, but much less severe for the blends as compared with the polyethylene reference. The blends of tr-PB and UHMW-PE possess in an enhanced resistance against high energy radiation.

Beckham and Spiess [43] described a polymer that can be crosslinked preferentially in the crystalline state, the polymer is poly-(1,2,3-tetracosadiyne). It is thought that such systems offer possibilities for realising ductile crosslinked products, as the amorphous phase is not crosslinked. Crosslinking in the crystalline phase is possible because of the segregated crystallisation of the double bond pairs. Selective crosslinking occurs to doses up to 100 kGy.

5.3.4.2 Photo-crosslinking of the drawn fibre

Photo-crosslinking of ultra-high strength polyethylene fibres, impregnated before drawing, is described by Yan [44], and Penning [45,46] and de Boer et al. [47].

Penning studied the effect of crosslinking by UV irradiation of a gel-spun fibre (strength 3.8 GPa) impregnated with dicumyl-peroxide from a 12% solution cyclohexane. Crosslinking was realised through UV-irradiation during 20-150 hours. The crosslink to scission ratio was relatively low; approximately 1. A small decrease of the plateau creep rate (by a factor 6) was observed. The duration of the irradiation

did not have a significant influence on the creep rate improvement. Unexpectedly, it was found that the UV resistance of the impregnated samples was improved.

De Boer et al demonstrated UV-crosslinking of a gel-spun UHMW-PE fibre [47]. The fibre was impregnated before drawing, and contained 17% di-cumyl-peroxide. Irradiation was performed directly after drawing. The gel fraction was up to 64%, the maximum strength of the fibre was 1.8 GPa. It was concluded UV-crosslinking is an option for the realisation of high strength crosslinked fibre. Creep data were not reported.

Chen and Rånby [48,49] impregnated gel-spun UHMW-PE fibres (Spectra 900) with benzophenone in the vapour phase, at a temperature of 100°C. The initiator absorption was up to 0.8 %. UV-crosslinking was performed at 130°C using radiation with a wavelength ≥ 300 nm. A high gel fraction (up to 90%), and an increased temperature resistance were reported. The primary, reversible, creep increased. An improved resistance to secondary creep was claimed. The data available do not allow to quantify the creep improvement.

Zamotaev [50] demonstrated the possibility to impregnate and crosslink highly oriented gel-spun tapes and fibres with sulphuryl-chloride, by exposure to its vapour at room temperature, followed by UV-irradiation.

5.3.4.3 Chemical crosslinking

De Boer et al. [47] studied the crosslinking of gel-spun fibres containing di-cumyl-peroxide (DCP). Up to 50 % DCP was introduced in the non drawn fibres by swelling them in a solution of n-hexane. Drawing was done at 150°C, implying that some decomposition of the peroxide and crosslinking of the fibre occur already during drawing. The mechanical properties were poor, especially at high initiator content, because of the lower maximum draw ratio. Crosslinking resulted in brittle failure, and in elimination of the fibrillar structure. The time rupture under load was significantly longer. Creep data were not reported.

Chemical crosslinking of gel-spun fibres using chloro-sulphonation was studied by Penning et al. [46]. Chloro-sulphonation showed to be ineffective in an

drawn gel-spun fibre. For a fibre pre-treated with chloro-sulphonic acid before drawing, lower creep was observed, both initially and on further treatment. Prolonged chloro-sulphonation however also resulted in a significant strength reduction.

Yagi [51] reported grafting silane to the polymer chains before spinning. The drawn fibres were crosslinked in boiling water. An especially effective combination is vinyl-tri-ethoxy-silane, grafted with Perhexa B (2-5 di-methyl- 2-5 di(terts-butyl-peroxy)-hexine-3). Also Toyobo applied a patent on silane grafted and crosslinked gel-spun fibres [52].

5.4 Discussion

Improving the creep resistance of highly oriented polyethylene has been a subject of intensive research. All successful routes for improving the creep resistance of melt-spun fibres also have been tried for gel-spun fibres. However, due to the limited success, other routes have been evaluated too.

Methods for improving the creep properties that rely on modification of the polymer before drawing also influence the drawability; the maximum draw ratio decreases significantly, typically by a factor 2 (easy draw, easy creep). Using the results and model parameters reported in chapter 3, the effect of drawing can be estimated. The creep rate typically is increased by 1 to 2 orders of magnitude if the draw ratio is reduced by a factor 2. For evaluating improvements in the creep resistance two situations can be considered; creep properties at equal draw ratio (or Young's modulus), and creep properties at the maximum draw ratio for each fibre. Mostly the first possibility has been chosen; and the effect of the method tested is overestimated.

Polymer concentration [45,46], branching [13, 25, 26,28], chlorinating [27] and crosslinking before drawing [2] or early in the drawing process [29, 30, 32,33] are methods that influence draw ratio. The improvement realised at maximum draw ratio typically is one order of magnitude or less. The merit of using any of the methods mentioned above is, that by these methods fibres can be produced with a fair balance between short term (Young’s modulus, and strength) and creep properties.

Optimisation of any of these methods mentioned above can result in a limited further improvement of the creep properties. The most obvious candidate is the use of branched polymers, the results obtained with melt-spun as well as gel-spun fibres are at least as good as with any of the other methods. Furthermore the impact on the process is smaller than with crosslinking before drawing or chlorinating, that requires an additional processing step on the feedstock polymer.

Crosslinking of the drawn fibre using high energy has resulted in a decrease of the creep resistance [31,15] due to an unfavourable crosslinking to chain scission ratio [31,36-39]. The possibilities of crosslinking gel-spun fibres in a sensitising atmosphere have not been evaluated fully; low dose crosslinking of gel-spun fibres in acetylene atmosphere is an option [3] that has not been evaluated. Annealing before irradiation is instrumental for minimising chain scission [41].

Low energy crosslinking such as photo-chemical and thermal crosslinking has several merits; chain scission is reduced and is limited to the non-crystalline phase. A major problem is the addition of the reactants to the fibre. Adding a reactant early in the process is possible, but it is complicating the production process. Furthermore it has been shown that large quantities of the reactant are required for obtaining any improvement [45,46]. Impregnation of the drawn fibre is hindered by its high crystallinity and diffusion barrier properties. Vapour phase impregnation may be an option. UV-crosslinking of gel-spun fibres after gas or vapour phase impregnation of gel-spun fibres has been demonstrated [48-50]. Rånby et al. [48] suggested that by this method creep improvements can be realised for gel-spun fibres.

Most methods for improving the creep resistance of gel-spun polyolefin fibres mentioned above, are optimisations of methods that have been tried before on melt-spun fibres.
Two methods can be mentioned that use a mechanism that has not been tested before.

In the first method a polymer is used that can be crosslinked (after drawing) in the crystalline phase. Beckham and Spiess [43] studied such a polymer; 1,2,3 tetra-cosecadiyne, a linear flexible polyolefin with conjugated double bonds at regular

distances. They demonstrated selective crosslinking in the crystalline phase by high energy irradiation. This peculiar behaviour is caused by the presence of segregated double bonds in the crystalline phase. Crosslinking exclusively this crystalline phase is expected to result in a highly ductile product [43]. For these study non-oriented samples have been used; it is not known if the double bonds interfere with the drawing process.

In the second method use is made of the fact that irradiation of the fibre at an advanced stage of drawing with high energy radiation, results in an enhanced drawability. The reason of the enhanced drawability is due to chain scission, most probably of taut tie molecules [40]. A enhanced yield stress at 100°C was reported after further drawing such the irradiated fibre [31]. This suggest that improvements in the creep resistance can be realised in this way. Preferably, irradiation should be done shortly before drawing, and drawing in inert atmosphere, as this will help to eliminate remaining radicals.

5.5 Conclusions

All methods evaluated for improving the creep properties that rely on modification of the polymer (branching, chlorinating, crosslinking) before drawing also influence the drawability. Compared at the maximum draw ratio of the fibres the creep of the modified fibres is comparable or only slightly better than that of the non modified fibres. Branching seems to be the most effective of this type of modification. The advantage is, that it enables production of fibres with intermediate modulus with relatively good creep properties.

Photochemical and thermally induced crosslinking are options for crosslinking drawn gel-spun polyethylene fibres with minimal chain scission. In this way a network can be formed without degradation of the short term mechanical properties. Initiators introduced in the fibre before drawing are little effective, furthermore the presence during the process interferes with the gel-spin process. The initiators should be therefore be introduced after drawing of the fibres. Impregnation of drawn fibres with initiators from the vapour phase has is a possibility. In the following chapters several methods for impregnation and crosslinking of gel-spun fibres will be studied.

5.6 References

1 M.A .Wilding and I.M. Ward, Plastics and Rubber Proc. Appl., **1**, (1981), 167

2 P.G. Klein , J.A. Gonzalez-Orozco, I.M. Ward, Polymer, **35**, 10, (1994), 2044

3 J. Rasburn, P.G. Klein and I.M. Ward, J. Polym. Sci., B, Polym. Phys., **32**, (1994), 1329

4 X. LU, Z. Zhou, N. Brown, Proc. Antec, (1996), 2107

5 L.J. Rose, A.D. Channel, G. Capaccio, J. Appl. Polym. Sci., **54**, (1994), 2119

6 I.M. Ward, Macromol. Symp., **98**, (1995), 1029

7 J. de Boer, P.F. van Hutten, J. Mater. Sci., **19**, (1984), 428

8 R. Hikmet, P.J. Lemstra and A. Keller, Coll. Polym. Sci., **265**, (1987), 185

9 K. Yagi, H. Hiroyiku, Japanese patent, JP 304484/87, (1987)

10 J. de Boer, A.J. Pennings, Polym. Bull., **5**, (1981), 317

11 J. de Boer, A.J. Pennings, Polym. Bull., **7**, (1982), 309

12 I.M. Ward and M.A. Wilding, J. Polym. Sci., Polym. Phys., **22**, (1984), 561

13 Ohta et al, J. Polym. Sci., B, Polym. Phys., **32**, (1994), 261

14 Y. Ohta, H. Yasuda, A. Kaji, Polym. Pre-prints Japan, **43**, 9, (1994), 3143

15 P.G. Klein, D.W. Woods, I.M. Ward, J. Polym. Sci., B, Polym. Phys., **25**, (1987), 1359

16 P.G. Klein, N.H. Ladizeski, I.M. Ward, J. Polym. Sci., B, Polym. Phys., **24**, (1986), 1093

17 Raychem Corp., WO-86-05739

18 W.G. Perkins, V.T. Stannett, R.S. Porter, Polym. Eng. Sci., **18**, 6, (1978), 527

19 I.M. Ward, D.W. Woods, W.K. Busfield, GB8332952, (1983), and EP 0145 475, (1984)

20 D.W. Woods, W.K. Busfield, and I.M. Ward, Polym. Comm. **25**, 9, (1984), 298

21 D.W. Woods, W.K. Busfield, and I.M. Ward, Plastics and Rubber Proc. Appl., **5**, 2, (1985), 157

22 D.W. Woods, W.K. Busfield, and I.M. Ward, Plastics and Rubber Proc. Appl., **9**, 3, (1988), 155

23 D.W. Woods, I.M. Ward, Report IRC in Polym, Sci, and Technology, University of Leeds.

24 R.W. Appleby and W.K. Busfield, J. Mater. Sci., **29**, (1994), 227-231

25 C.W.M. Bastiaansen, NL 8602745, JP194856, (1987), EP 269151, (1987)

26 K. Yagi, EP 0 290 141, (1988)

27 R. Steenbakkers-Menting, Thesis Eindhoven University of Technology, (1995), ch. 5

28 Canadian patent 1 276 065, (1984)

29 N.J.A.M. van Aerle, G. Crevecoeur, P.J. Lemstra, Polym. Comm., **29**, (1988), 128

30 G. Akay, F. Cimen, T. Tincer, Radiat. Phys. Chem., **36**, 3, (1990), 337

31 M.E.M. Burkhard, N.S.J.A. Gerrits, DSM internal report, April (1993)

32 H. Nishigawa et al, JP 63-326899, (1988), JP 63-326900, (1988)

33 I. Sakano, JP 88-326898, (1988)

34 D Suwanda, X.L. We, S.T Balke, (1993), Canadian patent 2,147 746

35 J.A. Webb, D.I. Bower, I.M. Ward, P.T. Cardew, Polymer, **33**, 6, (1992), 1321

36 J. de Boer and A.J. Pennings, Polym. Bull., **5**, (1981), 309

37 J. de Boer and A.J. Pennings, Polym. Bull., **5**, (1981), 317

38 D.J. Dijkstra and A.J. Pennings, Polymer Bull. **17**, (1987), 507

39 D.J. Dijkstra and A.J. Pennings, Polymer Bull. **20**, (1988), 557
40 D.J. Dijkstra and A.J. Pennings, Polymer Bulletin **19**, (1988), 73
41 D.J. Dijkstra and A.J. Pennings, Polymer Bulletin **19**, (1988), 481
42 Y.M.T. Engelen, C.W.M. Bastiaansen, P.J. Lemstra, Polymer, **35**, 4, (1994), 729
43 H.W. Beckham and H.W. Spiess, Macromol. Chem. Phys., **195**, (1994), 1471
44 Q. Yan, Hecheng Xianwei Gongye, **14**, 4, (1993), 15
45 J.P. Penning, Ph-D Thesis University of Groningen, February (1994), ch. 6.
46 J.P. Penning, H.E. Pras, A.J. Pennings, Coll. Polym. Sci., **272**, (1994), 664
47 J. de Boer, H.-J. van den Berg, and A.J. Pennings, Polymer, **25**, (1984), 515
48 Y.L. Chen and B. Rånby, J. Polym Sci, A, Polym Chem., **27**, (1989), 4051
49 Swedish patent, SE 8802943, (1988)
50 I. Chodak and P.V. Zamotaev, Die Angewandte Makromolekulare Chemie, **210**, (1993), 119
51 K. Yagi, M Hitoshi, EP 0 229 477, (1986)
52 Japanese Patent 4-214205, (1992)

Chapter 6 Improvement of the creep resistance of gel-spun UHMW-PE fibres by vapour phase impregnation with chlorine containing photo-initiators and UV irradiation

6.1 Introduction

From the previous chapters the conclusion is that the interesting option for improving the creep resistance of gel-spun UHMW-PE fibres is to reinforce the strength of the network process. The network process can be strengthened by increasing the slip resistance of a relatively small fraction of the molecular chains.

Although high energy irradiation induced crosslinking is at least partly successful for creating a network in melt-spun fibres [1,2] it is not applicable for highly drawn gel-spun fibres [3-5]. On the one hand, crosslinking in the crystalline phase is not possible because the chains are too far apart to form a covalent bond. On the other hand the effect of chain scission is more important in gel-spun UHMW-PE fibres, because of the high molecular weight, even a small degree of chain scission has a significant influence.

Low energy crosslinking, using radical forming compounds, such as peroxides, and UV initiators, are options for crosslinking polyethylene with a minimum of chain scission [6]. Both methods require the presence of initiators in the fibre. The initiators can be added to the fibre in different stages of the process: a) to the polymer in the solvent [7,8], b) to the non-drawn gel-spun fibre [5], c) to the fibre at an intermediate stage of drawing [9,10], and d) in the fully drawn fibre [6,11,12]. Introducing the initiator in the fully drawn fibre, has the advantage that it does not interfere with the fibre production process.

UV-crosslinking of highly oriented gel-spun UHMW-PE fibres, after impregnation of the drawn fibre, is possible without deteriorating the mechanical properties [6,11,12]. Chen and Rånby [11] impregnated a commercial gel-spun fibre (Spectra 900, rather surprisingly the Young's modulus measured, 46 GPa, was much lower than expected for this fibre) by exposing the fibre to benzophenone vapour at elevated temperature (100°C) for 24 hours. Efficient crosslinking (gel-fraction up to 91%) and

an improvement of the thermal resistance was demonstrated. A single creep experiment (stress 0.46 GPa at room temperature during 1 week) was reported. The creep of the treated fibre is initially higher than that of the reference, after 6 days the creep of the treated fibre is lower than that of the reference, at the end of the experiment the creep rate of the treated fibre is significantly smaller than that of the reference.

Penning [6] crosslinked a fibre with a Young's modulus of 129 GPa by UV radiation (during 24-100 hours) using di-cumyl-peroxide as an initiator. Impregnation was done from a solution in cyclohexane. A relatively small creep improvement at a high stress (1.9 GPa) was reported.

Zamotaev and Chodak [12] demonstrated the possibility to impregnate and crosslink gel-spun tapes of different draw ratio and a commercial gel-spun fibre (Spectra 900) with sulphuryl-chloride by exposure to the vapour phase at room temperature, followed by UV-irradiation for a few minutes. Creep data were not reported. Table 6.1 summarises the literature data on impregnated and UV crosslinked fibres.

Table 6.1 Literature data on post drawing impregnation and UV crosslinked fibres.

	Rånby [11]	**Penning [6]**	**Zamotaev [12]**
Young's modulus	46 GPa	129 GPa	66 GPa
Breaking stress ref./treated	2.5/2.5 GPa	3.8/3.8 GPa	2.2/2.1 GPa
Initiator	BP	DCP	$S0_2Cl_2$
Impregnation temperature	100 °C	60 °C	Ambient
Duration	48 hour	120 hour	24 hour
Radiation	HP Hg lamp	Hg, 253 nm	HP Hg lamp
Atmosphere	N_2	N_2	Air
Temperature during irradiation	135 °C	50 °C	Ambient
Irradiation time	8 min	25 hr	1 min
Creep rate (stress GPa)	none (0.46 GPa)	1-2 $10^{-}6$ s^{-1} (1.9 GPa)	-
Thermal resistance	> 195 °C	-	>200°C

Many initiators exist for photo-treatment of polyethylene [13,14]. Inorganic and organic chlorinated compounds belong to the most effective photo-initiators for polyethylene [15]. Low molecular weight chlorine containing initiators seem to have certain advantages relevant for crosslinking gel-spun fibres; a) the crosslink yield is high, allowing to use a low irradiation dose and a short irradiation time, b) their high vapour pressure enables impregnation in a short time at room temperature, and c) the relatively small molecules may be able to penetrate relatively well into the fibres.

Photo-chemical reactions in polymers containing a photo-initiator are: grafting, crosslinking and chain scission [13]. The first two are expected to contribute to an enhanced creep resistance. Side groups grafted on the polymer chain can also influence other properties such as: hydrophilicity and thermal stability [16], especially Sulphur containing initiators, such as S_2Cl_2, and $PSCl_3$ can improve the thermal stability of the treated polyethylene [17] because sulphur grafted to the chain acts as radical scavenger.

It is the objective of this chapter to investigate the possibilities for improving the creep (and thermal) resistance of gel-spun UHMW-PE fibres of different draw ratio by vapour phase impregnation and irradiation at room temperature using chlorine containing initiators.

6.2 Initiators

Four inorganic chlorine containing photo-initiators: sulphur-monochloride (S_2Cl_2), thio-phosphor-trichloride ($PSCl_3$), phosphor-trichloride (PCl_3), sulphuryl-chloride (SO_2Cl_2), and also four organic initiators: tetra-chloromethane (CCl_4), hexa-cloroacetone (CCl_3-(C=O)-CCl_3), di-fluoro-tetra-chloroethane ($CFCl_2$-$CFCl_2$), and tri-chloroethylene ($CHCl=CCl_2$), have been used. The initiators have been proposed and made available by P. Zamotaev, Institute of Bio-organic and Oil Chemistry Research in Kiev. Selection criteria were: the efficiency for UV crosslinking of PE, stability, compatibility with polyethylene and high vapour pressure at room temperature. The initiators are of the photo-fragmentation or photo-cleavage type; when UV light of a suitable wavelength is absorbed, the initiator splits off a chlorine

atom or decomposes otherwise. Typical examples of photochemical reactions with sulphuryl-chloride and sulphur-mono-chloride are given in schemes 1 and 2 [17]

Scheme 1 Possible reactions in polyethylene containing SO_2Cl_2

$SO_2Cl_2 + h\nu$	$\rightarrow$	$^{\bullet}SO_2Cl + Cl^{\bullet}$	
$Cl^{\bullet} + RH$	$\rightarrow$	$R^{\bullet} + HCl$	
$R^{\bullet} + Cl^{\bullet}$	$\rightarrow$	RCl	(I)
$R^{\bullet} + {}^{\bullet}SO_2Cl$	$\rightarrow$	RSO_2Cl	(II)
$RSO_2Cl + h\nu$	$\rightarrow$	$RSO_2^{\bullet} + Cl^{\bullet}$	
$RSO_2^{\bullet}$	$\rightarrow$	$R^{\bullet} + SO_2$	
$R_1^{\bullet} + R_2^{\bullet}$	$\rightarrow$	$R_1\text{-}R_2$	(III)
$R_1^{\bullet} + R_2SO2^{\bullet}$	$\rightarrow$	$R_1SO_2R_2$	(IV)

Scheme 2 Possible reactions in polyethylene containing S_2Cl_2

$S_2Cl_2 + h\nu$	$\rightarrow$	$^{\bullet}SCl + {}^{\bullet}SCl$	
$2^{\bullet}SCl + S_2Cl_2$	$\rightarrow$	$2SCl_2 + S_2$	
$^{\bullet}SCl + h\nu$	$\rightarrow$	$S^{\bullet} + Cl^{\bullet}$	
$S^{\bullet} + SCl$	$\rightarrow$	$S_2 + Cl^{\bullet}$	
$R^{\bullet} + Cl^{\bullet}$	$\rightarrow$	RCl	(I)
$RH + Cl^{\bullet}$	$\rightarrow$	$R^{\bullet} + HCl$	
$R^{\bullet} + S_2$	$\rightarrow$	$RS_2^{\bullet}$	
$R^{\bullet} + S_2Cl_2$	$\rightarrow$	$RS_2Cl + Cl^{\bullet}$	(II)
$R_1^{\bullet} + R_2^{\bullet}$	$\rightarrow$	$R_1\text{-}R_2$	(III)
$R_1^{\bullet} + R_2S2^{\bullet}$	$\rightarrow$	$R_1S_2R_2$	(IV)

Reactions especially relevant for creep improvement are grafting side groups (I,II), and direct and indirect crosslinking (III, IV). Increased thermal stability has been observed due to non oxidised sulphur groups grafted to the chain by reactions II and IV [17].

The inorganic compounds are extremely reactive, in the presence of water the compounds decompose forming hydrochloric acid. This is a disadvantage for practical application. The organic compounds are stable compounds under the conditions required for the application and can be used more easily. The crosslink efficiency of such organic compounds generally increases with the number of chlorine atoms [16].

6.3 Experimental

6.3.1 Fibres

The properties of the fibres used are given in table 6.2.

Table 6.2 Mechanical properties of fibres used for impregnation and crosslinking experiments.

	Titre	Modulus	Strength	Elongation	Crystallinity
	tex[1]	GPa	GPa	%	%[2]
Sp900	132	88	2.7	3.5	~80
PE1	58	38±0.5	1.7±0.09	5.7	56
PE2	43.	63±0.7	2.3±0.10	4.5	63
PE3	33.	86±1.6	2.8±0.12	3.9	71
PE4	25.	111±2.3	3.2±0.20	3.4	77
PE5	21.	131±3.8	3.3±0.35	3.0	82
PE6	11	135±3.7	3.6±0.29	3.6	77

[1]tex: weight in gram/10000 m.

[2] calculated from the enthalpy

Spectra 900 ® and PE6 (Dyneema SK75) are commercial gel-spun fibres. PE1-PE5 (M_w 2 10^6 D), are experimental gel-spun fibres of different draw ratio supplied by DSM

6.3.2 Impregnation

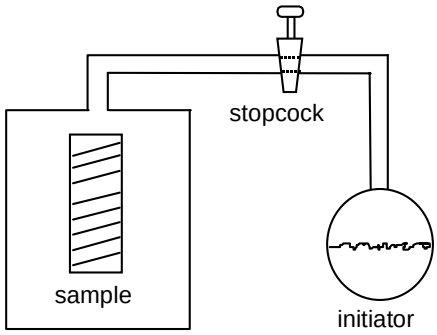

Figure 6.1 Impregnation set up

The fibre sample to be impregnated was wound tightly on, and fixed wit adhesive tape onto a quartz tube with a diameter of approx. 20 mm. A single layer of fibres was applied. The tube was placed in a chamber connected to a flask containing the liquid initiator, see figure 6.1.
The weight gain was determined on separate fibre samples exposed to the vapour, or (for the PE1-PE5 series) on the samples to be treated. In the latter case the weight gain of the tube with sample was determined. The temperature during impregnation was 20±2°C.

The impregnation was performed by exposing the fibre to the initiator vapour at room temperature during 24 hours. For impregnating PE1-PE6 fibres a selection of initiators was used: tri-chloro-ethylene ($CHCl=CCl_2$), phosphorous-tri-chloride (PCl_3) and sulphuryl-chloride (SO_2Cl_2). For tri-chloro-ethylene the absorption in 24 hours was small, therefore the minimum impregnation time for this initiator was extended to 48 hours.

6.3.3 UV-Irradiation

Immediately following impregnation, the sample, while still wound on the quartz tube, was irradiated. The sample was placed on a rotating table (rotation period 3 seconds) in front of the light source. The temperature was not controlled, due to the irradiation, the temperature increased, the estimated maximum temperature is 50°C.

The irradiation time was 3 minutes, unless specified otherwise. The light source was a 1 kW high pressure Mercury lamp (DRT-1000), giving a broadened line spectrum with a total flux of approx. 35 kLumen. The spectrum extends from 200 nm to 600 nm, with a maximum intensity at 366 nm. The for this research most important lines are: 254 nm, 265 nm. 302 nm and 313 nm. The lamp to sample distance was approx. 180 mm. The irradiation treatment was done in air. For studying the effect of the irradiation dose the sequence of impregnation and irradiation was repeated for PE1-PE5.

For PE6 (PE2-PE5): the irradiation source was a Hannovia 673 medium pressure mercury lamp, 0.4 kW, with the glass envelope removed. The sample to lamp distance was 100 mm.

6.3.4 Characterisation

Gel-fraction

The gel-fraction was determined by extraction for 14 hours of the soluble fraction in boiling xylene containing di-t-butyl-p-cresol as a stabiliser, while refreshing the solvent every two hours.

Thermal properties

The melting enthalpy, from which the crystallinity was calculated, was determined using a Perking Elmer DSC7. The calibration was done with Indium assuming a melting enthalpy of 28.45 J/g. About 0.5 mg fibre, cut to approx. 3 mm length was put with a small droplet of silicone oil in a 25 µl pan. The temperature scanned was 20-200°C, scan rate 10 °C/min.

Constrained melting and re-crystallisation experiments were performed at the University of Reading [18], on samples that were constrained in length by winding the fibre around a copper spool. Five Heating and cooling cycles were performed between 110°C and 190°C. The heating and cooling rates were 10 K/min.

Mechanical properties

The tensile properties of the PE1-PE6 fibres were determined using a Zwick 1474 universal tensile tester, fitted with pneumatic fibre grips (Orientec). The specimen

length was 300 mm, the test speed 50 %/min. The fibre cross-section was determined from the weight of a unit length of (non treated) fibre assuming a density of 970 kg/m^3.

The creep properties were determined using a temperature controlled creep rig. The elongation was determined with an optical displacement system with a resolution of 30 micron, and a maximum displacement of 100 mm. Before starting a creep experiment the sample was loaded for about 1 minute and allowed to relax for at least 15 minutes. The free sample length was 500 ± 2 mm. The limiting (or flow) creep rate was determined using the procedure given by Sherby and Dorn [19]. PE1-PE5 fibres were tested at a temperature of 40°C and a load of 0.6 GPa

IR-characterisation

Infra-red spectra were taken with 2 cm^{-1} resolution using a Matsson FTIR spectrometer, using non polarised radiation. The sample was a thin (single) layer of parallel filaments. The intensity of the 615 cm^{-1} band (C-Cl) relative to the intensity of the 720-722 cm^{-1} PE doublet ($GT_{m>4}G$) is used as an estimate for the amount of bound chlorine.

6.4 Results

6.4.1 Screening of UV-initiators

Table 6.3 gives the results of the screening experiments: the (approximate) concentration of the initiator in the fibre, the gel-fraction and the limiting creep rate.

Table 6.3 Results of treatment of Spectra 900 fibre

Initiator	**Vapour pressure (20 °C)** [20]	**Weight gain**	**Gel-fraction**	**Creep rate/ stress**
	Mbar	%	%	$s^{-1}*10^{-8}$/GPa
Untreated	-	-	0	4.5/0.46
S_2Cl_2	13 (27.5°C)	0.2	5	<1/0.50
CCl_3-(C=O)-CCl_3	-	0.3	10	3.1/0.82
$PSCl_3$	29 (25°C)	0.5	17	1.5/0.50
$CFCl_2$-$CFCl_2$	34.6	0.3	25	≈1/0.76
CCl_4	123	0.5	30	1.6/0.54
PCl_3	131	1.3	43	0.3/0.46
SO_2Cl_2	142	3.7	49	1.6/0.50
CHCl=CCl_2	80	0.4	65	<0.2/0.82

All treated samples possess a lower plateau creep rate than the untreated samples. Due to experimental limitations the load level could not be made equal in all experiments. In order to compare the results of the different initiators the creep rates were recalculated to equal stress using the relation given by Govaert [21,22]: $\varepsilon' \propto \sigma^{3.7}$. This correction does not change the conclusion that the most effective initiators, at least for the conditions chosen, are: tri-chloroethylene (CHCl=CCl_2) and phosphorous-trichloride (PCl_3, for PE6: S_2Cl_2). Treatment with sulphuryl-chloride (SO_2Cl_2) results in a relatively high gel-fraction, the effect on the limiting creep rate is however small. The three initiators mentioned were use for crosslinking fibres of different draw ratio.

Sulphur monochloride (S_2Cl_2) is relatively efficient for improving the creep, however not for crosslinking, because the gelcontent is very low.

6.4.2 Impregnation and UV crosslinking fibres of different draw ratio

Weight gain and gel-fraction

The weight gain was determined for fibres exposed to tri-chloroethylene at room temperature is given in figure 6.2.

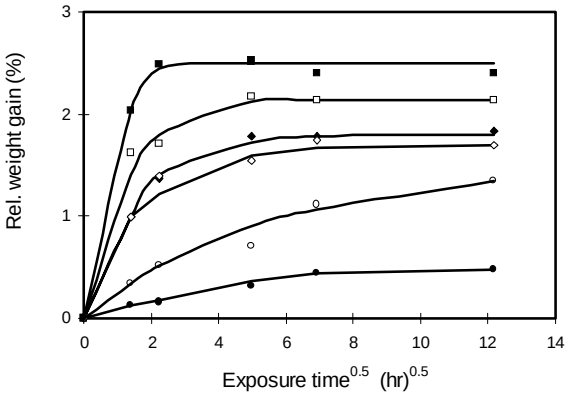

Figure 6.2 Weight gain for PE1-PE6 fibres exposed to tri-chloro-ethylene vapour at room temperature as a function of the square root of the exposure time. ■: PE1, □: PE2, ◆: PE3, ◊: PE4, ●: PE5, ○:PE6.

The equilibrium initiator uptake decreases with increasing draw ratio (PE1-PE5), especially for PE5 it is low. The behaviour of PE6, a commercial fibre, is at variance with that of the series PE1-PE5: the initiator uptake is higher than that of PE5 (whereas its modulus is even higher) and also the time dependence if the uptake is different. The commercial fibre PE6 (produced later than the experimental series PE1-PE5), is morphologically different (caused by differences in spinning/ quenching conditions). The absorption rate decreases with increasing draw ratio; equilibrium is reached for PE1 in a few hours, and for PE6 it requires more than 150 hours. The normal exposure time to tri-chloroethylene was 48 hours

The weight gain for the fibre samples to be crosslinked was determined from the weight gain of the sample wound on a quartz tube. The weight gain (table 6.4) given

is therefore the sum of the weight gain of the fibre sample itself and that of the quartz tube. Several samples were impregnated and irradiated for a second time, in table 6.4 the results are referred to as 1st and 2nd.

Table 6.4 Weight gain and gel-fraction of treated fibres

	$CHCl=CCl_2$				**PCl_3 (PE6:S_2Cl_2)**				**SO_2Cl_2**			
Fibre	Initiator %		Gel-cont. %		Initiator %		Gel-cont. %		Initiator %		Gel-cont. %	
	1st	2nd	1st	2nd	1st	2nd	1st	2nd	1st	2nd	1st	2nd
PE1	1.6		91		3.7	5.8	88	93	6.1	10.2	81	90
PE2	1.5		93		4.3	-	91	-	5.6	9.0	84	90
PE3	2.5	9.5	83	96	3.1	7.7	86	88	5.7	10.6	87	88
PE4	1.5	12.1	82	86	5.3	9.2	68	84	6.2	10.4	86	80
PE5	0.4		86		5.5	12.8	56	61	5.0	6.8	60	72
PE6	0.8		78		-		variable		-		80	

For $CHCl=CCl_2$ the weight gain during 48 hours exposure was 0.4-2.5%, roughly equal to that measured on the separate fibre samples. The weight gain at the second impregnation, after the first UV irradiation is significantly higher 7-10%. For SO_2Cl_2 and PCl_3 the weight gain during 24 hours impregnation is 3-6% for all samples, and approx. the same during the second impregnation.

The much larger amount of absorbed tri-chloro-ethylene at the second exposure could be due to physical changes (increased porosity caused by the first treatment) or chemical changes (an increase in compatibility or solubility due to chlorine containing groups grafted to the chain).

The gel-fraction decreases somewhat with increasing draw ratio (most clearly for PE5 and for fibres treated with the inorganic compounds PCl_3 and SO_2Cl_2). Treatment with of PE6 S_2Cl_2 resulted in a strongly varying gel-fraction (6-47%).

Repeating the impregnation and UV irradiation resulted in some further crosslinking.

Mechanical properties of the treated fibres

The effect of the treatment of fibres on the short term mechanical properties is given in table 6.5.

Table 6.5 Effect of treatment on the mechanical properties of PE1-PE6

Sample	Gel-content	Modulus	Breaking stress		Elongation
	%	GPa	GPa	%	%
PE1 reference	-	38.7±0.4	1.74±0.09	100	5.7
PE1 C_2HCl_3	91	-	1.26±0.03	72	-
PE1 PCl_3	88	-	1.11±0.13	64	-
PE1 SO_2Cl_2	81	-	1.37±0.16	79	-
PE2 reference	-	59.0±0.7	2.22±0.10	100	4.5
PE2 C_2HCl_3	93	60.5±1.1	1.48±0.06	67	2.8±0.1
PE2 PCl_3	91	-	1.63±0.21	73	-
PE2 SO_2Cl_2	84	63.1±1.0	1.66±0.11	75	3.0± 0.3
PE3 reference	-	80.9±1.6	2.58±0.12	100	3.9
PE3 C_2HCl_3	83	81.5±1.6	1.77±0.06	69	2.3±0.1
PE3 PCl_3	86	-	2.06±0.13	80	-
PE3 SO_2Cl_2	87	82.8±1.9	2.04±0.08	79	2.7±0.1
PE4 reference	-	107.5±2.2	2.91±0.19	100	3.4
PE4 C_2HCl_3	82	104.6±1.6	2.09±0.09	72	2.3±01
PE4 PCl_3	68	-	2.03±0.13	70	-
PE4 SO_2Cl_2	86	102.0±1.8	2.19±0.10	75	2.4±0.1
PE5 reference	-	125.2±3.7	3.02±0.34	100	3.4
PE5 C_2HCl_3	86	116.9±2.2	2.23±0.16	74	2.1±0.2
PE5 PCl_3	56	-	2.09±0.13	69	-
PE5 SO_2Cl_2	60	131.0±1.9	2.22±0.12	74	2.2±0.1
PE6 reference	-	126± 3.6	3.50±0.3	100	3
PE6 $CHCl_3$	78	123±3.4	3.1±0.2	89	2.6
PE6 S_2Cl_2	4-47	120±3.7	3.2±0.2	91	2.8
PE6 SO_2Cl_2	80	126±2.7	3.2±0.2	91	2.7

The effect of the treatment on the modulus is small, if any at all, however both breaking stress and strain to failure of the treated fibres are significantly smaller than that of the non-treated fibres. The effect of treatment on mechanical properties does not depend on draw ratio (PE1-to PE5); the average strength retention is between 65% and 75% for fibres treated with C_2HCl_3 and with PCl_3, and between 70% and 80% for SO_2Cl_2 treated fibres. PE6 is more resistant with 90% retention. Repeating the treatment does not result in a significant further decrease of the short term mechanical properties. The relation between gel-content (crosslinking) and decrease of strength (chain scission) is not strong, viz data for PE5 and PE6. Both processes may well be independent, it suggests that different sites are involved.

Creep

Creep curves for $CHCl=CCl_2$ treated and non-treated fibres PE1-PE5 are given in figures 6.3 and 6.4

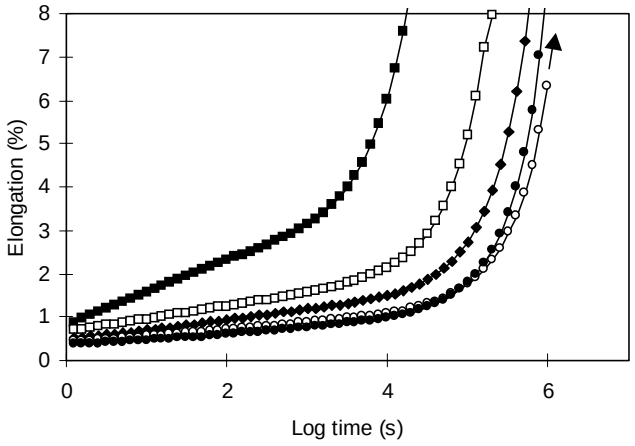

Figure 6.3 Creep of non crosslinked PE1-PE5 fibres. ■: PE1, □: PE2, ♦: PE3, ●: PE4, ○: PE5

The non-treated fibres show both reversible creep deformation, proportional to log-time, and flow creep. For the treated fibres the flow creep contribution is absent; only shortly before rupture, an increase in the creep rate is observed (figure 6.4).

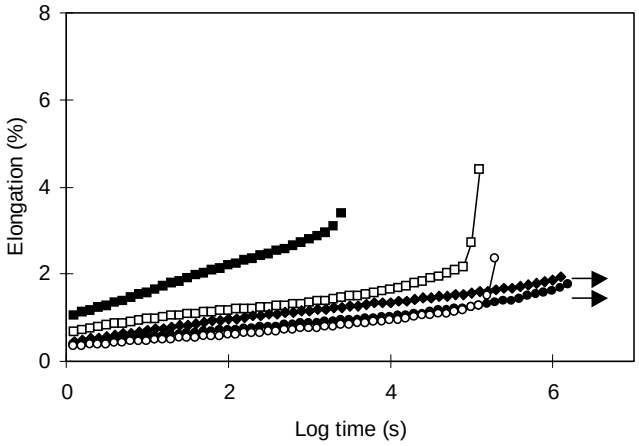

Figure 6.4 Creep of CHCl=CCl_2 crosslinked PE1-PE5 fibres. ■: PE1, □: PE2, ♦: PE3, ●: PE4, ○: PE5

The effect of the treatment on the creep behaviour of PE3, for different initiators is shown in figure 6.5

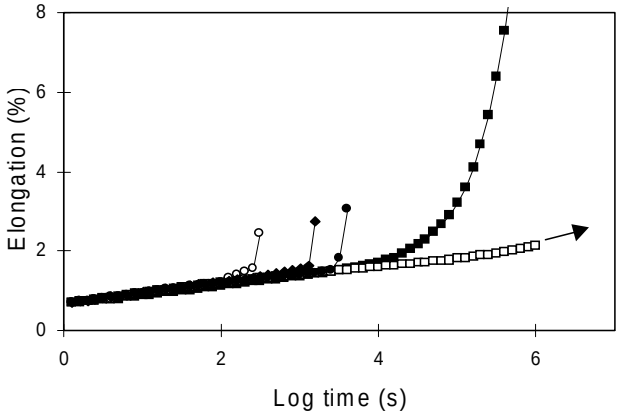

Figure 6.5 Creep of a crosslinked PE3 fibre.■: untreated, □: CHCl=CCl_2, ♦:CHCl=HCl_2 (2) ●: PCl_3, ○ SO_2Cl_2*

The reversible creep is not influenced. The treated fibres fail before any significant flow creep has been observed. The time till rupture for some treated samples (PCl_3, SO_2Cl_2 and CHCl=CCl_2 twice treated) is short.

Figure 6.6 gives Sherby and Dorn plots for the creep curves of figure 6.5.

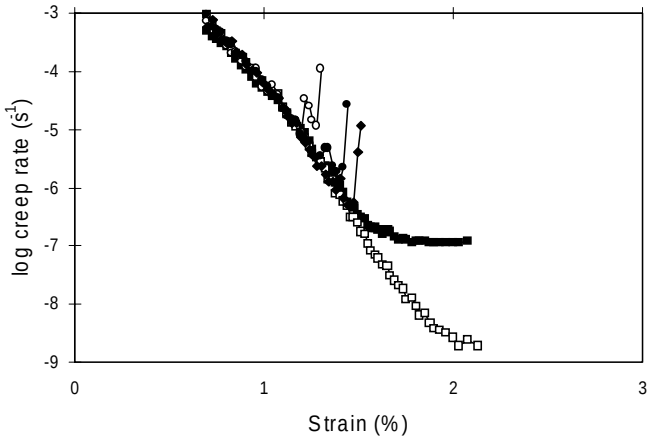

Figure 6.6 Sherby and Dorn plot for $CHCl=CCl_2$ treated PE3 fibre, □: $CHCl=CCl_2$, ♦:$CHCl=HCl_2$ (2) ●: PCl_3, ○: SO_2Cl_2.*

For $CHCl=CCl_2$ treated PE3 fibres a limiting creep rate of about than 10^{-9} /s can be estimated; while for untreated fibre the plateau creep rate is 1.5 10^{-7}/s.

Temperature resistance of crosslinked fibres.

The crosslinked fibres resist melting (at least partially) when they are constrained. Figure 6.7 gives the result of temperature cycling between 380 and 477 K for several fibres, crosslinked with sulphuryl-chloride. Shown are the first heating curve for PE3 (the melting curves for PE1 and PE5 were like that of PE3 and are left out) and the second heating curve for PE1, PE3 and PE5. Further cycling did not have a significant influence; the third, fourth, and fifth heating curves are essentially equal to the second.

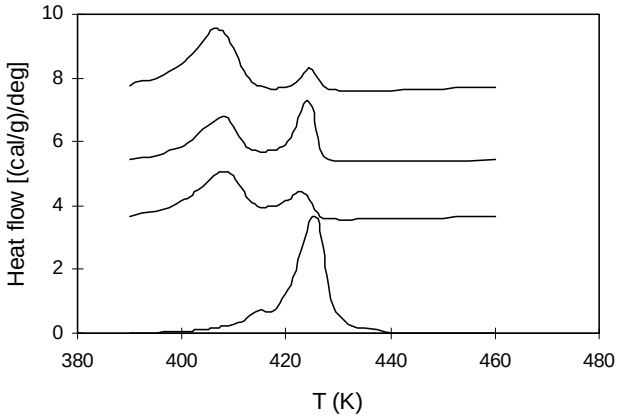

Figure 6.7 Restrained temperature cycling of SO_2Cl_2 crosslinked PE3 fibre, reproduced with permission from J.C. Teckoe [18]

The first heating cycle shows a weak melting peak for folded chain crystalline polyethylene (at 415 K) and a strong orthorhombic to hexagonal transition (at 427 K). The re-melting curves (2nd–5th heating run) show two peaks, one peak at about 407K for melting of folded chain polyethylene, the other peak at about 424 K for the orthorhombic-to hexagonal transition. It shows that for PE3 approx. 50% of the chains has resisted coiling and is re-crystallised in the extended chain conformation. The fraction of chains that shows reversible orthorhombic to hexagonal transition is much larger for PE3 than for either PE1 or PE5.

The creep of PE6 and (PE4) impregnated with: tri-chloroethylene, suplhuryl-chloride and sulphur-monochloride was measured at 60°C and a load of 0.8 GPa. Figure 6.8 gives a typical result for tri-chloro-ethylene treated PE4 and PE6 (impregnation time 48 hours, irradiation time 3 minutes) fibres and the references. For PE6 the creep of the treated and untreated fibre is the same. In contrast for treated PE4 (and PE3) flow creep was not observable.

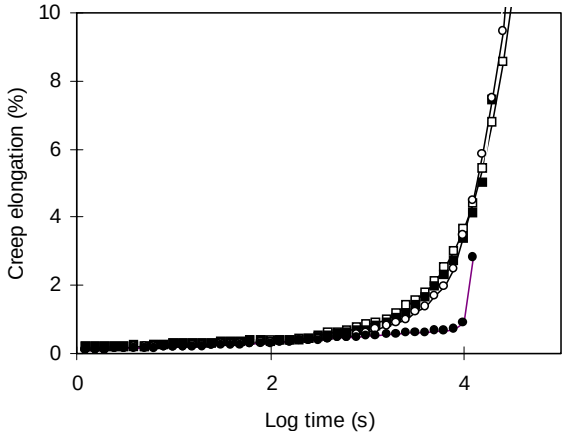

Figure 6.8 *Creep of UV crosslinked PE4 and PE6 fibres, stress 0.8 GPa, temperature 60°C. □: PE6 untreated, ■: PE6 CHCl=CCl$_2$ treated, ○: PE4 untreated, ●: PE4 CHCl=CCl$_2$ treated*

6.5 Discussion

While vapour phase impregnation followed by UV-irradiation results in a network, and in suppression of the flow creep, not all fibres can be crosslinked equally easily. For instance PE1-PE4 can be crosslinked more easily than Spectra 900, PE5 and PE6. For PE6 the crosslinking had no influence on the flow creep (at a of load: 0.8 GPa). Below the factors that determine the efficiency for UV crosslinking of the fibres tested, are considered.

Creep improvement, by UV-crosslinking or by grafting side groups, relies on the presence of an initiator at locations where crosslinking or grafting can occur, and thus contribute to an increased resistance to chain slip. Impregnation resulted in a mass gain varying from 0.2% to 12%, depending on the initiator, the fibre and impregnation conditions. An estimate can be made on the quantity of initiator required for effective crosslinking and grafting.

Only few crosslinks per chain are required for influencing the creep significantly; Hikmet and Lemstra [23] showed a significant effect on the creep, when the average segment length between crosslinks was reduced from 10^6 to $5x10^5$ kD. According to

Chodak [24], the amount of initiator required for crosslinking UHMW-PE with di-cumyl-peroxide, is less than 0.1%. Chen et al. [11] crosslinked gel-spun PE fibres containing 0.5-0.8% benzophenone. Given the low molecular weight of the most effective chlorine compounds, a concentration of the 0.1% should be adequate. Moreover creep can also be reduced by the presence of branches. Chlorinating of the chain, through direct substitution is one possible process. More bulky side groups can also be grafted onto the chain. Some possible reactions are given in schemes 1 and 2.

There are large differences in the mobility of the initiator. Whereas the lesser drawn fibres can be impregnated at room temperature to equilibrium in a short time, about 1 hour, for the more highly drawn PE5 and PE6 several days are required. The mobility of the initiator molecules (in the non-crystalline phases) is clearly restricted in the fibres of high draw ratio. At a more elevated temperature the chain mobility is higher and impregnation and crosslinking are enhanced. Treatment of the Spectra 900 fibre by room temperature impregnation and crosslinking resulted in relatively low gel-content. Rånby et al. reported gel-fractions up 91% after impregnation at 100°C and irradiation for 8 minutes at 120°C [11].

Constrained DSC measurements on crosslinked PE1, PE3 and PE5 fibres [18, figure 6.8], showed that the fraction chains that shows reversible orthorhombic to hexagonal transition is much larger for PE3 than for either PE1 or PE5. In PE3 a large fraction, about 50%, of the chains is constrained in the extended chain conformation in the melt. For both PE1 and PE5, this fraction is only about 10%. It is concluded that in PE1 the network is present but not able to constrain the extended chains.

The relative degree of reaction between the fibre and initiator can be estimated by concentration of bonded Cl-atoms (see reaction in scheme 1 and 2). In the infrared spectrum an absorption band at about 615/cm can be assigned to C-Cl bonds [28]. In figure 6.9, IR spectra are shown for PE2, PE4, and PE6.

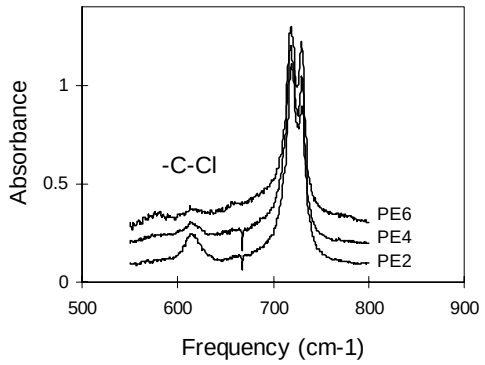

Figure 6.9 C-Cl absorption band in IR-spectra for PE2, PE4, and PE6.

The intensity of this band, relative to that of the strong polyethylene doublet at 720-722/cm is calculated as:

$$I_{C-Cl} = \frac{Abs_{615}}{0.5(Abs_{720} + Abs_{722})} \qquad 6.1$$

The values for $I_{C\text{-}Cl}$ are 0.145 (PE2), 0.08 (PE4) and <0.03 (PE6) respectively. The low concentration of bound chlorine atoms in PE4 and PE6 cannot be caused by a too low initiator content. The low degree of Cl-bonding may be due to a very low degree of penetration in the fibre, or to preferential formation of HCl in stead of R-Cl.

The most suitable initiator is tri-chloro-ethylene. For PE1-PE5 the flow creep and ductility can be suppressed completely (at a stress of 0.6 GPa), see figures 6.4, and 6.5, also for Spectra the creep and ductility are reduced significantly.

For most of the fibres the crosslink results in a deterioration of the (short term) mechanical properties, this is variance with the literature data (table 6.1), notably with those of Zamotaev [12]. PE1-PE5 seem to be more sensitive to UV damage than Spectra 900 and Dyneema SK75.
For PE1 to PE5 fibres produced from the same precursor, the sensitivity to the treatment does not depend on the draw ratio. Based on the invariance to short term and long term loading, it was suggested in chapter 4 that a load bearing structure is

formed at relatively low draw ratio, and that this structure remains invariant on further drawing. The existence of such an invariant structure can also explain that the degradation due to UV-irradiation after impregnation does not depend on the draw ratio.

Several experimental conditions can be changed for improving the efficiency of crosslinking and reducing the negative effects.
The experiments reported above, have been done in air. Oxygen reacts with the radicals created during the treatment, and is therefore competitive with crosslinking, furthermore oxygen can induce chain scission. Elimination of oxygen during the irradiation, adds to the complexity of the process, but should not be prohibitive.
Both impregnation and irradiation have been performed at low temperature. At higher temperature the chain mobility will be increased resulting in an acceleration of the impregnation process, and in enhancing the crosslink yield. This can be expected to be most effective in the more highly drawn fibres.
The irradiation has been performed using a high or medium pressure mercury lamp. The radiation contains short wavelength components (down to 240 nm). Elimination of the radiation with a wavelength lower than 300 nm, can be expected to reduced chain scission [11].

6.6 Conclusions

Gel-spun UHMW-PE fibres of different draw ratio can be impregnated at room temperature by low molecular weight UV initiators from the vapour phase and crosslinked by UV irradiation. The treatment also results in grafting side groups to the chain. Tri-chloro-ethylene has shown to be a particularly useful initiator.

Elimination of flow creep, and an increased thermal resistance have been realised in fibres of different draw ratio, especially so in fibres of intermediate draw ratio. Impregnation and UV irradiation at room temperature do not influence the short term modulus nor the reversible creep rate.

The treatment results in a reduced ductility, a decrease of the strength and strain to failure, and of the time till rupture under load. The negative effects observed are

caused by chain scission. It is assumed that stressed tie molecules rupture during the irradiation phase. It is assumed that the chain scission can be reduced by: the use of radiation of longer wavelength, elimination of oxygen during impregnation and irradiation, by relaxation fibres prior to irradiation, and by elimination of the radicals before the fibres are exposed to air, the latter to prevent delayed reactions with oxigen.

Large differences in the effects of treatment have been observed for different fibres, with respect to crosslinking, the enhancement of the creep resistance, and to its effects on the short term mechanical properties.

For PE1 to PE5 fibres produced from the same precursor, the sensitivity to the treatment does not depend on the draw ratio. This can be explained by assuming that a load bearing structure is formed early in the process, and that this structure remains relative unchanged on further drawing.

6.7 References

1 D.W. Woods, W.K. Busfield and I.M. Ward, Plastics. and Rubber Proc and Appl., **5**, (1985), 157

2 D.W. Woods, W.K. Busfield and I.M. Ward, Polym. Comm., **25**, 9, (1984), 298

3 J. de Boer and A.J. Pennings, Pol. Bull., **5**, (1981), 317

4 J. Penning, Ph-D Thesis university of Groningen, February (1994), ch. 5

5 J. de Boer, H.J. van de Berg, A.J. Pennings, Polymer, **25**, (1984), 513

6 J.P. Penning, H.E. Pras, A.J. Pennings, Coll. Polym. Sci., **272**, (1994), 664

7 K. Yagi, M. Hitoshi, EP 0 229 477, (1986)

8 Japanese Patent 4-214205, (1992)

9 H. Nishigawa et al, JP 63-326899, (1988), JP 63-326900, (1988)

10 I. Sakano, JP 88-326898, (1988)

11 Y.L. Chen, and B. Rånby, Polymers for Advanced Technologies, **1**, (1990), 103

12 I. Chodak and P.V. Zamotaev, Die Angewandte Makromolekulare Chemie, **210**, (1993), 119

13 Y.L. Chen, and B. Rånby, J. Polym. Sci., A, Polym. Chem., **27**, (1989), 4051

14 P.V. Zamotaev, O. Mityukhin, S. Luzgarev, Polym. Degradation. Stab., **35**, (1992), 195

15 A.A. Katchan and P.V. Zamotaev, Photochemical modification of polymers, Kiev, (1990)

16 P.V. Zamotaev, Macromol. Chem., Macromol. Symp., **28**, (1989), 227

17 P.V. Zamotaev and Z.O. Streltsova, Polymer Degradation and Stability, **36**,(1992), 267

18 J. Teckoe, R.H. Olley, D.C. Bassett, Meeting, Polym. Physics Group , Bristol, Sept. (1997)

19 D. Sherby, J.F. Dorn, J. Mech. and Phys. of Solids, **6**, (1958), 145

20 Hommel, Handbuch der gefährliche Güter, 7. Edition, Springer Verlag Berlin (1995)

21 L.E. Govaert, Ph-Thesis Eindhoven University of Technology, (1989), ch. 3

22 L.E. Govaert, P.J. Lemstra, Colloid Polym. Sci., **270**, (1992), 455

23 R. Hikmet, P.J. Lemstra, A. Keller, Coll. and Polym. Sci., **265**, (1987), 185

24 I. Chodak, Progress. Polym. Sc., **20**, (1996), 1165

25 Y. Ohta, H. Yasuda, A Kaji, Polym. Prep. Japan, **43**, 9, (1994), 3143

26 C.W.M. Bastiaansen, Y. Ohta, H. Sugiyama, EP 0 269 151 B1

27 R. Steenbakkers-Menting, Ph-Thesis University of Eindhoven, (1995), ch. 5

28 V.I.. Vettegren, A.F Ioffe Physical technical Institute, Personal Communication

Chapter 7 Supercritical CO_2 assisted impregnation and UV-crosslinking of gel-spun UHMW-PE fibres.

7.1 Introduction

In the preceding chapter it was reported that gel-spun UHMW-PE fibres can be UV-crosslinked after impregnation with a UV-initiator from the gas or vapour phase. Compounds have been used, that possess a sufficiently high vapour pressure at room temperature. A disadvantage of using high vapour pressure initiators is that these compounds also readily evaporate from the fibre, requiring that UV crosslinking must be performed directly after exposure to the initiator.

Of interest for post drawing impregnation are low molecular weight initiators that are mobile in polyethylene below the melting point. Well known initiators for UV-crosslinking polyolefins are benzophenone (BP), quinones, xantone and their derivatives [1,2,3]. Also peroxides are widely used for crosslinking polyolefins. Low molecular weight peroxides are di-benzoyl-peroxide (DBP) and di-cumyl-peroxide (DCP), the latter has been used by de Boer for UV-crosslinking gel-spun fibres [4].

Benzophenone (BP) can be diffused into polyethylene at elevated temperature. Whereas diffusion in isotropic polyethylene is possible at 50°C [5], for gel-spun polyethylene fibres, a higher temperature is required [6]. Impregnation of the fibre with BP from solution in benzene or carbon tetrachloride [6] or with DCP from immersion in the liquid initiator [4] was not successful. Chen and Rånby [6] demonstrated impregnation of gel-spun polyethylene fibres (Spectra 900) with BP at a temperature of 100°C. Impregnation at a much higher temperature is not practical because of the deterioration of the mechanical properties due to relaxation processes. In the case of impregnation with peroxides there is an additional constraint, that the impregnation must be done at a temperature at which decomposition of the peroxide is negligible.

Impregnation of polymers using supercritical media is a rather novel technology which might provide new possibilities for impregnating in particular for gel-spun polyethylene fibres. Supercritical fluids are highly penetrating media with a low

viscosity. A wide range of chemical compounds can be dissolved in a suitable supercritical medium. The potential of supercritical fluids for extraction of organic compounds is known already for a long time [7,8]. Examples of industrial activities based on supercritical medium extraction are extraction of: caffeine from coffee and tea, acids from hop, nicotine from tobacco, flavours from many foodstuffs, oils from seeds and monomers from polymers [7,8].

Impregnation of polymers using supercritical fluids is relatively new. In 1985 a patent was filed for impregnating polymers with various compounds using supercritical media [9]. Examples of compounds that can be diffused in polymers using supercritical media are: naphthalene, xylene, 1-hexanol, ethyl laureate, ethyl benzoate, di-methyl-phthalate and benzophenone (BP). PVC, polyurethane and polycarbonate were impregnated with BP using supercritical trifluoro-methane and sulphur-dioxide as media [9]. Impregnation of synthetic fibres with dyes using supercritical carbon dioxide is being studied as an alternative to water based textile dyeing [10,11,12]. Even highly oriented polyethylene fibres can be impregnated, to some extent, in supercritical CO_2 with dyes with a molecular mass up to at least 300 dalton [13].

Examples of media used for supercritical extraction/impregnation are: trifluoro-methane, sulphur-dioxide, water, ethylene, nitrous oxide (N_20), and carbon-dioxide.

Carbon-dioxide is of particular technological interest for impregnation of polymers because of various practical reasons such as: availability, it is non-toxic, non-flammable, low cost, and it possesses easy to obtain supercritical conditions at a temperature of 31.3°C and a pressure 7.4 MPa [12].

Supercritical carbon dioxide (s-CO_2) is a solvent for non polar or weakly polar compounds with a molecular mass up to about 1000 dalton. Furthermore s-CO_2 is a swelling agent for polyethylene [9], rendering the mobile phase of the polymer more easily accessible. S-CO_2 is inert to peroxides, preventing their premature decomposition, allowing their use up to the normal decomposition temperature. In conclusion, s-CO_2 seems to be a favourable medium for impregnation of highly oriented polyethylene with different initiators.

This chapter describes the possibilities for the UV-crosslinking of gel-spun UHMW-PE fibres after impregnation with BP using s-CO_2 as a carrier and benzophenone as the initiator. Some additional experiments have been performed using di-benzoyl-peroxide (DBP) as the initiator.

In order to compare the efficiency of s-CO2 assisted impregnation with vapour phase impregnation at elevated temperature, a fibre was also impregnated with BP from the vapour phase at 100°C using the procedure described by Chen [6].

7.2 UV crosslinking and grafting of polyethylene with benzophenone

Benzophenone is activated by absorbing a UV-photon. The activated benzophenone can extract a hydrogen atom from the chain and thus start the reaction [14]. The most relevant reactions of benzophenone [1] are presented below schematically (R = Polymer Chain):

$BP + h\nu$	$\rightarrow$	BP^*		
$BP^* + RH$	$\rightarrow$	$BPH^\bullet + R^\bullet$		
$R^\bullet + R^\bullet$	$\rightarrow$	R-R	(I)	Crosslinking
$BPH^\bullet + R^\bullet$	$\rightarrow$	RBPH	(II)	Grafting
$BPH^\bullet + 0_2$	$\rightarrow$	$BP+O_2H^\bullet$	(III)	
$BPH^\bullet + BPH^\bullet$	$\rightarrow$	$(BPH)_2$		

The most important reaction is reaction (I) resulting in crosslinking of polyethylene. Also grafting reactions, i.e. the introduction of side groups on the chain (II) are relevant, the side groups can contribute to a higher creep resistance [see chapter 8]. Oxygen, present in a limited amount, recycles the initiator (reaction III) and contributes to a higher efficiency of the initiator. Oxygen however also competes with the crosslinking reaction. Oxygen reacts with the radicals in forming alcohol- and ketone-groups. The dimer (IV) and the grafted benzophenone (II) are UV sensitive which can result in secondary photochemical reactions, leading to detachment of the

group and separation of the dimer respectively. In crosslinking polyethylene often a bridging agent as: a diene, acrylic acid, and especially tri-allyl-cyanurate is added [14]. Chen and Rånby [6], however demonstrated that the latter was not effective in promoting UV crosslinking gel-spun fibres, most probably because the compound did not penetrate in the fibre. As it was demonstrated that the fibres could be crosslinked in a short time using only benzophenone, in the present experiments no bridging agent was used.

7.3 Experimental

7.3.1 Materials

Table 7.1 gives an overview of the fibres used, all fibres are multifilament yarns.

Table 7.1 Properties of gel-spun fibres

Sample	Titre	Cross Section	Modulus	Strength	Failure strain
	tex*	mm^2	GPa	GPa	%
PE1	58.0	0.060	38	1.7	5.7
PE2	43.4	0.045	63	2.3	4.5
PE3	33.9	0.035	86	2.8	3.9
PE4	25.2	0.026	111	3.2	3.4
PE5	21.3	0.022	131	3.3	3.0
PE6	22.0	0.023	135	3.8	3.7
SK65	44.0	0.045	95	3.0	3.6

*tex: mass in gram/1000 m.

The samples were supplied by DSM. PE1-PE5 are experimental grades, Dyneema SK65 and PE6 (Dyneema SK75) are commercial fibre grades (remark: PE6 is the same fibre as PE6 in the preceding chapter, however with twice as much filaments). For removing the spin oil present on the fibres during spinning, the samples were extracted with boiling acetone in a Soxhlet for 70 minutes. The cross-section was determined from the mass per unit length, assuming a density of 970 kg/m^3.

Benzophenone (BP) supplied by Fluka, melting point 46-49°C, and di-benzoyl-peroxide (DBP) , supplied by AKZO-Nobel, were used as received.

7.3.2 Impregnation with BP and UV-crosslinking

The process conditions for supercritical CO_2 impregnation with BP are determined by the solubility of the initiator. In the case of peroxides (reference experiments), the decomposition temperature is an additional parameter to consider. The solubility of BP, respectively DBP, was tested in a high-pressure cell fitted with optical windows. The process was observed visually. For BP the optimum temperature and pressure conditions were 100°C and 88 bar, respectively.

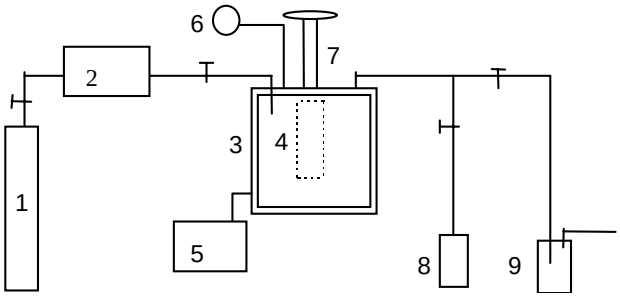

Figure 7.1 Schematic representation of the s-CO_2 impregnation equipment, 1: gas pressure vessel, 2: compressor, 3: autoclave, 4: sample holder (quartz tube), 5: heater, 6: manometer, 7: magnetically coupled stirrer, 8: vacuum pump, 9: gas wash bottle

For impregnation in supercritical carbon dioxide a static high pressure apparatus was used. The set-up is shown in figure 7.1. The impregnation vessel is a 400 millilitre autoclave (10), fitted with a stirring device. The initiator (as a powder) was put into the vessel before closing. The yarn sample was wound on a quartz tube, mounted inside the vessel sample holder. After closing the vessel it was pressurised with CO_2 and heated. Operating conditions are: pressure up to 50 MPa and temperature up to 300^0C.

The impregnation cycle was typically 1 hour, including heating, pressurising, and cooling/de-pressurising, from which 30 minutes at specified temperature and pressure conditions. The quantity of BP added was varied between 2.5% and 15% based on the yarn mass, corresponding to a concentration in s-CO_2 between 0.0125 to 0.075 %.

Before UV-irradiation, the sample which was still on the quartz tube, was placed in a quartz container flushed with nitrogen for two hours in order to remove oxygen. The closed container was placed in a Rayonet RPR-100 photochemical reactor, containing 16 low pressure mercury lamps (35 Watt each), producing mainly 253 nm radiation. The temperature of the reactor was kept constant at 65°C. The fibres were irradiated for different periods, from 20 seconds up to 30 minutes. Directly after irradiation the container with the sample was placed in an oven at 100°C for 15 minutes for eliminating any remaining radicals. During this annealing procedure, the container was flushed with nitrogen.

7.3.3 Reference experiments

Vapour phase impregnation with BP

The yarn sample (tightly wound on a quartz tube) was placed in a desiccator that also contained an open beaker filled with BP. After evacuation, the desiccator was placed in an oven at 100°C for 48 hours. UV irradiation was performed following the procedure as described above, the irradiation time was 5 minutes.

Surface precipitation of BP

Precipitation of BP on the fibre surface was performed by immersing a fibre in a 0.25 wt % solution of BP in methanol for 30 seconds. The solvent uptake in the yarn, viz. between he individual fibres, was about twice the yarn mass (capillary uptake). Hereafter the yarn was dried at ambient conditions. The mass gain of the dried yarn was approximately 0.5%. The UV irradiation procedure was the same as for vapour impregnated samples.

Impregnation with DBP

For DBP the solubility increases with temperature and pressure; the impregnation pressure was chosen to be 260 bar. The decomposition temperature of DBP in supercritical carbondioxide was determined in a high pressure DSC equipment built by DTNW. The system was filled with CO_2 at 260 bar. The scan speed was 10 K/min. Dissociation of the peroxide results in an exothermic peak at 120°C. Consequently, impregnation was performed at temperatures up to 115°C, just below the decomposition temperature. UV irradiation was performed using the procedure described above, irradiation time varied from 3 minutes to 30 minutes.
Some DBP impregnated samples were heat cured at temperatures varying from 115°C to 135°C, for a period up to 48 hours.

E-beam crosslinking

Non-impregnated samples were irradiated with doses of 0 (reference), 20, 60, 100 or 150 kGy. The temperature during irradiation was either 30°C or 100°C. Before, during and for 4 days after irradiation the sample container was flushed with nitrogen.

The experiments concerning supercritical CO_2 impregnation have been performed at the Deutches Textilforschungsinstitut Nord-West (DTNW) in Krefeld, Germany.
E-beam irradiation was performed with the 3 MeV van der Graaff generator of the Inter-university Reactor Institute in Delft
.

7.3.4 Characterisation

The mass increase due to the s-CO_2 treatment due to initiator uptake was determined by weighing. For some samples the initiator (BP) was extracted in 30 ml boiling methanol in a Soxhlet apparatus for 70 minutes. The extract was diluted to 50 ml. The UV-absorption at 253 nm was used to calculate the amount of BP. Infrared spectra were taken using a Mattson FT-IR spectrometer. Spectra were taken from a thin (mono)layer parallel filaments, wound tightly on a paper frame. The relative BP fraction was calculated from the absorbance of the 1277/cm and 1665/cm bands relative to that of the 1465/cm PE band.

The gel fraction was determined by extraction of the sol fraction for 48 hours in boiling xylene, containing 0.5 % by mass di-t-butyl-p-cresol. The non-dissolved gel was dried at 100°C for 2 hours and conditioned for 1 hour at room temperature, before weighing.

Melting endotherms were determined using a Perkin Elmer DSC-7. Temperature scans were taken from 30°C to 180°C at a scan rate of 10 °C/min. A first scan was taken to check any changes in crystallinity caused by the impregnation and crosslinking. After cooling, at 50°C/min and re-crystallisation, a second scan was made to reveal changes in the melting and re-crystallisation behaviour.

Tensile tests were performed using a Zwick 1445 universal tester equipped with pneumatic fibre clamps. The sample length was 200 mm, the test speed was 100 mm/min. The modulus reported is the secant modulus for a strain interval of 0.3-1%.

Yield stress measurements and stress relaxation experiments were performed on a Frank universal tester, equipped with a thermostatically controlled oven and fibre grips. The free sample length was 100 mm. The yield stress was measured at 80°C, using strain rates of $1.6\ 10^{-6}$ to $5\ 10^{-3}$/sec.

Stress relaxation experiments were performed using the Frank tester on samples 100 mm long, the temperature was 80°C.

Creep was measured using dead weight loading at 80°C (Frank tester) or at 30°C, using the test equipment of DSM as described in chapter 4.

The heat resistance of constrained samples was determined on samples of 200 mm wound on and fixed to a steel frame by placing the samples in an oven for 30 sec at 165°C or 200°C for 15 sec. If a sample did not melt at 165, the mechanical properties were measured using the procedure described above.

7.4 Results

7.4.1 BP impregnated PE3 fibre.

Most experiments were performed on a fibre with an intermediate draw ratio (PE3). The amount of BP put in the autoclave was a fraction of the mass of the fibre sample 2.5% to 15%). The BP concentration in the fibre, as determined by the mass increase of the fibre sample and by extraction was 0.3% for 2.5 % BP added, and

0.5±0.1%, for 10% and 15% BP. The crosslinking experiments were performed on fibres that were impregnated using an addition of 10% BP.

Gel fraction and short term mechanical properties

The gel fraction of PE3 as function of the irradiation time and treatment conditions, and the effect of the treatment on the mechanical properties of the fibres at room temperature are shown in table 7.2. The table gives data on crosslinked fibres and several control experiments, relevant for the process steps as: spin finish removal, annealing, exposure to s-CO_2, and irradiation.

Table 7.2 Gel fraction and mechanical properties as a function of treatment conditions and irradiation time for PE3.

Sample treatment	**Gel fraction**	**Modulus**	**Strength**
	(%)	GPa	GPa
Reference, untreated	0±0.5	78.9±0.8	2.3±0.1
Spin finish removed	-	71.0±0.6	2.2±0.1
Annealed at 100°C	-	70.8±1.4	2.2±0.2
S-CO_2 exposed	-	64.3±1.5	2.4±0.1
S-CO_2 exposed, 3 min irradiated	4±2	64.2±1.8	2.3±0.1
Impregnated, 0.33 min irradiated	67±1	64.3±0.5	2.3±0.1
Impregnated, 1 min irradiated	86±5	64.5±1.6	2.2±0.2
Impregnated, 3 min irradiated	93±5	65.5±0.5	2.3±0.1
Impr, stored 18 days, irrad. time 3 min	92±4	-	-
Impregnated, 5 min irradiated	93±5	66.3±2.0	2.1±0.3
Impregnated, 30 min irradiated	97±5	62.7±1.3	1.8±0.3

Fibre handling (spin finish removal) results in an apparent loss of modulus, due to difficulties in measuring the properties of the treated fibres. Fibres treated with s-CO_2 show a real decrease in Young's modulus of approximately 10%. This decrease is caused by partial relaxation of the fibre. Exposure to a temperature of 100°C and

UV-irradiation do not affect the short term mechanical properties. After long UV-irradiation a significant decrease of strength was observed, most probably due to chain scission. The result for the sample that was stored for 18 days between impregnation and irradiation shows that loss of BP is not important on this time scale.

Thermal properties

DSC analysis of non-constrained fibres, showed that neither the crystallinity (70%) nor the (onset) melting point is influenced by crosslinking.

The thermal resistance increases with increasing irradiation time. The maximum temperature that a highly crosslinked fibre (irradiated for 5 minutes) could sustain for 15 seconds without breaking was 200°C.

The effect of heating the crosslinked fibres above the melting temperature is shown in table 7.3. This table gives the mechanical properties (at room temperature) of fibres heated to 165°C in a constrained condition for 30 seconds.

Table 7.3 Mechanical Properties of (crosslinked) PE3 fibre after heating to 165°C

Sample treatment	**Modulus**	**Strength**
	GPa	GPa
Reference, untreated	Ruptured	-
Crosslinked, 0.33 min irradiated	Ruptured	-
Crosslinked, 1 min irradiated	7	0.3
Crosslinked, 3 min irradiated	18±2	0.7±0.1
Crosslinked, 5 min irradiated	34±2	1.1±0.1

Long-term mechanical properties

The yield stress was determined by slow tensile tests (figure 7.2).

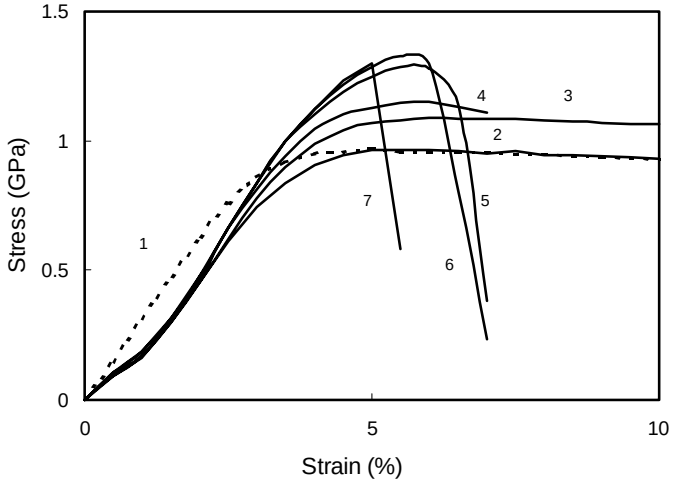

Figure 7.2 Stress-strain curves for an untreated and a crosslinked PE3 fibre at 80°C, strain rate 10^{-4} s^{-1}. 1: untreated, 2: only impregnated. 3-6 crosslinked, irradiation time: 20 sec (3), 1 min (4), 3 min (5), 5 min (6), 30 min (7).

Figure 7.2 shows the effect of the impregnation treatment on the stress strain curve. Due to partial relaxation, impregnation results in a low initial modulus, while the modulus at higher strain is not influenced. The plasticity is suppressed progressively with increasing irradiation time. The maximum load increases and strain to failure is reduced. The fibre irradiated for 30 minutes shows a brittle failure behaviour.

In figure 7.3 the maximum stress, or 'yield stress' , is plotted as a function of irradiation time. The maximum stress approaches to a constant value at long irradiation time.

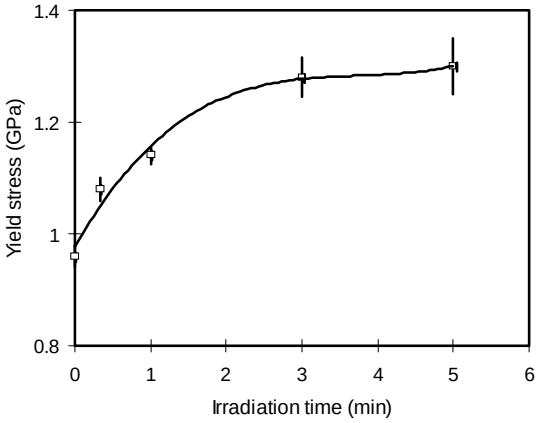

Figure 7.3 Yield stress PE3 fibre as a function of the irradiation time. Strain rate 10^{-4} s^{-1}, temperature 80°C.

The combined results of slow tensile tests at different strain rates and of creep tests at different loads are plotted in a single figure.

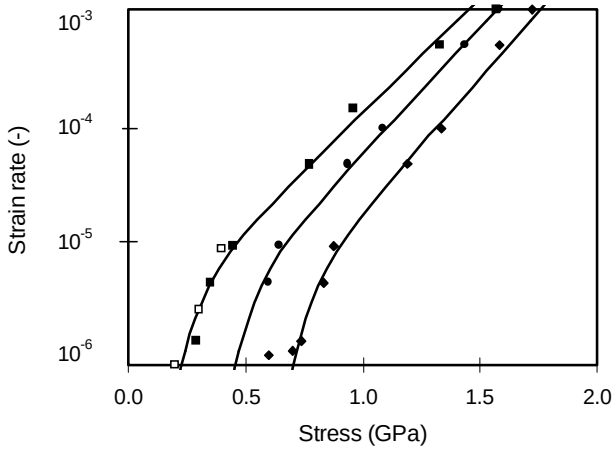

Figure 7.4. Strain rate or flow creep rate of the crosslinked PE3 fibre as a function of stress, temperature 80°C, ■,□: untreated, ●: 0.33 min irradiated, ♦: 5 min. irradiated. Closed symbols: constant strain rate, open symbols: constant load experiments.

The flow creep rate is suppressed significantly, especially for intermediate loads, the effect of the treatment increases with the irradiation time. At a higher stress, >1.5 GPa, the effect of crosslinking on the strain rate is small. For the fibre irradiated during 5 minutes, no flow creep could be observed within experimental limits (creep rate > 10^{-6} s^{-1}) at stresses lower than 0,6 GPa.

Long term creep experiments were performed at a temperature of 30°C, and at stresses of 0,5 and 0.7 GPa. Figure 7.5 gives the measured creep curves for the crosslinked and non treated PE3 fibre.
At short loading time, in the region of the primary creep and dominated by the reversible creep, the deformation of the treated fibres is higher than that of the non-treated fibre. At longer loading time, a significant reduction of the creep is observed. The crosslinking treatment has a negative effect on the reversible creep, but improves the resistance against flow creep

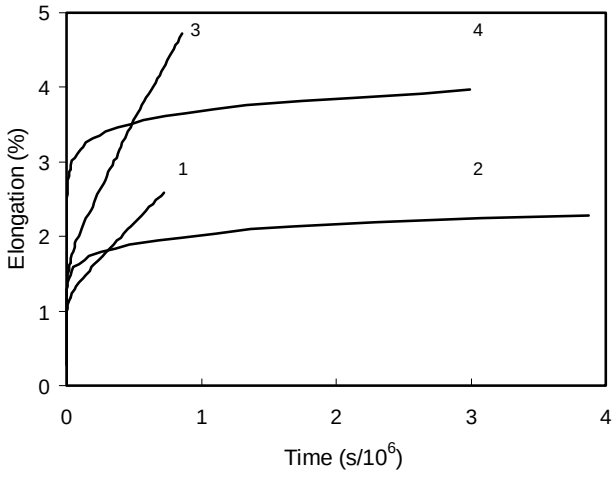

Figure 7.5 Creep of PE3 and crosslinked PE3,temperature 30°C, 1: untreated 0.5 GPa, 2: crosslinked 0.5 GPa , 3: untreated 0.7 GPa, 4: crosslinked 0.7 GPa

The influence of crosslinking on the long term creep is also shown in the Sherby and Dorn plot in figure 7.6. For the non-treated fibres a limiting, or plateau, creep rate

was observed. For the treated fibres the creep rate decreases steadily till the end of the experiments (<10^{-9} s^{-1}). The more pronounced (reversible) creep at short loading times is also seen in the Sherby and Dorn plots of figure 7.6.

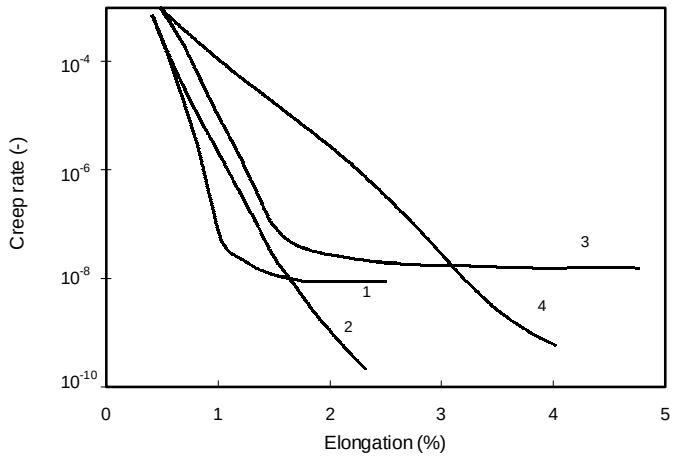

Figure 7.6 Sherby and Dorn plot, PE3 and crosslinked PE3, irradiation time 5 min, temperature 30°C. 1: untreated 0.5 GPa, 2: crosslinked 0.5 GPa, 3: untreated 0.7 GPa, 4: crosslinked 0.7 GPa

The effect of crosslinking on stress relaxation is given in figure 7.7.

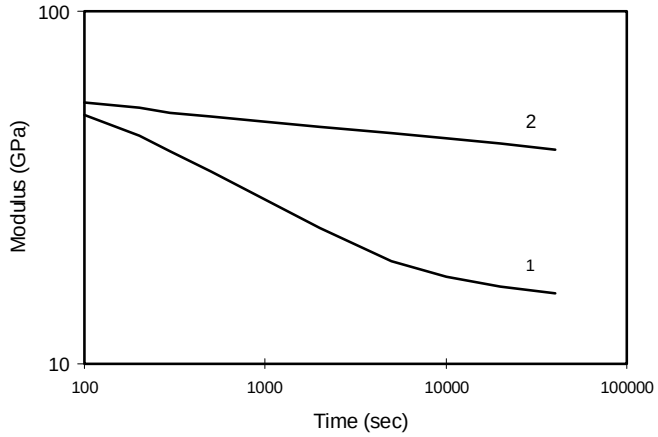

Figure 7.7 Stress relaxation modulus of PE3 and crosslinked PE3 fibre, temperature 80°C, strain 2.5%. 1: untreated, 2: crosslinked

The relaxation modulus of the crosslinked fibre is well described by equation :

$$E(t) = E_0\, t^{-m} \qquad 7.1$$

with m = 0.049. Such a behaviour has been observed in situations, where relaxation due to irreversible plastic processes is negligible [15]. For the non treated fibre an additional relaxation is observed, due to irreversible molecular reorganisations.

7.4.2 Crosslinking of fibres with different draw ratio

A range of fibres with different modulus were impregnated under standard conditions: 10% BP, 88 bar, 100°C, 5 minutes irradiation time. The results are summarised in table 7.4.

Table 7.4 Properties crosslinked fibres with different modulus

Sample	Modulus	BP cont.	Gel cont.	Yield stress, 80°C, 10^{-4}/s GPa		
	GPa	%	%	untreated	treated	% incr.
PE1	38	1.0	89±3	0.47	0.62	32
PE2	63	1.2	90±2	0.68	0.91	33
PE3	86	0.7	93±5	0.95	1.30	36
PE4	111	0.7	89±4	1.03	1.29	25
PE5	131	1.0	87±2	1.21	1.24	2
SK65	95	0.7	87±3	1.11	1.33	20
PE6	135	0.6	77±3	1.14	1.29	13

The initiator content (relative to PE3) was determined by IR spectroscopy. For PE3 the initiator content was also determined by the mass increase. Figure 7.8 gives representative IR-spectra.

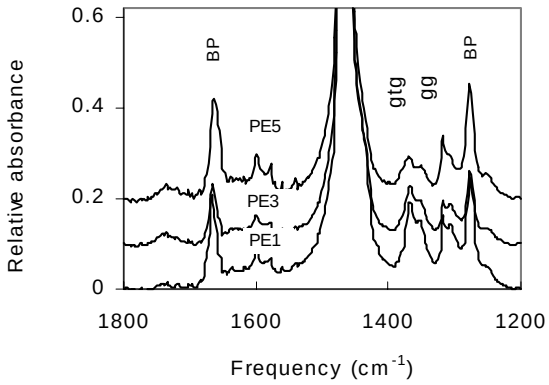

Figure 7.8 Infra-red spectra of PE1, PE3 and PE5

The infrared spectra of the impregnated fibres show bands of BP at 1277 cm^{-1} and 1665 cm^{-1}. In all fibres tested a significant amount of initiator was absorbed. There is

no clear relation with the degree of drawing of the fibre. Figure 7.10 shows that the BP content of PE5 is equal to that of PE1.

All fibres studied can be crosslinked using the procedure optimised for PE3; however the crosslinking is less effective for the more highly drawn fibres. The yield stress increases for all fibres, except for PE5. The relative increase of the yield stress generally is smaller for highly drawn fibres, the absolute value seems to be constant around 1.3 GPa. Also the gel fraction decreases with increasing draw ratio. Figure 7.8 shows weak lines at 1355 cm^{-1} and 1368 cm^{-1}, representing lines for non extended polyethylene chain segments: gauche-trans-gauche and gauche-gauche respectively [16]. The strength of these lines decreases with increasing draw ratio, demonstrating the decrease of the concentration of mobile chain segments.

7.4.3 Reference experiments

A number of reference experiments were performed for testing alternative treatments; table 7.5 summarises the results. The first two samples are references; a non-treated PE3 fibre and an UV-crosslinked PE3 fibre impregnated with BP as described above. Vapour phase impregnation at 100°C was performed repeating the procedure described by Chen and Rånby [6]. UV irradiation of PE3 fibres, with initiator on the surface, was performed for checking if initiator present on the surface contributes to the crosslinking. Impregnation with di-benzoyl-peroxide (DBP) showed to be little effective for crosslinking either PE3 or Dyneema SK65. In the table the best results obtained with PE3 are given. The fibre was impregnated with DBP in s-CO_2 at a temperature of 80°C. The mass increase was 0.4-0.7%. Post treatment was either by UV-irradiation during 5 min or by oven exposure at a temperature of 115°C during 48 hours. E-beam irradiation of PE3 with doses varying from 20 to 150 resulted in a relatively low gel fraction and a low yield stress. In table 7.5 the results for a dose of 150 kGy are given.

Table 7.5 Results of reference experiments on PE3

Sample (PE3) treatment	**Gel fraction**	**Yield stress**
	%	GPa
Reference, non treated	<4	0.94
S-CO_2 impregnated with BP, 5 min UV-irradiated	93	1.30
Vapour phase impregnated with BP, 100°C, 48 hour	93	1.26
Surface precipitated BP (0.8% BP)	<3	0.95
S-CO_2 impregnated with DBP, 5 min UV-irradiated	<2	0.97
S-CO_2 impregnated with DBP, 48 hours 115°C	<3	0.98
E-beam irradiated 150 kGy, 30°C	30	0.21
E-beam irradiated 150 kGy, 100°C	70	0.46

Vapour phase impregnation is as effective as s-CO_2 impregnation, but requires a much longer impregnation time. Initiator present on the surface does not contribute significantly to crosslinking of the fibre.
DBP treated fibres could not be crosslinked neither using UV irradiation nor with heat curing. The gel fraction was essentially zero, a slight increase of the yield stress was observed. Figure 7.9 gives a representative result.

The stress-strain graphs in figure 7.9 also show the effect of relaxation of the fibre, that is most pronounced at the highest treatment temperature. Curing at a higher temperature, 135°C, leads to some further degradation and loss of ductility without increasing the yield stress.

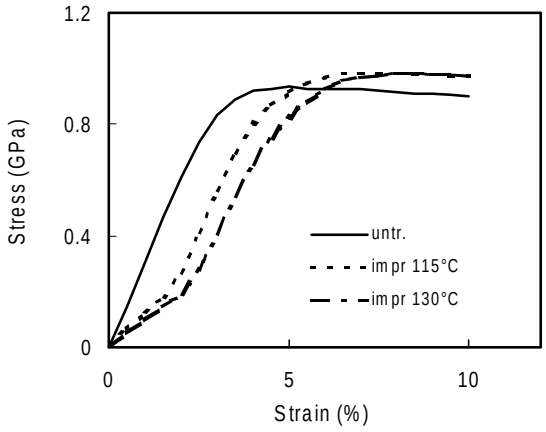

Figure 7.9 Yield stress measurement DBP treated fibre

High energy (e-beam) irradiation results in a highly reduced yield stress see table 7.5, especially when irradiated at low temperature, in this case the reduction is nearly 80%. The result implies a strongly reduced creep resistance,.

7.5 Discussion

The high gel fraction and thermal resistance well above the melting point demonstrate effective crosslinking of s-CO_2 impregnated gel-spun fibres using BP as initiator.

A high gel fraction, more than 90% was observed for an initiator concentration of about 0.5%. Also Chen and Rånby [6] found gel fractions up to 90% for UV crosslinked Spectra 900 fibre. The crosslink yield seems to be much higher than for fibres that are crosslinked with initiator introduced in the fibre before drawing. De Boer et al. [4] obtained gel fractions of 16%, 69% and 100% for a fibre containing of 1%, 8%, and 17% DCP. The low crosslink efficiency reported by the Boer seems to be specific for the high modulus fibres, as for crosslinking UHMW-PE with DCP usually less than 1 % initiator is required [18]. A large fraction of the initiator introduced before drawing is clearly not effective. When the initiator is diffused into

the fibres after drawing, it only penetrates into non-crystalline zones where crosslinking is possible.

The effect of the irradiation time on the gel fraction (for PE3) allows to estimate the chain scission to crosslink ratio. For UV-crosslinking a modified procedure as proposed by Chen et al. [14] can be applied. The procedure and results are shown in appendix 7.1. The analysis results in an estimated crosslink-to chain scission ratio of 2-2.5.

The flow creep rate is strongly reduced, especially at intermediate load. In chapter 2 and 3 it was shown that the rate of the irreversible creep (plateau creep rate) of gel-spun polyethylene fibres can be described by two activated processes acting in parallel. The results of the yield stress and creep rate measurements of figure 7.4 were fitted with this model, that describes the data well. The change in the network strength is modelled by a change in the rate factor for this process. In addition a small change of the activation volume of the crystalline process is required. This accounts for the change in the slope of the plot of strain rate versus stress at high stress.

Table 7.6 Two process fit parameters for PE3 and crosslinked PE3.

	Network process		**Crystalline process**	
	$\dot{\varepsilon}_{01}$ s^{-1}	v_1 nm^3	$\dot{\varepsilon}_{02}$ s^{-1}	v_2 nm^3
PE3	2.10^{-9}	0.160	10^{-5}	0.025
PE3 20 “ irradiated	$1\ 10^{-12}$	0.160	10^{-5}	0.028
PE3 5 min. irradiated.	4.10^{-16}	0.160	10^{-5}	0.030

Other fits, for instance, one assuming constant rate factors and changing the activation volumes, are possible, but require more pronounced changes in the crystalline process. The fit parameters are given in table 7.6. The observed improvements of the creep resistance can therefore be fully accounted for by an

enhanced strength of the network process. Analogous results had been reported by Klein [19, chapter 5, figure 5.2] for the creep of melt-spun fibres crosslinked before drawing.

It is shown, see figure 7.2, that the plasticity is suppressed to a high extent. Crosslinking results in a network that allows only a small deformation, the description by activated flow processes is therefore only valid for small deformations.

The additional contribution of the first process depends the irradiation dose, for the results reported above between 0.15 GPa (irradiation time 20 sec) and 0.45 GPa (5 min) for PE3. The effect is analogous to that (but larger than)reported for the melt spun fibre studied by Klein: 0.02 to 0.12 GPa [19].

The increase of the activation volume for the crystalline process suggests that less chains contribute to this process, due to a more inhomogeneous load distribution. The rate factor of the crystalline process seems to be constant.

The primary creep is enhanced in crosslinked fibres. This is at variation with the observations in the preceding chapter for fibres impregnated at room temperature. An increase of the primary creep was also observed by Chen [6] who impregnated a fibre at 100°C, and irradiated at 135 °C. The increase is due to a (partial) relaxation of the fibre. This causes also the Young's modulus to decrease during the impregnation step, see figures 7.2 and 7.9.

The stress relaxation, see figure 7.7, does not show any effect of annealing. The explanation is, that the strain (2.5%) was sufficiently high to eliminate the extra strain induced by the relaxation of the chains. The stress relaxation experiments confirm the absence of plastic flow in the crosslinked fibre.

The strength of the PE1-PE5 fibres is not influenced by impregnation with benzophenone followed by UV-irradiation in nitrogen atmosphere. This is in contrast with the result reported in the preceding chapter for impregnation with chlorine compounds at room temperature.

The most probable cause is the absence of oxygen during irradiation in the present experiments. Oxygen is known to compete with the crosslinking reaction [14] and cause chain scission. However the results of the treatment of Spectra fibres [chapter 6] and of gel-cast tapes demonstrate that the presence of oxygen does not necessarily result in strength loss in highly oriented polyethylene [20].

Several other possible causes have been identified: the size of the initiator, and the impregnation temperature. The relatively small chlorine compounds or a chlorine atom split of may be able to penetrate more deeply in the fibre than BP can do. Therefore less mobile chains may be involved. Room temperature impregnation did not result in significant chain relaxation, as was observed with the high temperature impregnation. Room temperature impregnation results in exposure of taut non crystalline chains to reactive species. Taut chains are more susceptible to chain scission than lax chains.

As in the previous chapter, treatment of highly drawn fibres seems to be less efficient; the gel fraction is lower and the relative increase of the yield stress is smaller. For PE5 hardly any increase in yield stress has been observed. Optimisation may result in some further improvement for the highly drawn fibres. Table 7.4 and figure 7.7 show that all fibres absorb approx. equal amounts of initiator independent of draw ratio. it is therefore concluded that the smaller effect in highly drawn fibres not due to insufficient initiator present in the fibre.

While impregnation and UV-irradiation gel-spun UHMW-PE fibres with benzophenone as an initiator has shown to be an efficient way for crosslinking gel-spun fibres, the method does not seem to work with di-benzoyl-peroxide. This initiator was chosen because of its molecular size, comparable to di-azo-dyes and benzophenone (compounds that can well be introduced in the fibre), and its relatively low decomposition temperature, τ_{50} 10 minutes at 130°C [23], allowing curing without important degradation of the mechanical properties of the fibre. The reason of the failure is not known. Premature decomposition might be a factor but is not expected to occur in the experiments at 80°C, furthermore the stability in s-CO2 was verified. Solubility of the initiator in s-CO2 does not seem to be limiting, because the polarity

of s-CO2 increases with pressure, especially above 20 MPa (the pressure during impregnation was 28 MPa). Solubility of DBP in polyethylene may well be limiting as DBP is a polar molecule. Evaporation or diffusion of the peroxide out of the fibre before decomposition can also have occurred.

7.6 Conclusions

Fibres of different draw ratio can be impregnated with benzophenone using supercritical CO_2. UV irradiation of the impregnated fibres results in effective crosslinking, this in turn resulting in improved creep and stress relaxation resistance. Also the thermal resistance is increased. Improvement of the creep properties by UV-crosslinking is thought to result from a relatively low chain-scission to crosslink ratio. In contrast, treatment with high energy radiation, where this ratio is approx. 1, only leads to degradation of the creep properties.

The creep improvement realised by impregnation and crosslinking can be attributed fully to an increase of the strength of the first or network process. The effect of chain scission is relatively small.

Fibres of low and intermediate draw ratio can be crosslinked readily and effectively. For highly drawn fibres the efficiency of the process of crosslinking by impregnation and UV-irradiation is relatively low. It is assumed that, that this is due a low concentration of chains that can be crosslinked, and to a limited accessibility of such chains for initiator molecules.

7.7 References

1 P.V. Zamotaev, Makromol. Chem., Macromol. Symp.,**28**, (1989), 287

2 P. Zamotaev and O. Mityukin, Polymer degradation and stability, **35**, (1992), 195

3 Y.L. Chen, B. Rånby, J. Polym. Sci., A: Polym Chem., **27**, (1989), 4051

4 J. de Boer, H.-J. van den Berg, A.J. Pennings, Polymer, **25**, (1984), 513

5 G. Oster, G.K. Oster, H. Moreson, J. Polym. Sci., **34**, (1959), 671

6 Y.L. Chen and B. Rånby, Polym for Adv. Techn., **1**, (1990), 103

7 G.M. Schneider, E. Stahl, G. Wilke, Extraction with supercritical gases, Verlag Chemie, Weinheim, (1980).

8 E. Stahl. K.W. Quirin, A. Glatz, G. Ran, Ber. Bunsenges. Phys. Chem., **88**, (1984), 900

9 EP 02222 207 B1, the B.F. Goodrich Company, (1987)

10 W. Saus, D. Knittel, E. Schollmeyer, Textile Praxis Int., (1993), 32

11 K. Poulakis et all, Chemiefaser/Textilindustrie, **43/93**, (1991),142

12 E. Bach, E. Cleve, E. Schollmeyer, High Pressure Chemical Engineering, Ph. von Rohr and Ch. Trepp (ed.) 581

13 E. Bach, E. Cleve, E. Schollmeyer, J. Text. Inst., **89**, 1, 4, (1998), 657

14 Y.L. Chen, B. Ranby, J. Polym. Sci., A, Polym. Chem., **27**, (1989), 4051

15 L.E. Govaert, Ph-D Thesis Eindhoven University of Technology, (1990), ch. 3

16 R.G. Snyder J. Chem. Phys., **47**, (1967), 1316

17 A. Charlesby and S.H. Pinner, Proc. Royal Soc. London, **A249**, (1959), 367

18 I Chodak , Prog. Polym. Sci., **20**, (1995), 1065

19 P.G. Klein , D.H. Ladizeski, I.M. Ward, J. Polym. Sci., Polym. Phys. **24**, (1986), 1093

20 I. Chodak, P.V. Zamotaev, Angew. Makromol. Chem., **210**, (1993), 119

21 D.L. Tzou, T.-H. Huang, A.F. Saraf, P. Desai, Polymer, **32**, 2, (1992), 426-428

22 B.E.Krishuk, V.A. Marikhin, L.P. Myasnikova, N.L Zaalishvilli, Int. J. Polym. Mater., **22**, (1993), 161

23 Brochure Akzo Chemical

24 L. Zhang, M. Zhou, D. Chen, Radiat, Phys. Chem., **44**, 3, (1994), 303

25 Jones et al, Nuclear Instruments and Methods in Physics Res., B, **151**, (1999), 213

26 Y. Qing, X. Wenying, and B. Rånby, Polym. Eng. Sci., **31**,22, (1991), 1561

27 J. de Boer and A.J. Pennings, Polymer Bulletin **5**, (1981), 317

Annexe 7.1 Charlesby and Pinner analysis for UV-crosslinked fibres

The gel-content data of table 7.2 can be used to estimate the crosslinking/chain scission ratio, using the Charlesby and Pinner (C-P) analysis [17,24].
For analysing UV-crosslinking efficiency, and for estimating the crosslink to chain scission ratio, a modified form of the Charlesby and Pinner equation can be used [14, 25]:

$$s + s^{0.5} = \frac{G_s}{2G_x} + \frac{1}{G_x MC} \qquad 7.2$$

S is the soluble fraction, Gs and Gx are the chain scission and crosslink yields (a factor 2 is added following the usual convention because crosslinking requires two reactions, while scission requires only a single reaction), M the molecular weight and C the initiator concentration used in the process [14]
When the initiator concentration is sufficiently high, the reacted concentration is approximately proportional to the irradiation time [14]. C is then approximately proportional to the irradiation time.

$$s + s^{0.5} = \frac{G_s}{2G_x} + \frac{\text{const.}}{G_x t} \qquad 7.3$$

Equation 7.3 has been used for estimation the crosslink to chain scission ratio in the present experiments.

Analysis of the assumptions on which the C-P-analysis is based [17] shows that this method is suitable for analysing the effect of UV-crosslinking gel-spun fibres. The assumptions are: (a) each monomer unit has the same probability of being crosslinked (and its related primary bonds being broken), (b) the number of crosslinks is small compared with the number of monomer units available, (c) the effect of end groups and intra-molecular crosslinking can be neglected, and (d) the initial molar mass distribution is random. Furthermore (e) the crosslink and scission yield is assumed to be proportional to the dose. The C-P analysis gives reasonable results for polyethylene irradiated with e-beam or γ-radiation, especially for non-branched linear polyethylene, if the dose is not very high nor very low [24]. Recently it has been shown that [25], that because in polyethylene treated by e-beam and y-

irradiation, chain reactions are involved the usefulness of the C-P analysis is limited. The arguments most probably hold also for UV-crosslinking.

The factors (b), (c) and (d) do not depend on the type of treatment, they should hold for UV-irradiation as well as for high energy irradiation. For linear UHMWPE the requirements are met reasonably well. For gel-spun fibres, crosslinked with UV radiation two aspects (a) and (e) have to be considered.

The first aspect (a): the probability that each monomer group for being involved in any of the reactions is the same for each monomer group. Drawn gel-spun polyethylene fibres are highly crystalline, and the initiator does not penetrate in the crystalline phase. In the absence of initiator, neither crosslinking nor chain scission will occur, as the energy of 253 nm UV radiation used, has a low yield for direct chain scission in the crystalline phase. For the UV-irradiation used in the present experiments the crystalline fraction can be considered to be inert. For the analysis only the non-crystalline fraction has to be considered. In the non-crystalline phase some chain scission can occur due to the short wavelength used [14]. This can results in a lower gel fraction that can be realised, however it will not invalidate the analysis. The irradiation should also be constant over the cross-section of the fibre. In the present experiments the sample was a thin (approx. 50 μm) layer of fibres. As the penetration depth of UV-radiation in polyethylene typically is 1 mm, the irradiation can be assumed to be homogeneous.

The second critical assumption is that the yields are proportional to the irradiation dose. This point was discussed above, and is believed to hold reasonably well. The amount of benzophenone in the fibres was approx. 0.5%. This can be considered ample sufficient, on the one side because the molecular weight is high, therefore a low crosslink density results in a high gel-content. On the other side a large fraction of the fibre is inert, therefore the local concentration in the non-crystalline domains is enhanced.

It is therefore believed that a C-P analysis gives a reasonable estimate for the chain scission to cross-link ratio.

In the C-P analysis the quantity $s+s^{0.5}$ is plotted against the inverse of the irradiation dose. The dose was assumed to be proportional to the irradiation time (equation 7.3).

If the data fit the C-P relation a straight line against the reciprocal dose (1/t) should be obtained. The result is given in figure 7.10.

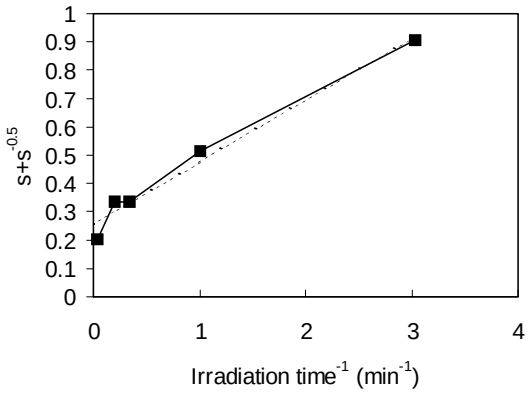

F igure 7.10 Charlesby and Pinner plot for UV crosslinked PE3 fibre

A straight line gives a reasonable fit except for long irradiation times, extrapolating to zero gives $s+s^{0.5} = 0.255$ for infinite irradiation time,1/t = 0, implying that G(s)/G(x) is approx. 0.5. Taking into account the deviations due to chain reactions [25] deviations of a straight line are expected and an intercept of 0.2, or G(s)/G(x) = 0.4.
is more probable.

The result shows, that chain scission is not negligible. The chain-scission to crosslink ratio however is more favourable than with high energy radiation. Data of De Boer [20] imply a Gs/Gx ratio of 1. The result is in line with a result reported by Qing, who compared crosslinking of low density polyethylene by UV radiation and by γ-radiation. [27]. He found a ratio of 0.55 for UV-crosslinking and 0.88 for γ-ray crosslinking. Further reduction of the chain scission may be possible by using UV-radiation of 300-330 nm instead of the 253 nm used in the present research [26], and by increasing the temperature during irradiation [14].

Chapter 8 Epilogue: Structure of UHMW-PE fibres and it's UV crosslinking

8.1 Introduction

The subject of the thesis is the creep behaviour of gel-spun polyethylene fibres, and the possibilities for improving their creep resistance. In this chapter the relation between the structure of the fibre, its creep behaviour and the possibilities for improvement, are discussed in retrospect.

Creep, as discussed before, is an intrinsic, and limiting, property of polyethylene fibres. Due to the small intermolecular interactions, viz. Van der Waals forces, chains can easily slip. Even a model fibre that consists of fully extended and oriented chains, viz. the fibre has no supermolecular structure, shows several aspects of the observed deformation behaviour [1,2]. However several other aspects of the deformation and creep behaviour, relevant to this work, can not be predicted by this model. For instance: plastic deformation is possible only to a very limited extent, because the breaking stress decreases at a small deformation (see chapter 2 figures 2.7 and 2.8), and the effect of the draw ratio cannot be described. There is no entanglement network in the model, therefore there is no network process that contributes to the load. Finally impregnation and (UV-) crosslinking is not possible in the model fibre. For describing these additional aspects of deformation and creep and the effects of impregnation and treatment a more complicated structure is required.

The structure of a fibre is formed during the process of drawing. In the preceding chapters, it has been shown that fibres of widely different draw ratio show qualitatively the same creep behaviour. In fact, the effect of the drawing on the creep properties can be understood, by assuming that the number of chains that carry the load is essentially invariant during drawing.
Due to production related limitations, commercially produced gel-spun fibres are not drawn to their maximum extent. The draw ratio applied to commercially produced fibres is determined by practical considerations, such as the production speed and the probability of fibre breakage during the process. There is no lock-in mechanism

that poses a natural limit to drawing. *Consequently, creep and drawing are the same, albeit at a different time-temperature scale.*

As flow creep and drawing are essentially the same, or at least strongly related processes [3, ch. 2], studies concerning the molecular processes that play a role during drawing, are also relevant for describing the molecular basis of the creep process. Many authors have studied the formation of highly oriented (polyethylene) fibres [4-30]. As a result, a large number of structural and deformation models have been proposed for highly oriented (polyethylene) fibres, each describing some aspects of the observed structure and deformation behaviour [7-12,22,24,25,31-44]. For the present research, especially those studies are relevant, that describe the structural changes, that occur under typical drawing conditions [4,11-13,20-25], and those studies, that address molecular or structural aspects of the deformation process [1,2,5,11,26,27,35-37,39,45-49].

A drawn fibre is characterised by a high degree of chain extension and a high crystallinity (typically 80%). Phase structural analysis by solid state NMR show that 4 different phases can be observed: an orthorhombic crystalline phase (the main constituent), a small fraction of monoclinic crystalline phase, a small fraction of disordered non-crystalline phase, and an 'interphase' [50-59]. The latter phase has the characteristics of a somewhat disturbed orthorhombic crystalline phase and is not always considered as a separate phase. For the present discussion the distribution and properties of the non-crystalline phase is most relevant.

The size and distribution of the crystalline and non crystalline domains have been studied using TEM [39,60], SAXS, [24,25,58,61,62], and WAXS [24,25,58,63]. The studies have indicated that in highly (and even in moderately drawn fibres) the distribution of low density domains lacks conspicuous regularity, (a long period is weak or absent) and causes more lateral scattering than longitudinal scattering, indicating that the density variations are most pronounced in the lateral direction.

Highly drawn gel-spun polyethylene fibres possess a fibrillar structure. Fibrillar units of different scale have been observed: macrofibrils, with a typical diameter of 1 μm

[18,34,35,54], microfibrils, with diameters of 20-50 nm, (by some authors also referred to as nanofibrils [14,19,34,35,63-70], and even smaller nanofibrils (5-10 nm) [71,72].

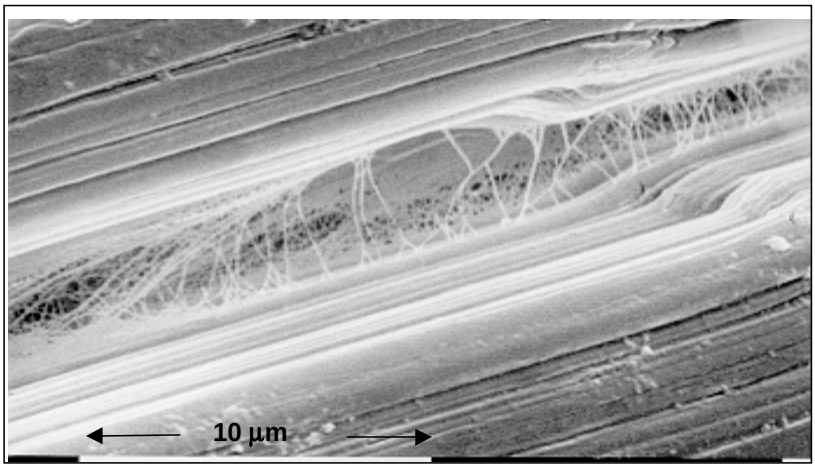

Figure 8. 2 Fibrillar structure of a gel spun UHMW-PE fibre. On the body of the filaments a macro-fibrillar structure is observed. In the space between the filaments (bundles of) very thin fibrils can be seen. The thin fibrils were separated from the thicker ones during the drawing process, [73].

It is still a subject of debate, whether this supermolecular structure is relevant for the deformation behaviour of highly drawn fibres, and if so, what the contribution of relative movements of supermolecular units is to the total deformation [13,15,34,35,44,74-79]. Marikhin et al [11, 34,35] assume that the macroscopically observed deformation is the result of slip processes acting on scales from a single molecular chain up to that of macrofibrils [34,35]. Van Hutten [13] and Pennings [15] assume that creep is purely an intrafibrillar process, and is caused by slip of taut tie molecules. Several authors [44,78-81] including Bastiaansen (80) and Smith (81), do not consider the supermolecular structure to be of any relevance to the deformation behaviour.

8.2 Structure of a drawn fibre

In the process of drawing the initial morphology, lamellar semi-crystalline polyethylene, or for pre-oriented fibres a mixture of lamellar and extended chain domains, is transformed into a fibre consisting mainly of fibrillar domains with a high degree of chain extension. The structural changes, that occur during ultra-drawing polyethylene in the solid state, have been described by several authors [11-13,20-22,24,25,35-37,82].

As discussed in chapter 2 there are two temperature regions, wherein gel-spun UHMW-polyethylene can be drawn isothermally, the processes are called solid state drawing and melt-drawing or hot-drawing respectively. Hot drawing is less effective, for realising a high degree of chain extension and good mechanical properties, at least when starting from isotropic samples [24,25], however it is important for commercial gelspinning, as the later stages of drawing are in the temperature window for hot drawing.
With increasing draw ratio the fraction of extended chain phase increases, and drawing can be done effectively as long as the temperature is below melting temperature of the constrained fibre as a whole [24]. In this regime a (small) fraction of the fibre can be in the melt. After cooling, the remaining melt re-crystallises, and can form a lamellar overgrowth layer on the extended chain domains [12,13].

Also solid state drawing results in fibrillar domains separated by domains with lower chain extension [21,22,24]. Whatever the actual drawing mechanism is, solid state drawing or hot drawing, that part of the fibre that is not yet incorporated in the fibrillar domains forms an interlayer between these domains. This fraction is a function of the draw ratio, and is small in highly drawn fibres. The domains of high chain extension form the main component of the fibre.

Several authors propose that the fibrils consist of microfibrils or weakly connected bundles of microfibrils (or nanofibrils) [12,34-38,63,66,67,70]. Such a microfibril has an essential constant cross-section (typical diameter 20-40 nm) independent of the draw ratio. The internal structure of a microfibril is characterised by regular

alternations of crystalline blocks (with the same diameter as the microfibril itself) separated by non-crystalline zones.
Microfibrillar structures with alternating bands of different lateral compliance have been observed by AFM [63,65-67,70]. The banded structure is obvious in fibres of a low draw ratio, but it can also be observed in highly drawn fibres [66,67,70]. It is however not clear that the regular alternation of the compliance along a fibril is intrinsic to the bulk of the fibril. It has also be attributed to an overgrowth layer [66].

An alternative model for the highly extended chain phase was proposed by Berger [39]. Following the suggestion of Chanzy [60], and supported by dark field TEM pictures, he proposes that the extended chain domains of a fibre are relatively coarse fibrils that are aggregates of irregularly shaped crystal domains, typical dimensions: 10-40 nm wide and 40-200 nm long. The crystal domains are separated by narrow boundaries (less a few nm wide), containing mainly kinks. The directions of the boundaries do not have a strong relation with the drawing direction. Adjacent crystal domains are slightly disoriented with respect to the a- and b-axes.

In conclusion; a drawn fibre consist mainly of fibrillar domains (either microfibrils or aggregates of crystal blocks), these domains are separated and connected by interphase layers of a much lower chain extension.
The long period observed by SAXS at relatively low draw ratio [12,13,20-22], and the banded structure seen by AFM, is caused by diffraction in the interphase and is not intrinsic to the domains of extended chains.
A typical chain has segments in the interfibrillar phase and intrafibrillar segments, that cross several crystal domains.

8.3 Plastic deformation and creep

When the fibre is loaded, the fibrils carry the load. The chains of the interphase follow the local deformation, unfold and are converted into extended chain phase. This is due either to elongation of the fibrillar domains, or their to their relative movement, or both. At low or intermediate stresses, most relevant for this study, the deformation mode is elongation of fibrillar units.

The deformation rate is determined by stress assisted, thermally activated, slip of intrafibrillar crystalline chain segments. The small activation volume of the crystalline process, the main process responsible for irreversible creep, demonstrates that many chains are involved and share the load. This suggests that elongation of the fibrils is the dominating deformation mode.

Elongation of the fibrils is due to the slip of chain segments through crystalline domains, both the crystalline process (diffusion of chains mediated by Reneker defects), and the network process (contribution of chains with a resistance more than average) contribute. If a fibril elongates, chains of the interphase are reeled-in, and become part of the fibril. When fibrillar slip to occurs, the reverse process occurs; the chains of the interphase are drawn taut, and once taut will be pulled out of the fibril, or rupture. For elongation of a fibril essentially all chains in a section must be involved, for fibrillar slip only the chains in the surface of a fibril.

The more mobile chain segments in the interfibrillar layers follow the deformation of crystalline parts, essentially without contributing to the load. Elongation of the fibrils, causes these to become thinner, the reduction of the cross-section is partly compensated by the added mass of new extended chains. Chain segments are reeled in, and thus become part of the extended chain phase [12]. As soon as the interfibrillar phase is exhausted an increasing number of chain ends are drawn into the fibril.

8.4 Creep improvement by impregnation and UV irradiation

UV treatment can increase the creep resistance both by forming chemical crosslinks and by grafting side groups. Crosslinking and grafting reactions can only occur in the defect-rich interphase layers, and in sufficiently large defects in the extended chain domains. The fibrillar structure with low density interfibrillar layers, facilitates the penetration of reactants deep into the fibres.

The interfibrillar phase is readily accessible to the initiators or reaction products [83]. It can be expected that in the interphase crosslinking occurs readily.

It is less certain if crosslinking and grafting side groups also occur in intrafibrillar defects. Krishuk et al. [83] demonstrated that in highly drawn films nitroxyl radicals (TEMPO) cannot penetrate in the fibrils, but only in large pores (identified as interfibrillar void space). Tiño et al. [84], showed that the rotational mobility of TEMPO diffused in fibres increases with increasing draw ratio (PE1 to PE4). While it was suggested, that this is due to chain rupture and formation of local defects; the data can also be explained assuming that the probe is progressively excluded from the more dense non-crystalline intrafibrillar phases, and an increasing fraction is in larger pores. Also with ^{129}Xe-NMR the non-crystalline phase of several fibres used in this research (PE1, PE3, and PE5) was probed, it was found that the mobility of Xe atoms diffused in non-crystalline phase decreases with increasing draw ratio [85].

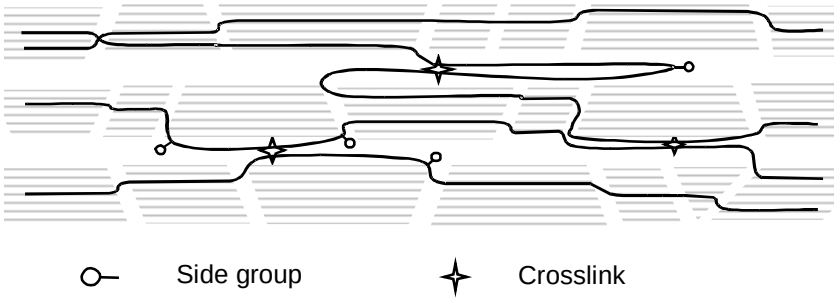

Figure 8.2 Schematic representation of a fibre after impregnation and UV-treatment. A fibre consists of fibrillar units consisting of irregularly shaped crystal domains and defect borders. Crosslinks and grafted side groups are formed primarily in the interfibrillar layers..

It is concluded, that for highly drawn fibres accessibility of the intrafibrillar phase is limited. Consequently it is assumed that for such fibres the reactions are primarily in the interfibrillar layers. Figure 8.2 gives a schematic picture of a modified fibre of high draw ratio.

Interfibrillar crosslinking and grafting interfere with elongation of the fibrils. Chains containing a large side group or a crosslink will resist being reeled in, the groups or crosslinks are arrested at the surface of the fibril. The possibilities for improving the

creep depend on the fraction of the chains in the interfibrillar layers. As this fraction is small the flow creep can be suppressed only up to a limited stress level.

The effect of grafting small side groups, such as Cl-atoms, is probably different from that of large side groups and crosslinks. Chains with small side groups, $-CH_3$ or a Cl-atom, can slip through the crystalline phase, although with an increased slip resistance [86-88]. Chains with small side groups can be drawn into the crystalline phase and thus cause an increased resistance against slip, but still allowing plastic deformation. Larger side groups and crosslinks form large defects, that resist the pulling-in of chains into the crystalline domains.

Intrafibrillar reactions, both crosslinking and grafting, probably also take place, especially so for the fibres of a lower draw ratio. Intrafibrillar crosslinks and side groups prevent the slip of chains and thus oppose the elongation of a fibril.
As the accessibility of suitable sites for modification and the mobility of initiator is critical, the size of the reacting species is important. The smallest reacting species is much smaller when using chlorine compounds (chorine atoms) as compared with benzophenone (BP is activated by an internal reorganisation). Intrafibrillar reactions resulting in chain scission could be the cause of degradation of the mechanical properties of fibres treated with chlorine compounds.

The accessibility for initiators and reaction products can be enhanced by relaxation of non-crystalline chains at elevated temperature. This results in less stress on the non-crystalline chains, and in a lower density of the non-crystalline domains. The enhanced accessibility for initiator molecules and increased mobility of chain segments, could result in more favourable conditions for impregnation and UV-crosslinking.

Impregnation and UV-crosslinking results in suppressing the flow creep of gel-spun polyethylene fibres with a Young's modulus of about 100 GPa up to a threshold stress (for the presently tested fibres between 0.5 and 1 GPa). The most interesting alternative is the use of a polymer with small side groups. In order for the fibre to remain drawable, there are limits to the concentration and size of the sidegroups. This also implies that the flow creep is reduced, but not fully suppressed.

Furthermore the chemical network formed by crosslinking results in an enhanced temperature resistance.

8.5 Conclusions

A structural model that is suitable for describing highly, but not ultimately, drawn polyethylene fibres is proposed. According to this model, a fibre consists mainly of fibrillar extended chain domains separated by a small fraction of interfibrillar material with a low degree of chain extension. Plastic deformation, is due to elongation of the extended chain domains.

Chain segments, that are accessible to initiator molecules, are present mainly in the intermediate layers. Crosslinking and grafting of such chain segments interfere with reeling in of chains into the fibrillar domains, and thus contribute to an enhanced creep resistance. Intrafibrillar crosslinking and grafting, also contributing to an enhanced creep resistance, is also possible especially so in fibres of a low draw ratio.

(UV)-crosslinking of the drawn fibre depends on the presence of a fraction of chains that do not form part of the main structure of the extended fibrillar domains. In highly drawn fibres this fraction is small, and formation of a strong network is not possible with this method. Fibres of an intermediate draw ratio are most suitable for UV-crosslinking after drawing. The method results in elimination of the flow creep up to a threshold stress.

8.6 References

1 Y. Termonia, P. Smith, High modulus polymers, A. Zachariades, and R.S Porter Ed. Marcel Dekker New York, (1988), ch. 11

2 Y. Termonia, P. Smith, Macromol., **26**, (1993), 3738

3 L.E Govaert, Ph-D Thesis Eindhoven University of Technology, (1990), ch. 1

4 J. de Boer, P.F. van Hutten, A.J. Pennings, J. Mater. Sci., **19**, (1984), 428

5 J. de Boer, H.J. van en Berg, A.J. Pennings, Polymer **25**, (1984), 513

6 G. Cappacio, I.M. Ward, Polym. Eng. Sci., **15**, 3, (1975), 219

7 A.G. Gibson, G.R. Davies, I.M. Ward, Polymer, **19**, (1978), 683

8 A.G. Gibson, G.R. Davies, I.M. Ward, Polym. Eng. Sci., **20**, 14, (1980), 941

9 A. Peterlin, J. Mater. Sci, **6**, (1971), 490

10 A. Peterlin, Polym. Eng. Sci., **18**, 6, (1978), 488

11 V.A. Marikhin, L.P. Myasnikova, D. Zenke, R. Hirte, Polym. Bull., **12**, (1984), 287

12 P.F. van Hutten, C.E. Koning, J. Smook, A.J. Pennings, Polym. Comm., **24**, (1983), 237

13 P.F. van Hutten, C.E. Koning, A.J. Pennings, J. Mater. Sci., **20**, (1985), 1556

14 J. Smook and J. Pennings, Colloid. Polym. Sci., **262**, (1984), 712

15 A.J. Pennings, J. Smook, J. de Boer, S. Gogolevski, and P.F. Hutten, , Pure and Appl. Chem., **55**, 5, (1983), 777

16 B. Bönigk, Ph-D Thesis TU Berlin, (1995)

17 F.T. Ohta, A. Takada, T. Yamamura, A. kawaguchi, S. Murakami, Polymer, **26**, 11, (1995), 2181

18 P. Smith, P.J. Lemstra, J. Mater. Sci., **15**, (1980), 505

19 P. Smith, P.J. Lemstra, J. Polym. Sci., B. polym. Phys., **19**, (1981), 877

20 N.A.J.M. van Aerle, P.J. Lemstra, Makromol. Chem., **189**, (1988), 1253

21 N.A.J.M. van Aerle, C.W.M Braam, J. Mater. Sci., **23**, (1988), 4429

22 N.A.J.M. van Aerle, Ph-D Thesis Eindhoven University of Technology, (1989), ch. 3

23 D. Hofmann, E. Schulz, Polymer, **30**, (1989), 1964

24 P.J. Lemstra, N.A.J.M. van Aerle, C.W.M. Bastiaansen, Polymer J. **19**, 1, (1987), 85

25 N.A.J.M. van Aerle, Ph-D Thesis Eindhoven University of Technology, (1989) ch. 4

26 W. Hoogsteen, H. kormelink, G. Eshuis, G ten Brinke, A.J. Pennings, J. Mater. Sci., **23**, (1988), 3459

27 W. Hoogsteen, R.J. van der Hooft, A.R. Postema, G ten Brinke, A.J. Pennings, J. Mater. Sci., **23**, (1988), 3467

28 R. Kirschbaum, H. Yasuda, E.H.M. van Gorp, Proc 25 Int. Chem. Fibres Congress, Dornbirn, Sept.(1986), 229

29 J Smook, Ph-D-thesis Groningen University, (1984), ch. 2

30 T. Ogita, R. Yamamoto, N. Suzuki, F. Ozaki, M. Matsuo, Polymer, **32**, 5, (1991) 822

31 R.S. Porter Polym. Prep. **12**, 2, (1971), 39

32 R.S. Porter, T. Kanamoto, Polym. Eng. Sci., **34**, 4, (1994), 266

33 E.S. Clark, L.S. Scott, Polym. Eng. Sci., **14**, 10, (1974), 682

34 V.A. Marikhin, Makromol. Chem. Suppl., **7**, (1984), 147

35 V.A. Marikhin, L.P. Myasnikova, Makromol. Chem., Makromol,. Symp., **41**, (1991), 209

36 G.K. Elyashevich, B. V. Streltzev, E.A. Karpov, E. Y. Rosova, V.A. Marikhin, L.P. Myasnikova, E.A. Ro, Fibres ans Textiles, March-June 1994, 33

37 V.A. Marikhin, L.P. Myasnikova, Progress in Colloid and Polym. Sci., **92**, (1993), 39

38 D.C. Prevorsek, H.B. Chin and S. Murthy, J. Polym. Sci., Polym. Symp., **75**, (1993), 81

39 L. Berger, Ph-D-Thesis, EPFL Lausanne, (1997)

40 A. Zachariades, T. Kanamoto, J. Appl. Polym. Sci., **35**, (1988), 1265

41 Zachariades. And T. Kanamoto, High modulus polymers, A. Zachariades, and R.S Porter Ed., Marcel Dekker New York, (1988), ch. 10, 299

42 D.J. Dijkstra and A.J. Pennings, Polymer Bull., **19**, (1988), 73

43 Kausch 1996 H.H. Kausch, L. Berger, C.L.G. Plummer, Proc. 35th Int. Manmade fibre Congress, Dornbirn, (1996)

44 L.E. Govaert, Ph-D Thesis Eindhoven University of Technology, (1990), ch. 4

45 W.F. Wong, R.J. Young, J. Mater. Sci., **29**, (1994), 510

47 J.A.H.M. Moonen, W.A.C. Roovers, R.J. Meier, B.J. Kip, J. Polym. Sci., B, Polym. Phys. **30**, (1992), 361

48 B.J. Kip, M.C.P. van Eijk, R.J. Meier, J. Polym. Sci., B, Polym. Phys. **29**, (1991), 99

49 W.F. Wong, R.J. Young, J. Mater. Sci., **29**, (1994), 520

50 N. Nakagawa, F. Horii, R. Kitamaru, Polymer, **31**, (1990), 323

51 A Kaji, Y. Ohta, H. Yasuda, M. Murano, Polym. J., **22**, 6,(1990), 405

52 A Kaji, A. Yamanaka, M. Murano, Polym. J., **22**,10, (1990), 893

53 A Kaji, A. Ahimoto, M. Murano, J. Polym. Sci, A, Polym Chem., **29**, (1991), 1987

54 H. Deckmann, Ph-D Thesis Universität Freiburg im Breisgau, (1991), 54

56 D.L. Tzou, T.H. Huang, P. Desai, A.S. Abhiraman, J. Polym. SCi, B, Polym. Phys., **31**, 8, (1993), 1005

57 D.L. Tzou, K. Schmidt-Rohr, H.W. Spiess, Polymer, **35**, 22, (1994), 4728

58 Y. Fu, W. Chen, M. Pyda, d. Londono, B. Annis, A Boller, A. Habenschluss, J. Cheng, B. Wunderlich, J. Macromol Sci., B, Phys., **35**, 1, (1996), 37

59 J. Cheng, M. Fone, Y, Fu, W. Chen, J. Thermal Anal., **47**, 3, (1996), 673

60 H.D. Chanzy, P. Smith, J.V. Revol, R. St. John Manley, Polym Comm. **28**, (1987), 133

61 D.T. Grubb , K. Prasad, Macromol., **25**, (1992), 4575

62 W. Hoogsteen, G. ten Brinke, A.J. Pennings, J. mater. Sci., **25**, (1990), 1551

63 S.S. Sheiko, S.N. Magonov, M. Möller, Polym. Prep.,**37**,2, (1996), 788

64 D. Snetivy, H. Yang, G.J. Vansco, J. Mater. Chem., **2**,8, (1992), 891

65 A. Wawchuschewski, H-J Cantov, S.N. Magonov, Polym. Bull., **32**, 2, (1994), 235

66 A. Wawchuschewski, H-J Cantov, S.N. Magonov, J.D. Hewes, M.A. Kocur, Acta Polymerica, **46**, 2 ,(1995), 168

67 A. Wawchuschewski, H-J Cantov, S.N. Magonov, S.S Sheiko, M. Möller, Polymer Bulletin, **31**, (1993), 699

68 S. Halaoua, Memoire fin d'étude, ENSAIT, (1995)

69 S.S Sheiko, M. Möller, H-J Cantow, S.N. Magonov, Polymer Bulletin, **31**, (1993), 698

70 S.S Sheiko, M. Möller, M. Kunz , H. Deckmann, Acta Polymerica, **47**, (1996), 492

71 G.J. Vancso, Polym. Prep.,**37**,2, (1996), 550

72 Kashu 1996 Y. Kashu, T. Adachi, Y. Tomita, Proc. Symp. Japan Mech. Soc.,

73 C. Veillat, Thesis ENSAIT, (1995)

74 D.C. Prevorsek, Oriented Polym. Mater., (1996), 444, Eds.: Fakirov, Stoiko, Hüthig und Web Verlag, Zug

75 N.N. Peschanskaya, L.P. Myasnikova, Proc. 25, Europhys. Conf, St Petersburg, (1992), 224

76 N.N. Peschanskaya, L.P. Myasnikova, Physics soli state, **35**,11, (1993), 1484

77 N.N. Peschanskaya, P.N. yakushev, L.P. Myasnikova, V.A. Marikhin, A.B. Sinani, M. Jacobs, Physics Solid State, **38**,8, (1996), 2582

78 L.E. Govaert and P.J. Lemstra, Coll. and Polym. Sci., **270**, (1992), 455

79 L.E. Govaert , C.W.M. Bastiaansen, P.J.R. Leblans, Polymer, **34**, (1993),

80 C.W.M. Bastiaansen, P-D Thesis Eindhoven University of Technology, 1991

81 P.A. Irvine and P. Smith, Macromolecules, **19(1)**, (1986, 240

82 J.P. Penning, H.E. Pras, A.J. Pennings, Coll. Polym. Sci., **272**, (1994), 664-676

83 B.E. Krishuk, V.A. Marikhin, L.P. Myasnikova, N.L. Zaalishvili, Int. J. Polym. Mater. **22**, (1993), 161

84 J. Tiño, M. Klimová, I. Chodak, M.J.N. Jacobs, Polymer Int., **39**, (1996), 231

85 M. Horstmann, Thesis Gerhard Mercator University Duisburg, (1997)

86 Y. Ohta, H. Yasuda, A. Kaji, Polym. Preprints Japan, **43**, 9, (1994, 3143

87 C.L.H. van Heist, Ph-D Thesis Eindhoven University of Technology, (1994), ch.2

88 H.N.A. Steenbakkers-Menting, Ph-D Thesis Eindhoven University of Technology, (1995) ch. 5

Het gelspin proces, dat uitgevonden is bij DSM op het eind van de 70-er jaren maakt het mogelijk vezels met superieure mechanische eigenschappen te maken op basis van polyetheen met een ultra hoog moleculair gewicht. Vezels met een treksterkte tot 4 GPa en een Young's modulus tot 150 GPa worden commercieel geproduceerd. Het blijkt echter, dat de lange termijn belastbaarheid van deze vezels veel minder goed is dan die voor de korte termijn. Met name kruip is limiterend voor de lange duur belastbaarheid van de vezel. Kruip is van belang voor vele toepassingen van de vezels, bijvoorbeeld in touwen en kabels en in composieten. Bovendien worden de vezels voor vele andere toepassingen niet in overweging genomen, vanwege de kruip van de vezels.

Het verbeteren van de kruipeigenschappen van de vezels is niet eenvoudig. De vezels worden geproduceerd door uit oplossing versponnen vezels in een gel-toestand te brengen, te drogen en in zeer hoge mate te verstrekken. Elke verandering van de moleculen (vóór het verstrekken) interfereert met het verstrekproces, en resulteert in vezels met minder goede mechanische eigenschappen. Significante verbeteringen zijn geclaimd door het gebruik van polyetheen met zijketens of chemisch gemodificeerd polyetheen, de mate van verbetering wordt echter in het algemeen overschat omdat de eigenschappen worden vergeleken bij een gelijke en relatief lage verstrekgraad. Voor het verbeteren van de kruipeigenschappen van al verstrekte vezels is het een vereiste dat de nadelige effecten van ketenbreuk worden geminimaliseerd. Vanwege een te hoge mate van ketenbreuk resulteert het crosslinken van de vezel met behulp van hoog-energetische straling slechts in een achteruitgang van de korte duur en van de kruipeigenschappen.

De snelheid waarmee hoog-georiënteerde vezels kruipen onder belasting wordt bepaald door de snelheid waarmee ketensegmenten door kristallijne domeinen slippen. Voor het beschrijven van de permanente kruip is het concept van thermische geactiveerde diffusieprocessen toegepast en verder ontwikkeld. Tenminste twee van dit soort processen zijn nodig om de relatie de tussen de deformatiesnelheid en de belasting te beschrijven. Elk van deze processen is gekarakteriseerd door een limiterende snelheid, die bepaald wordt door de door de gemiddelde snelheid waarmee ketensegmenten door kristallijne domeinen

diffunderen, door een activeringsenergie en door een activeringsvolume. Het activeringsvolume, bepalend voor de spanningsafhankelijkheid van de kruipsnelheid, is omgekeerd evenredig met het aantal aan het proces bijdragende ketensegmenten.

Het blijkt dat de kruip, zowel de niet permanente kruip alsook de permanente kruip, zodanig met de verstrekverhouding schaalt dat vezels die met gelijke kracht belast worden dezelfde kruip vertonen. Deze waarneming wordt verklaard door aan te nemen, dat het aantal ketens in een doorsnede van de vezel dat bijdraagt aan de belasting, constant is, en tevens dat de weerstand van deze ketens tegen slip constant is.

Het ontwikkelde model van thermisch geactiveerde vloei processen is gebruikt om na te gaan welke mogelijkheden er zijn om de weestand tegen permanente kruip te verbeteren. Dit kan gebeuren door vergroten van het aantal ketens dat bijdraagt aan de belasting, of door het verhogen van de weerstand van (tenminste een deel van) de ketens tegen slip. De mogelijkheden om de kruipeigenschappen bij relatief hoge belasting te verbeteren, bijvoorbeeld door gebruik van polyetheen met een nog hoger moleculair gewicht, of het in nog hogere mate vertrekken van de vezels, zijn beperkt. Het verbeteren van de kruipweerstand bij lagere belastingen, is mogelijk door vergroten van de bijdrage van één van de processen, het netwerkproces. Dit is de meest interessante optie voor het verbeteren van de kruipeigenschappen na het strekken van de vezels.

Fotochemische en thermische methoden zijn in principe geschikt voor het crosslinken van door gelspinnen geproduceerde polyetheen vezels, omdat ketenbreuk hierbij alleen een secundair effect is. Het toevoegen van de benodigde initiator vóór het verstrekken heeft nadelen; het compliceert het produceren van de vezels, en de vooraf ingebrachte initiator blijkt weinig effectief te zijn. Impregneren van de vezel met initiator na het verstrekken wordt bemoeilijkt door de hoge dichtheid en hoge kristalliniteit van de vezels. Twee methoden voor impregnatie na verstrekken zijn gevonden en geëvalueerd, impregnatie met relatief kleine moleculen vanuit de dampfase, en impregnatie gebruik makend van een superkritisch medium.

Vezels van verschillende verstrekgraad zijn gecrosslinkt door middel van UV-straling na impregnatie met chloorhoudende initiators uit de dampfase. De mate waarin een gevormd vezel gecrosslinkt kan worden hangt af van de verstrekgraad. De effectiviteit van het netwerk, beoordeeld naar de mate waarin het netwerk in staat is de molecuulketens in gestrekte toestand te houden als de vezel boven het smeltpunt verhit wordt, is optimaal voor een hoog, maar niet volledig, verstrekte vezel, en is lager zowel voor vezels met lagere alsook met hogere verstrekgraad. Aangetoond is dat de permanente kruip kan worden geëlimineerd (bij een spanning van 0.6 GPa) voor vezels van verschillende verstrekgraad (met uitzindering van een enkele hoogverstrekte vezel), hierbij wordt de omkeerbare kruip niet beïnvloed. Het is vereist de behandeling in inerte atmosfeer uit te voeren, om achteruitgang van de korte duur mechanische eigenschappen te beperken.

Impregnatie met superkritische media is een techniek waarmee polymeren geïmpregneerd kunnen worden Verven gebruikmakend van een superkritisch medium is in ontwikkeling als een milieuvriendelijk alternatief voor het verven van kunststofvezels. Polyetheen vezels, geproduceerd door gelspinnen, met verschillende verstrekgraad zijn geïmpregneerd in superkritisch CO_2 met de initiator benzophenon en vervolgens gecrosslinktt met UV-straling. De weerstand tegen permanente kruip word significant verbeterd voor belastingen tot 1 GPa. De verbetering van de kruip kan geheel toegeschreven worden aan versterking van het netwerk. UV-crosslinking resulteert ook in een verminderde spanningsrelaxatie en in een verhoogde temperatuur weerstand

Het onderzoek naar de kruipeigenschappen van vezels van verschillende verstrekverhouding en de levert nieuwe inzichten op die relevant zijn voor de modellen die de structuur van de vezel beschrijven. Er wordt een model voorgesteld, waarin een vezel, die een verstrekgraad heeft die minder is dan de uiterste verstrekgraad; voornamelijk bestaat uit fibrillaire domeinen met daartussen een kleine fractie materiaal waarin de ketens relatief weinig gestrekt zijn. De fibrillen zelf bestaan uit materiaal waarin de ketens in hoge mate gestrekt zijn. Bij verder strekken, of ten gevolge van kruip, verlengen de fibrillaire domeinen; de ketens van de die zich er tussen bevinden worden erin getrokken en gaan aldus deel uitmaken van de fibrillen. Initiatoren kunnen in de ruimte tussen de fibrillen penetreren. UV-bestraling resulteert in crosslinking van deze intermediare fase en in het enten van

groepen aan de ketens. Beide processen verhinderen het intrekken van de moleculen in de fibrillen, hun verlenging wordt daardoor tegengewerkt.

This work and this thesis would not have been realised without the support of many. I would like to thank those who contributed in one way or another to the research and those who assisted in the preparation of this thesis. I would like to name especially:

- The management of DSM High Performance Fibers, for the financial support, and for allowing publication of this thesis.
- Many members of the Faculty of Chemistry. Furthermore the (former) students Danny Knoop, Nicole Heijnen, Natasja Kriele and Marc Mutsaerts.
- Valuable contributions stem from discussions with: Ian Ward, IRC in Polymer Physics University of Leeds, Leen Struik of DSM Research, Leon Govaert of the Faculty of Mechanical Engineering, Vatjesclav Marikhin and his group of A.F. Ioffe Physical Technical Institute in St Petersburg and of Takashi Nishino of Kobe University.
- Loek Vlugt and his colleagues of DSM Research for the assistance with literature research.
- Pavel Zamotaev and Oleg Mityukhin of the Institute of Biochemistry and Oil Chemistry in Kiev, for advising and making available UV initiators, and for performing impregnation and UV crosslinking experiments.
- Ivan Chodak of the Polymer Institute of the Slovak Academy of Sciences in Bratislava, for enabling part of the work to be done in the Polymer Institute, and for supervising experiments and discussing results.
- Elke Bach of the Deutsches Textilinstitute Nord-West (DTNW) in Krefeld, for advising on and assisting at experiments on supercritical CO_2 assisted impregnation and cross-linking of gel-spun fibres.
- My (former) colleagues of DSM High Performance Fibers; Koos Mencke for making available experimental gel-spun fibres, Miek Segers and Jean Goossens for performing experiments.
- Daniel Teckoe of Reading University for allowing the use of data concerning restrained DSC experiments on cross-linked fibres.
- Elly Langstad, Margit Roelofs and Marlène Dekkers for their co-ordinative activities in Eindhoven

  Marjon Jörissen for her contribution to the lay-out of the cover.

Last but not least I would like to thank my family, in the first place Lisa, for their continuing support, and patience.

a(T)	temperature dependent shift factor
c	coefficient logarithmic creep rate
c_L	load related coefficient logarithmic creep rate
f	fraction load bearing chains
k	Boltzman's constant
l_b	bond length
m	constant
n	constant
r_0	end to end distance
s-CO_2	supercritical carbon dioxide
tex	mass (g/1000 m)
v, v_e	activation volume, activation volume elementary process
BP	benzophenone
C, Cij	compliance
C_∞	characteristic chain stiffness
D	Dalton
D(T)	compliance
DBP	dibenzoylperoxide
DCP	dicumylperoxide
E, E_∞	Young's modulus, limiting Young's modulus
H(τ)	relaxation time distribution
L	length
L_f	fold length
M	molecular weight
M_e	mass of chain segment
Mw	weight average molecular mass
P	load
PA	polyamide
PE	polyethylene
PECO	polyketone
POM	polyoxymethylene
PP	polypropylene
PPTA	poly(p-phenylene terephthalamide)
PBO	poly-(phenylene benzoxazole)
PIPD	polypyridobisimidazole
PVAL	poly(vinyl alcohol)
S, Sij	stiffness
U, U_e	internal energy, internal energy elementary process
UHMW-PE	ultra-high-molecular-weight polyethylene

β	stress concentration factor
δ	chain diameter
ε	strain
$\dot{\varepsilon}$	strain rate, creep rate
$\dot{\varepsilon}_0$, $\dot{\varepsilon}_{0e}$	pre-exponential rate factor, for elementary process
$\dot{\varepsilon}_0(T)$,	temperature dependent pre-exponential rate factor
$\dot{\varepsilon}_{pl}$	limiting (plateau) creep rate
ε_{rev}	reversible strain
ε_{irrev}	irreversible strain
φ	polymer concentration in solution
λ	draw ratio
λ_{max}	maximum attainable draw ratio
σ	stress
θ	angle
Ψ	effective time

Stellingen

Behorende bij het proefschrift

" Creep of gel-spun polyethylene fibres, Improvements by impregnation and crosslinking"

van Martien Jacobs

1. The method for describing stress relaxation and creep of polyethylene fibres as used by Ward et al. and the method for describing stress relaxation of solids used by Kubát et al. are equivalent.
   *M.A. Wilding, I.M. Ward. Polymer **19**, (1978), 969. J. Kubát and M. Rigdahl, Phys Status Solidii, **35(1)**, 1976, 173, C.-G. Ek, B. Hagström, J. Kubát, M. Rigdahl, Rheol. Acta, **25**, (1986), 534.*

2. The model of Struik for physical ageing of semi-crystalline polymers, such as polyethylene, should take into account that chain segments can easily diffuse through crystalline domains at room temperature.
   *L.C. E Struik, Polymer, **28**, 1987, 1534*
   *J. Kubát, F.H.J. Maurer, M Rigdahl, M. Welander, Rheological Acta, **28**, 1989,147-153*

3. The observation, that the activation volume for the crystalline flow process is proportional to the inverse of the Young's modulus implies that the number of chains contributing to the stress is proportional to the modulus.
   This thesis chapter 3

4. Gel-spinning enables the production of a strong fibre, superdrawing enables the production of a long fibre.
   *P. Smith and P.J. Lemstra UK patents 2 040 414, 2 051 661 (1979), P. Smith, P.J. Lemstra, J.P.L. Pijpers, J. Polym. Sci., Polym. Phys., **20**, 1982, 2229*

5. A temperature rise is not sufficient to explain the wear of diamond tools when cutting polymeric materials.
   *J.W. Carr, C. Feger, Precision Engineering, **15(4)**, (1993), 221*
   A. Jacobs, Eindhoven University of Technology, WPA 310052

6. The trend to a single universal language in scientific publications, is well demonstrated by the number of scientific publications in various languages.
   Statistics Chemical abstracts 1967-1997

7. International policy concerning Sustainable Development as proposed in Kyoto in 1997does not necessarily imply an improvement of the environment on a foreseeable time scale.
   Kyoto Protocol to the United Nations Framework Convention on Climate Change

8. Computers with emotionally supporting, 'emphatic', agents have been invented too late.
   R. Picard, MIT symposium, Massachusetts, Oct 1999

9. The current trend in the petrochemical industry to scale down or even eliminate corporate research is surprising in view of the fact that the exponential growth of polymers in this century was based on the many discoveries made by individual scientists and engineers.